Analysis of the spatial and temporal distribution of stable isotopes and their driving factors in the Upper Claro River Basin, Colombian Andes

TECHNISCHE UNIVERSITÄT DARMSTADT

Master Thesis of

Andrés Tangarife Escobar, Matr. -No.: 2341479

Institut für Angewandte Geowissenschaften
Darmstadt, December 2019

Declaration of Authorship

Hereby I certify, Ferney Andrés Tangarife Escobar (Matrikel No. 2341479) that the complete work of this master thesis

"Analysis of the spatial and temporal distribution of stable isotopes and their driving factors in the Upper Claro River Basin, Colombian Andes"

was done by myself and only by using the referenced literature and the described methods. This thesis was not submitted in identical or similar form to another examination authority and it was not published before.

…….. ……

Place, date Signature

First supervisor: Prof. Dr. Christoph Schüth

Second supervisor: Dr. Paul Königer

Acknowledgment

I would like to thank to the Deutscher Akademischer Austauschdienst (DAAD) for the funding and support during my Master studies and the development of this research project. I also give my special thanks to Prof. Dr. Christoph Schüth for allowing me to write the thesis under the supervision of his group. I would like to acknowledge Dr. Paul Königer and Nils Michelsen for the permanent supervision and advice throughout the whole research process. I am also very thankful with the Instituto de Hidrología, Meteorología y Estudios Ambientales (IDEAM) in Colombia for providing the data set on stable isotopes, and specially with Jorge Luis Ceballos for assisting and guiding me during the field stage as well as for sharing his valuable knowledge on the Colombian glaciers. Also, thanks to Liz Diaz and Eng. Francisco Gómez from IDEAM for his collaboration with the acquisition of meteorological data.

I owe my deepest gratitude to Carlos Vergara, Héctor Tangarife, Andrés Aguilar and Cristian Segura for the advices on data processing and their enriching discussions. Also, my special thanks to the staff members of the laboratories at Institute for Applied Geosciences, particularly to Stefanie Schmidt for the proofreading.

Finally, I am very much grateful to my parents, Alba Lucía Escobar and Héctor Elías Tangarife for the fight of an entire life to give me education. To Sofia Nalbadi and Hector Iván Tangarife, thanks for being the support, for being my rocks.

Table of content

List of Figures

List of Tables

Abstract

Stable isotopes and chemical composition of surface water and precipitation are recognized to provide information for hydrology and hydrogeology research. However, very limited data of the Upper Claro River Basin and the Central Colombian Andes are available. In this study, a total of 152 samples ranging a period of about two years are analyzed and the Local Meteoric Water Line $\delta^2H = 8.13\ \delta^{18}O + 12.5$, $R^2=0.98$ is defined. The results for δ^2H and $\delta^{18}O$ values showed a high range of variation due to the difference in altitude, meteorological conditions and seasons. Heavy isotopes content and deuterium excess in precipitation were clearly more negative during the rainy season. The seasonal variation of the stable isotopes concentration responded more to the change in rainfall periods and amounts than to the one of temperature. Altitude effect were calculated and their behavior showed non-linearity, namely, -0.36 ‰ of $\delta^{18}O$ / 100 for precipitation and -0.18 ‰ of $\delta^{18}O$ / 100 m for surface water. Data were compared with others collected by the Global Network of Isotopes in Precipitation (GNIP) and two patterns separated spatial and altitudinally were obtained.

Major ions and trace element analysis were conducted for rainy and dry season samples. The concentrations in precipitation were higher in the dry season. The influence of several factors such as (i) dilution caused by runoff availability, (ii) amount of volcanic emissions, (iii) size of the drainage area, (iv) input of baseflow, (v) lithology, and (vi) presence of thermal springs, were found to be the more relevant on the composition and concentration of the waters.

The obtained data and analysis allow to conclude that there is a high degree of complexity in the study site since the influence of winds coming from the Pacific and Atlantic oceans, surrounding ecosystems, evaporation sources, local meteorological phenomena and volcanic systems constitute all relevant driving factors on the isotopic and chemical signatures for the watershed. The present study provides an input to set up a methodology for the “National Network of Isotopy” and the “Glaciers and High Mountain Ecosystems Monitoring Program” ran by IDEAM.

Resumen

Los isótopos estables y la composición química del agua superficial y la precipitación proporcionan información clave para la investigación en hidrología e hidrogeología. Sin embargo, en la cuenca alta del Rio Claro y en los Andes centrales colombianos se dispone de datos muy limitados. En este estudio, se analizan un total de 152 muestras que abarcan un período de aproximadamente dos años y se define la línea meteórica local $\delta^2H = 8.13\ \delta^{18}O + 12.5$, R2 = 0.98. Los resultados para los valores de δ^2H y $\delta^{18}O$ mostraron un alto rango de variación debido a la diferencia de altitud, condiciones meteorológicas y estacionalidad. El alto contenido de isótopos y el exceso de deuterio en la precipitación fueron claramente más negativos durante la temporada de lluvias. La variación estacional de la concentración de isótopos estables respondió más al cambio en los períodos y cantidades de lluvia que al de la temperatura. Se calculó el efecto de altitud y su comportamiento mostró no-linealidad, a saber, -0.36 ‰ de $\delta^{18}O$ / 100 para precipitación y -0.18 ‰ de $\delta^{18}O$ / 100 m para agua superficial. Los datos se compararon con otros recopilados por la Red Global de Isótopos en Precipitación (GNIP) y se obtuvieron dos patrones separados espacial y altitudinalmente. Se realizaron análisis de iones mayores y elementos traza para muestras de temporada lluviosa y seca. Las concentraciones en precipitación fueron mayores en la estación seca. La influencia de varios factores, tales como (i) dilución causada por la disponibilidad de escorrentía, (ii) cantidad de emisiones volcánicas, (iii) tamaño del área de drenaje, (iv) entrada de flujo base, (v) litología y (vi) presencia de fuentes termales, se encontró que son las más relevantes en la composición y concentración de las aguas.

Los datos y análisis obtenidos permiten concluir que existe un alto grado de complejidad en el sitio de estudio, ya que la influencia de los vientos provenientes de los océanos Pacífico y Atlántico, los ecosistemas circundantes, las fuentes de evaporación, los fenómenos meteorológicos locales y los sistemas volcánicos constituyen factores influyentes relevantes sobre las firmas isotópicas y químicas de la cuenca. El presente estudio proporciona un aporte para establecer una metodología para la "Red Nacional de Isotopía" y el "Programa de Monitoreo de Glaciares y Ecosistemas de Alta Montaña" dirigidos por el IDEAM.

1. INTRODUCTION

This work is carried out within the frame of the "Glaciers and High Mountain Ecosystems Monitoring Program" of the Colombian Institute for Hydrology, Meteorology and Environmental Studies (IDEAM). This program is mainly focused on the identification, description and quantification of the ecosystems and water resources in the glaciers and associated basins in the Colombian Andes. According to this goal, the IDEAM has collected meteorological and hydrological data since 2006 and for the first time, stable isotopic composition data. The isotopes have been measured from precipitation and surface waters in the Upper Claro River Basin (UCRB) in the department of Caldas with the aim of monitoring the water resources behavior and the hydrologic response to different environmental and social variables.

The study area is characterized by having a strategic location where different high mountain ecosystems are present: Glacier, *Páramo*[1] and Andean Forest and in consequence is a suitable area to understand how the water characteristics react to variations in the meteorological conditions, geological properties and anthropogenic factors, etc. Additionally, diverse activities depend on the water provision from the UCRB: the development of agriculture, livestock, electricity generation, as well as the supply for different municipalities such as Villamaría and the 35 % of the water consumption of the capital city of the department, Manizales (Universidad Nacional de Colombia, 2014b).

However, despite of the relevance of this watershed and the fact that a first data set of stable isotopes has been gathered, this extensive amount of material has not been taken advantage of yet. Thus, this Master thesis makes use of the available information and generates a comprehensive set of new data to produce a base line of the temporal and spatial distribution of the stable isotopes in water and their driven factors in the UCRB. The present study integrates the analysis of meteorological (2 m above ground air temperature, regional wind direction and precipitation), vulcanological (ash fall events) and hydrochemical data along with the concentration of the stable isotopes of oxygen and hydrogen (^{18}O and ^{2}H, respectively) in surface and rainwaters over the period 2017 to 2019. It describes the driving factors of the distribution in the concentrations of stable isotopes across the altitudinal, seasonal, temperature, and precipitation gradients as well as researches deeper on the influence of the surrounding volcanic system in the water chemistry first proposed by Erazo et al., 2015.

Besides, the research aims to understand the role of the Glacier, Páramo and Andean Forest for the water distribution and to find relationships between the driving factors above mentioned and the presence of major ions and trace elements. To support the accomplishment of these objectives, the Local Meteoric Water Line (LMWL) is compared with those of others located in several locations of Colombia and available in the Global Network of Isotopes in Precipitation (GNIP) database provided by the International Atomic Energy Agency (IAEA). The fulfillment of all these traced goals will provide essential information for the decision making of the local communities, the environmental authorities and the IDEAM to adequately manage the water resources of the region in the context of the accelerated melting of the Santa Isabel glacier at the top of the UCRB (IDEAM, 2010).

The stable isotopes research on the Andes Cordillera and tropical Americas has not been recently abundant as in other regions of the world, as it can be seen in the publications of the symposiums on Isotope hydrology of 1997 and 2003 (IAEA 1997; IAEA 2003). Here, isotopic techniques have been commonly centered on the applications in hydrology and hydrogeology (Cortes et al., 1997; Gonfiantini et al., 2001). Nevertheless, the importance of this technique for the understanding of the water cycle has originated a series of studies focused on the characterization and modelling of the tropics climate.

[1] Páramo: ecosystem located in the high tropical Andes between 3100 and 4800 m a.s.l. (Buytaert et al., 2006) characterized by vegetation able to retain water. Páramos generally present low temperature and evaporation rate, high relative humidity and stable seasonality (in the maximum and minimum monthly temperatures) (Buytaert et al., 2006) and therefore are considered water regulators (Ortiz and Reyes, 2009). This ecosystem reports high biodiversity and endemism (Sklenáj et al., 2005) housing 17% of the floristic diversity of Colombia (Bernal et al., 2016). It is the main source of water for the high Andean areas (Buytaert et al., 2006).

The spatial and temporal distribution of ^{2}H and ^{18}O isotopes in South America[2] is influenced by four factors: a) the input from three atmospheric moisture sources (Atlantic and Pacific Oceans and Caribbean sea), b) the Andes mountains blocking free air flow and leading to enhanced condensation along the slopes and the associated depletion of rainfall in the heavy isotopes, c) the presence of the world largest continental evaporative basin (Amazon Basin) and d) the seasonal movement of the Intertropical Convergence Zone (ITCZ) over the central and northern part of the continent (Rozanski and Araguas, 1995). Furthermore, the Amazon Forest has been recognized for contributing large amounts of recycled moisture to the air masses transported by trade winds (Martinelli et al. 1996; Vallet-Coulomb et al. 2008) and for increasing the deuterium excess by the supply of recycled continental moisture (Esquivel-Hernández et al., 2019).

Regional models on the precipitation of $\delta^{18}O$ over the tropical Americas have stated that the variation of the isotope concentration does not depend on the local weather factors but on the interaction of several regional weather patterns, mainly the "El Niño" Southern Oscillation (ENSO) and the South American Monsoon (SAM), which in turn cause regional air masses transport (Vuille et al. 2003; Vuille and Werner 2005; Vimeux et al. 2005). In the Andes specifically, convective wind streams varying in direction during austral winter and austral summer also influence the isotopic composition of the atmospheric water vapor (Villacis et al. 2008; Samuels-Crow et al. 2014).

The spatial variability of isotopic composition in the Andean basins is dominated by the altitude effect where the gradient in precipitation ranges from 0.2 ‰ / 100 m in $\delta^{18}O$ (up to 3000 m a.s.l.), 0.5 ‰ / 100 m (above 3000 m a.s.l.) and -1.12 ‰ / 100 m in $\delta^{2}H$ (Rozanski and Araguas 1995; Windhorst et al. 2013). Nonetheless, this occur also in stream waters where the isotope concentration is generally modified by surface water recycling and/or evaporation (Bershaw et al. 2016). In high mountain ecosystems, like the páramos of Costa Rica and Ecuador the isotopes in precipitation were found to be influenced by the Amazon Forest air masses during the passage of the ITCZ in the wetter seasons and by orographic precipitation during the transition and drier seasons. García et al. (1997) added that the Andes are controlling the precipitation regime and the isotopes composition in that region causing the fluctuation of $\delta^{18}O$ annual mean to range from -11 to -14 ‰ in stations located above 3000 m a.s.l. The LMWL for Ecuador eastern Andes was $\delta^{2}H = 8.32\ \delta^{18}O + 18.5$ ‰ (r^2=0.99, n=62) which agreed with the intercept of 18 ‰ and 14.5 ‰ for other páramos located at the western slope (Windhorst et al. 2013; Mosquera et al. 2016). Nonetheless, the behavior of the evaporation depends on which slope of the Andes the basin is located. For example, in a humid páramo in the western slope, Mosquera et al. (2013) concluded that the fractioning occurs in equilibrium since there is almost no signal of evaporation.

The studies in the Bolivian Andes carried out by Gonfiantini et al. (2001) have shown that $\delta^{18}O$ and $\delta^{2}H$ have seasonal variations with lower values in the summer rainy months with respect to the winter dry months. In addition, Vimeux et al. (2011) attributed more influence in the intra-seasonal variation to atmospheric convective processes and Fiorella (2016) supported the hypothesis of an influence of water recycling in the high elevation regions. In Guatemala and Belize (Central America), the surface water line was defined as $\delta^{2}H = 8.0\ \ \delta^{18}O + 8.7$, which is like the MWL at San Salvador of $\delta^{2}H = 8.1 \cdot \delta^{18}O + 10.9$. Lachniet and Patterson (2009) demonstrated that, $\delta^{18}O$ precipitation values decreased by 1.24 ‰ each 100 mm of increase of monthly rainfall which in consequence allowed to conclude that only two variables: distance from the Pacific Ocean and mean catchment altitude, could explain 84% of the spatial isotopic variability.

In Colombia[3], several studies on stable isotopes have been developed in different hydrologic systems and investigative techniques (IDEAM, 2013). Rodríguez (2004) developed by the first time an Isotopic

[2] Geographical location of referenced studies in this section are shown in Appendix 1: Location of the study sites on stable isotopes referenced in this section across the tropical América

[3] Geographical location of referenced studies in this section are shown in Appendix 2: Location of the study sites on stable isotopes across Colombia.

Meteoric Line for Colombia *($\delta^2H = (8.03 \pm 0.28)\ \delta^{18}O + 9.6$, r = 0.994)* based on 800 data from different studies. In this paper, it was identified that δ in the rainy season (April to June and September to November for Bogotá) is higher than in the dry one, as well as it is lower near the oceans than inner the country due to the lower temperature and altitude at the sea level. However, these highest δ values did not coincide with the highest precipitations, which could be explained by the different provenance of the rain fronts in the central part of the country (Atlantic Ocean through either the Amazon basin or the Caribbean, and, Pacific Ocean). Furthermore, a gradient of 0.5 ‰ for ^{18}O and 4 ‰ for ^{2}H every 200 m in altitude variation was found in precipitation. When analyzed the data in the surroundings of the UCRB, it was found a slope of 10. For the samples taken from the area of Nevado del Ruiz (10 km northeast of the study area), the $\delta^{18}O$ was around -13.5 and $\delta^{2}H$ was between -80 and -90 ‰.

Other investigations have been mainly concentrated in: a) the Eastern Andes Mountains to determine the source of the water in the Tota lake and Ibagué fan (Mariño-Martinez et al., 2018). The isotope concentration showed a clear variation with altitude where $\delta^{18}O$ varies from -8 to 12.6 ‰ between 2800 and 3700 m a.s.l. Castrillon et al. (2003) and Saylor et al. (2009) found that the precipitation exerts the highest effect on $\delta^{18}O$ and $\delta^{2}H$ at the IAEA GNIP stations of the surroundings of Bogotá and that the corresponding streams signature falls on the GMWL, b) In the Morroa Aquifer to analyze the residence times and recharge areas (Herrera et al. 2009), c) In the aquifers located in the alluvial valleys of the Cauca River to identify recharge areas, where a LMWL of $\delta^{2}H = 8.3\ \delta^{18}O + 13.5$ was found for the mountainous region (1500 – 2500 m a.s.l.) and $\delta^{2}H = 8.50\ (\pm 0.24)\ \delta^{18}O + 11.3\ (\pm 1.2)$ for the lowlands (<120 m a.s.l.). Two altitude gradients for $\delta^{18}O$: 0.21 and 0.07 ‰ and a value of 0.47 $\delta^{2}H$ ‰ / 100 m of elevation were also defined (Betancur and Palacio 2007; Medina et al. 2009), d) In the Ciénaga system to find the connection between groundwater and the wetland (Santa et al. 2008), e) In the Caribbean region at the sea level for groundwater exploration (Toro et al. 2009) and to study the water supply for the region (Diaz-Granados, 1988), and f) In Pereira y Dosquebradas for the construction of a hydrogeological model (Otálvaro et al. 2008).

Finally, few studies have tangentially analyzed the behavior of stable isotopes in the surroundings of the study area. CARDER (2007) carried out a hydrogeological study in the Pereira Aquifer (in a neighbor basin of the UCRB) analyzing around 63 samples from groundwater, rainfall and surface streams. The results showed an isotopic range between -9.5 ‰ and -10.7 ‰ for $\delta^{18}O$ and between -67 ‰ and -78 ‰ for $\delta^{2}H$ in the aquifers located between 50 and 253 m of depth, which are close to the GMWL. This study also defined a value of 0.1 ‰ / 100 m as the isotopic gradient for $\delta^{18}O$ and established the different recharge areas of the geologic formations (Otálvaro et al., 2008). Besides, Otálvaro et al. (2009) examined the Otún river (3700 m a.s.l.) located 4 km away from the southern boundary of the UCRB, finding isotopic values of -13.15 for $\delta^{18}O$ and -96.1 for $\delta^{2}H$. In this study, a pH value of 7.1 and a conductivity of 55 µS/cm were measured, contrasting with the values found by Ruiz (2009) which spanned from 8.71 to 9.12 and conductivity from 160 and 3410 µS/cm.

Geologically, the UCRB is located inside a regional hot-springs system (associated to the Nevado del Ruiz – Santa Isabel volcanic complex) which presents two kind of waters from meteoric origin: chloride-type and sulphate-type waters, emerging from below 2500 and above 3000 m a.s.l., respectively. Chemically, the first type shows a pH around 7.3 and ions such as K^+, Li^+, Rb^+ and high concentrations of BO^{2-}, Na^+ and Cl^- (Arango et al., 1970). The water of the hot springs also exhibited an enrichment of $\delta^{18}O$ values (about 1.5 ‰) due to the exchange of the oxygen with carbonaceous rocks. The $\delta^{2}H$ and $\delta^{18}O$ values measured at 3600 m a.s.l. were -110.7 and -15.4 ‰, respectively, and for the samples taken between 2470 and 2600 m a.s.l. they were between -95 and -96.4 ‰ and -11.6 and -12 ‰, respectively, values that remain coherent with the records measured by Federico et al. (2017) in the Ruiz Volcano area.

All the focuses previously mentioned require a detailed characterization of the isotopic signal in precipitation and in stream waters and an adequate description of the environmental setting and local and regional weather patterns since this isotopic signal varies spatially and temporally due to the depletion of heavier isotopes when the water changes of physical state. The main variations in the

isotopic concentration are caused by temperature, amount (or precipitation), continentality, altitude and weather conditions modelled by the cyclicity of the season (Craig 1961; Dansgaard 1964; Siegenthaler and Oeschger 1980; Gat 1996).

As noticed by the previous studies, the stable isotope patterns in the tropical Americas have several influencing factors, even more when analyzing intra-Andean basins as the UCRB. In basins, such as this, the air temperature influence might be masked by the influence of air masses following seasonality patterns (Bendix et al., 2008). Therefore, this research presents detailed investigations on the complexity of the spatial and temporal distribution of isotope signatures in rainfall and surface waters. Water chemistry is described as well. This will enable researchers and communities to better identify flow paths of water, contribution of precipitation from different altitudes to discharge, hydrological impacts and changes in the water cycle and potentially might help to understand future glacier melting dynamics. With this understanding, it might be possible to contribute to sustainable management and provision of water for the population in this region.

2. STUDY AREA

2.1 Location

The UCRB is in the western flank of the central branch of the Andes Mountains of Colombia, on the hills of the Nevado de Santa Isabel Volcano (NSIV), to the south of the Caldas department in the municipality of Villamaría, 10 km southwest of Nevado del Ruiz Volcano (NRV), 30 km to the southeast of the city of Manizales and 140 km northwest of Bogotá (Longitude -74.0817, Latitude 4.6097100, Altitude 2600 m a.s.l.), see Figure 1. The NSIV is not properly an active volcano but a set of domes or convex surfaces created by lava effusion in the late Tertiary and early Quaternary (Flórez, 1992). On the other hand, the NRV is the second highest peak of the Colombian Central Andes and one of the most active volcanoes of Colombia (IDEAM 2019a; Servicio Geológico Colombiano 2019). The study site extends topographically from around 2700 to 4995 m a.s.l. crossing ecosystems such as glacier, periglacial, Páramo and Andean forest. It is inside the ash and lapilli fall area of the NRV (Servicio Geológico Colombiano, 2015). The Claro river flows towards the west to the Chinchiná river, which then flows to the Cauca river and from this to the Magdalena river, the biggest basin of the country that ends in the Caribbean Sea.

The UCRB is partially located inside the protected area: “Los Nevados Natural National Park” and its size is approximately 65 km². About 1.3% of the area is glacierized (Peña, 2016) whose equilibrium line is at 4870 m a.s.l.. The recent evolution of the glaciers in the NSIV (1850 to the present) has been conditioned by a rapid melting and the influence of volcanic eruptions and ash fall from NRV. This process has been so accelerated that the glacier has turned from being a continuous ice mass to a current fragmented area composed by eight different smaller glaciers (IDEAM, 2019b). Calculations for the Santa Isabel glacier showed an area of 0.66 km^2 in 2017 (IDEAM, 2019b). One of these small glacierized tops is the so-called “Conejeras”, located in the highest altitude of the UCRB with an area of approximately 0.2 km^2 (WGMS, 2017). This glacier makes part of the inventory of the *World Glacier Monitoring Service*-WGMS and is the only one in the inner tropics being monthly monitored which provides an important input to the comprehension of the glacier development over the Andes (Ruiz, 2009; Mölg et al., 2017).

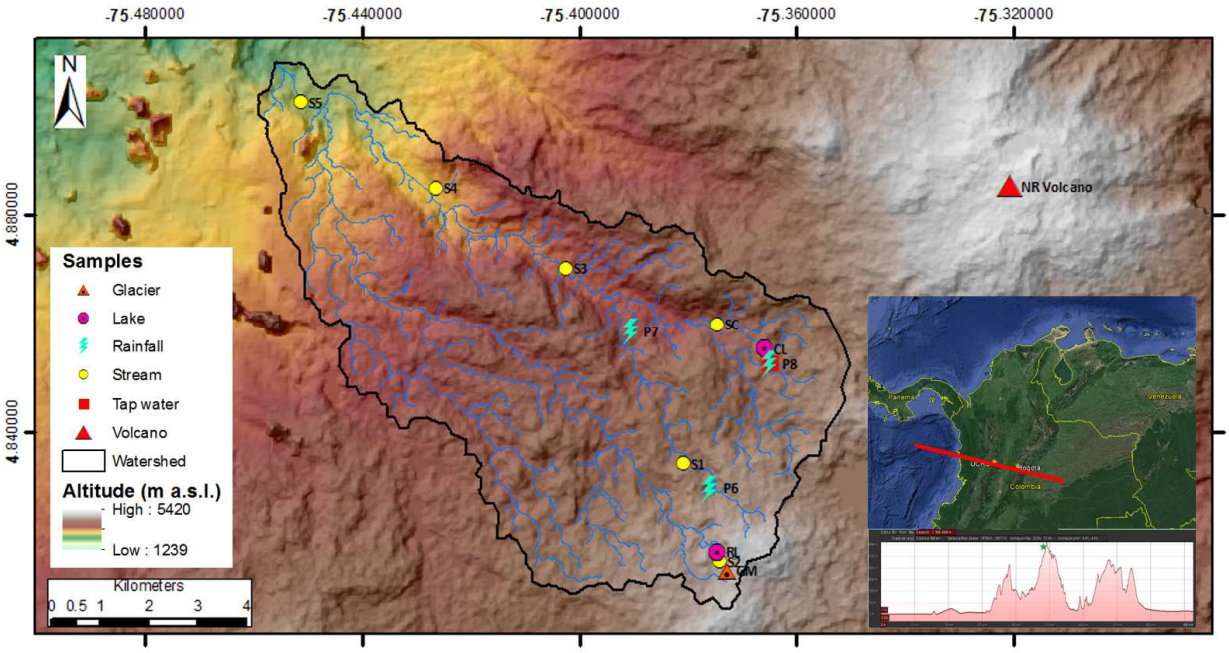

Figure 1: Location of the study site with samples by type, drainage network, Nevado del Ruiz Volcano. In detail: regional context with the northern section of South America and three branches of the Andes Mountains in Colombia. Samples renamed with short name only for visualization purposes as in Table 2.

2.2 Geology and soils

The geology of the basin has been extensively investigated by the Colombian Geological Survey (Servicio Geológico Colombiano, SGC) in the programs of cartographic recognition of the national territory. Geothermal potential and natural hazards associated to the NR and NSI volcanoes, this latter located in the upper part of the study area have motivated comprehensive research. The geology is strongly influenced by glacial and volcanic processes from the Quaternary (Figure 2). The principal composition of the volcanic bodies around NSIV and NRV area is andesitic of two pyroxenes with variations to dacite and basaltic andesites (Servicio Geológico Colombiano, 2019).

Figure 2: Glacial morphology in the surroundings of the sampling spot Stream 2 at 4500 m a.s.l.

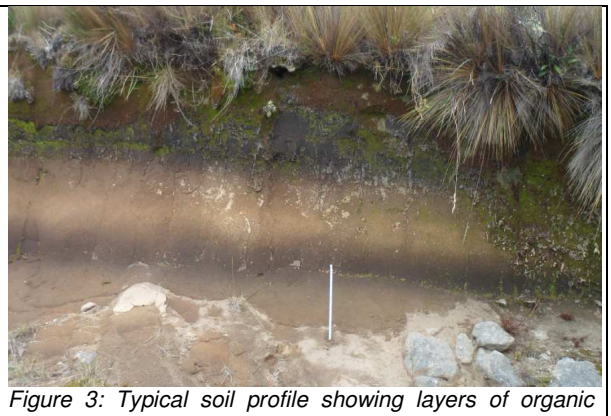

Figure 3: Typical soil profile showing layers of organic matter alternated with volcanic ashes. Scale equals 50 cm

The main geological units laying in the UCRB are: *Qg*, composed by clastic glacier deposits of lava fragments inside a sandy-clayey matrix originated during the recent glacier action, *Qfl*, formed by

volcanic mudflows constituted by ashes and boulders of volcanic and metamorphic rocks and sporadically andesitic lavas, *Qto*, non-lithified deposits composed by ash, lapilli and pumice clasts, *Qa,* effusive flows of andesitic lava which partially fill up former valleys, NgQa, andesitic flows which compose the most of the outcropping rocks and finally, *Pes,* quartz-sericite schists with mica, phyllites with intercalations of schists with chlorite and actinolite from Paleozoic age (Ingeominas, 1998). The geological map is displayed in conjunction with the hydrochemistry data in the Chapter 4 - Results. Arango et al. (1970) proposed a cross-section of the geological units of the NRV as in Figure 4 covering the UCRB and downstream until the outfall in the Cauca river. In this cross-section, the complexity of the study area is expressed with a set of fumaroles, springs and groundwater circulation paths.

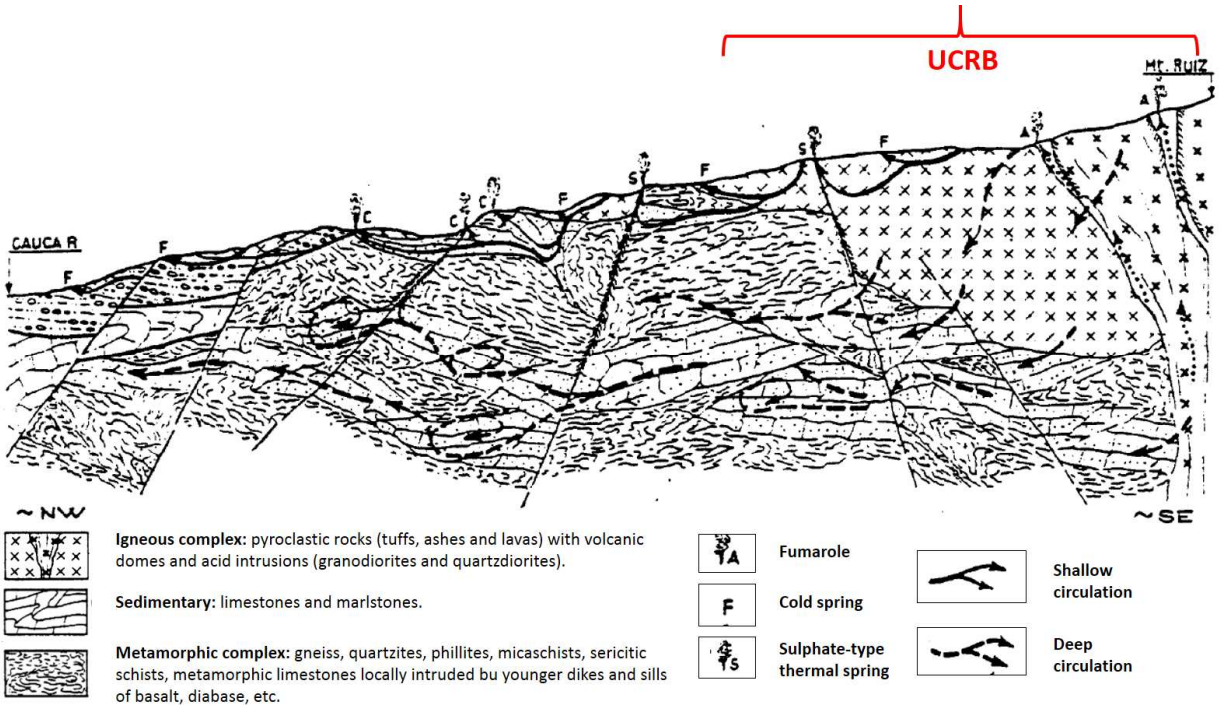

Figure 4: Cross section of the surroundings of the UCRB showing the geological units and the regional tectonic setting. Adapted from (Arango et al., 1970).

The soils are predominantly influenced by the emissions of volcanic ashes with high concentration of aluminic minerals, therefore they are acid and with low grade of evolution, causing soils of the *Entisol* type (Corpocaldas and Conservacion Internacional, 2007). On the other hand, they are rich in organic matter with alternation of sandy layers which produce well drained soils, with high cation exchange capacity, low content of calcium, magnesium and sodium and low amount of phosphorous absorbable for the plants (Prieto, 2008) (Figure 3).

2.3 Climate

The climate in the UCRB is defined not only by orographic factors but also by the displacement of the ITCZ, the trade winds coming from the Atlantic, the Pacific and the Amazon Basin (Jaramillo 2005; Gonzalez 2012) as well as a surface tropical stream called *Chocó Stream* (Poveda et al. 2006). The weather follows a bimodal behavior with two rainy and two dry seasons. The rainy periods are between April to May and October to November where the monthly average is higher in the second season (Ocampo-López, 2012).

General weather patterns in the UCRB show an annual average precipitation of 1300 mm, air temperature gradient of 0.52 °C/ 100 m and relative humidity of 83 % in average for the whole basin (Peña, 2016). For the highest areas, the mean temperature is between -2 ºC and 4 ºC with a relative humidity of 94% (WGMS, 2017). The annual evapotranspiration is between 300 and 500 mm (Ocampo-

López, 2012), with the highest values in December to January (51.7 and 52 mm) and the lowest in February and September (45.8 and 45 mm) and decreasing uphill (Universidad Nacional de Colombia, 2014a). The Conejeras glacier is more sensitive to the variability generated by the ITCZ and the ENSO dynamics than to annual variations of precipitation and air temperature (Mölg et al., 2017; WGMS, 2017). This small glacier has an elevation range between 4600 and 4900 m a.s.l. and in 2014 its average thickness was 22 m (Rabatel et al., 2018). By December 2015, based on ablation stakes, the thickness decreased by 10 meters (WGMS, 2017).

Wind direction in the study area varies across the meteorological stations and from day to night, the mean velocity is 1.2 m/s and the highest occur at higher altitudes (CARDER and IAvH, 2014). In el Cisne meteorological station, located at 4128 m a.s.l. in the eastern part of the UCRB, the average measured predominant wind direction was north, east and northeast between 2003 and 2012 (Vélez et al. 2015). According to the monthly cycle of wind direction studies by IDEAM and UPME (2017), regionally, the Central Andes of Colombia are a convergent area for air masses throughout the year. It receives winds coming from the Atlantic Ocean and the Pacific Ocean. During the first rainy season (May to June), the wind comes from the southeast and the west, while during the second rainy season (October to November) the winds come from the northeast and the west. In the first stage of the first dry season (December), winds come from the north, northeast and west and to the end of the season (March), it receives inputs from the southeast. In the second dry season (July to August) the winds come from the south and the west.

Climate change surveys in the region have suggested a strong variability in temperature and precipitation. In the higher elevations of the UCRB, the pluviometry is decreasing while heavy rainfall events are more usual (Ruiz et al. 2011). Analysis of precipitation records in two neighboring meteorological stations of the UCRB, have shown tendencies that suggest reductions in total annual rainfall between 811 and 1286 mm, by 2050 (Ruiz, 2009). On the other hand, the mean temperature has increased 0.5 °C for the period 1981-2010 compared with the historical records of 1951-1980 (Ocampo-López, 2012). The relative humidity showed reduction of 3.9 % / decade (Ruiz et al. 2008). According to Ruiz et al., (2009), if the current climate tendencies keep, the UCRB will face desiccation processes of bodies of water and swamps as well as decrease of the discharge rate.

2.4 Gauge stations

IDEAM accounts with a network of hydrological and meteorological stations distributed altitudinally to study the different high mountain ecosystems (Ceballos et al., 2006). Seven meteorological stations belonging to the IDEAM were used to obtain information about the air temperature and the precipitation (Figure 5) for each sampling point and in that way, to establish relationships between isotopic signatures and climate parameters with high precision. The stations are spread along the watershed and vary in type and measured variables, however, they measure 2 m air temperature and precipitation every 10 minutes from which daily records are calculated by IDEAM. In the Table 1, the most relevant information on the stations used in the present study is presented.

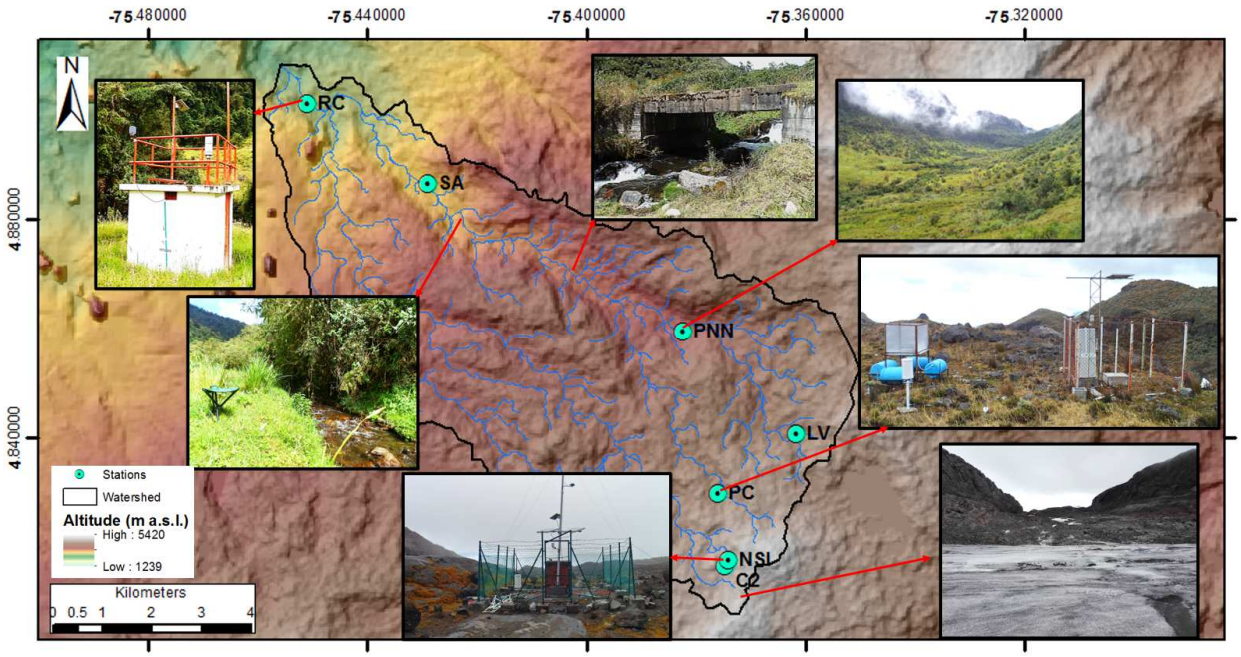

Figure 5: Location of the meteorological stations and detail on the land cover and the sampling points surroundings.

Table 1: Information on the meteorological stations located in the UCRB which are used for comparison with isotopic and chemical parameters.

Name	Short name	Long. (W)	Lat. (N)	Altitude (m a.s.l.)	Frequency of measurements and remarks
Conejeras 2	C2	-75.374444	4.816389	4699	Temperature: daily Precipitation: daily composed by NSI and PC
Nevado Santa Isabel	NSI	-75.373889	4.817500	4686	Precipitation: daily
Páramo de Conejeras	PC	-75.375833	4.829722	4413	Precipitation: daily Temperature: daily
Laguna Verde	LV	-75.361389	4.840556	4325	Precipitation: daily Temperature: daily
Parque Nacional los Nevados	PNN	-75.382222	4.859444	3637	Precipitation: daily Temperature: daily
San Antonio	SA	-75.428889	4.886389	3064	Precipitation: daily Temperature: daily
Rio Claro	RC	-75.450833	4.900833	2714	Precipitation: daily complemented from SA Temperature: daily taken from SA

3. METHODOLOGY

3.1 Field campaigns

Two different field campaigns were carried out. The first during the period January 2017 to October 2018 by the IDEAM, it was mainly focused on the periodic collection of water from three rainfall collectors and five streams. The sampling was intended to be conducted monthly, although this condition was not always fulfilled due to logistics aspects. A total of 140 samples for $\delta^{18}O$ and $\delta^{2}H$ analysis were collected, 91 for surface water spanning from January 2017 to October 2018 (Stream S1, S2, S3 and S4) and February 2017 to September 2018 (Stream 5). Besides, 49 of precipitation ranging from July 2017 to October 2018 (Precip. 6), May 2017 to October 2018 (Precip. 7) and August 2017 to September 2018 (Precip. 8).

The second campaign was conducted within the framework of this study between the 18 and the 22 June 2019, which corresponded to the end of a rainy season. Here, eight samples at the same spots as in campaign one were collected. The precipitation samples were taken from the collectors which were accumulating rainfall during approximately the last 6 months. Complementary samples from lakes, one stream, glacier and tap water for the same analysis and hydrochemistry were collected (See Table 2). During this campaign, physical parameters such as pH, conductivity and water temperature were measured, as well as the content of HCO_3^-. Furthermore, one sample of each station -eight in total- from the first campaign in the dry season of 2018 (March to April) were selected for hydrochemistry with the aim of comparing the response of the composition to contrasting weather conditions.

3.2 Sampling points

Sampling points for stable isotopes and hydrochemistry (major ions and trace elements) analysis were selected based on the location of different ecosystems, meteorological stations, and land use cover. Six spots (stream 1 to 5 and SC) for stream water along the Claro river and "Sietecuerales" tributary were sampled. Furthermore, two lakes (RL and CL), a stream draining the glacier melted water (GM), two tap water (in the Cisne hut – CTW- and in a house of the Villamaría municipality -VTW-) and three rainfall collectors were sampled (Precip. 6 to 8) (Figure 6 and Figure 7). In the Table 2 the main information is summarized. Not all the samples were considered for each kind of analysis.

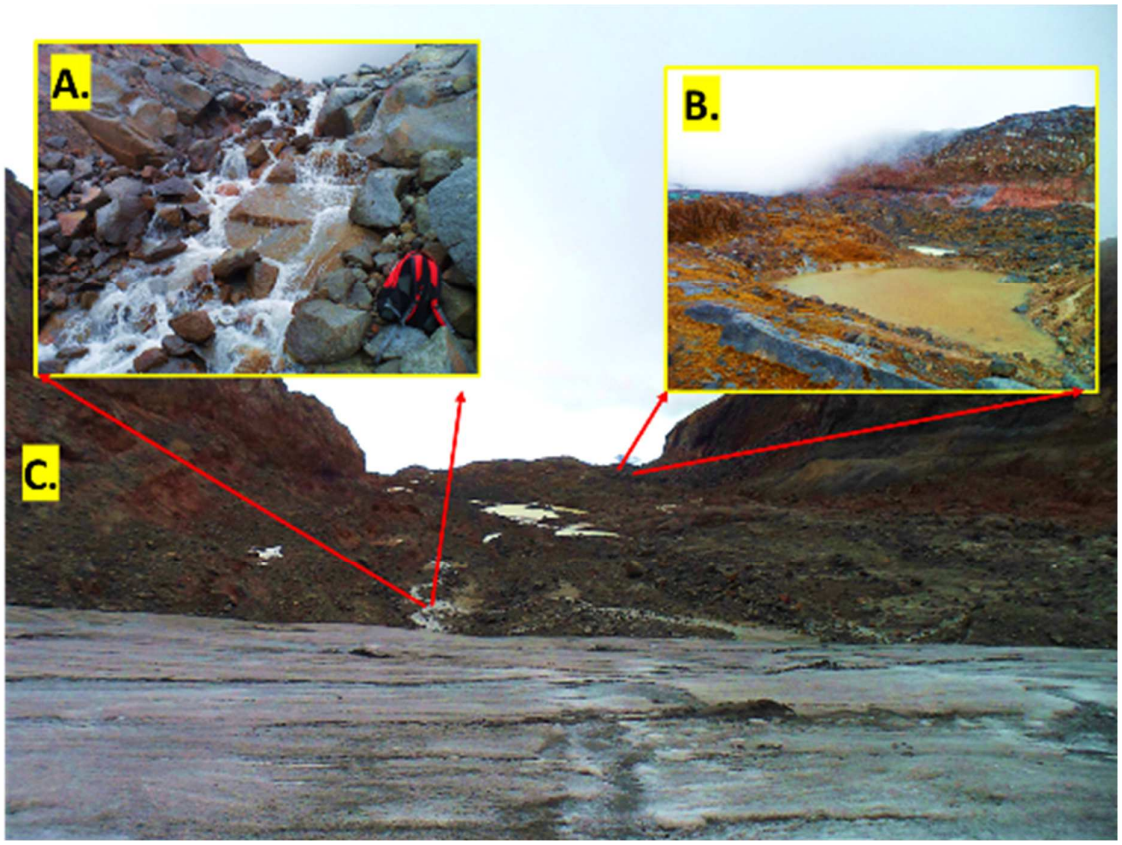

Figure 6: Conejeras glacier at 4700 m a.s.l. where sample GM was taken (C). In detail a) Stream 2 station taken from a tributary downstream of the glacier. b) RL station located in a lake 400 m downhill the Conejeras glacier.

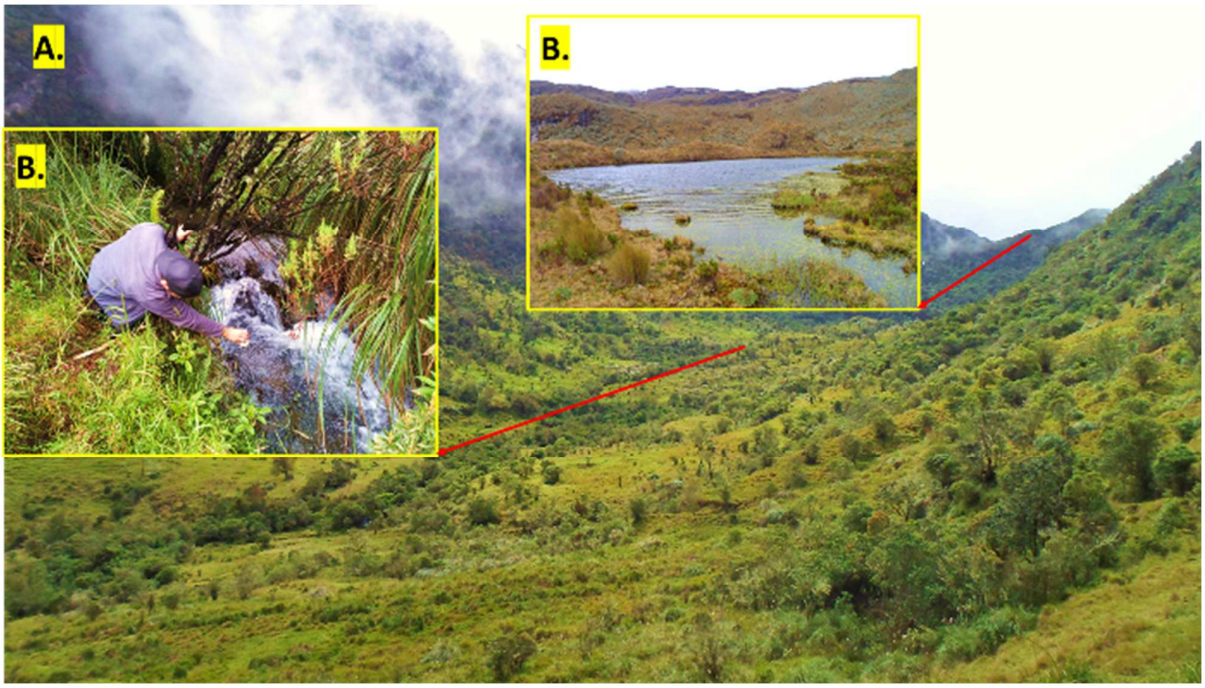

Figure 7: Sampling spot for surface water in SC (A) and CL -Cisne Lake- (B).

Table 2: Information about the samples for stable isotope composition and hydrochemistry.

Sampling point	Short	Type of water	Long. (W)	Lat. (N)	Elevation	Station used	Analysis: Num. samples
Stream 1	S1	Stream	75.3807	4.8342	4306, 4527 *	PC	Isotopes: 21 – MI: 2 – T: 2
Stream 2	S2	Stream	75.3744	4.8163	4681, 4727 *	NSI, PC, C2	Isotopes: 22 – MI: 2 – T: 2
Stream 3	S3	Stream	75.4024	4.8704	3473, 4089 *	PNN	Isotopes: 19 – MI: 2 – T: 2
Stream 4	S4	Stream	75.4263	4.8849	3084, 3364 *	SA	Isotopes: 19 – MI: 2 – T: 2
Stream 5	S5	Stream	75.4511	4,9007	2608, 3839 *	RC and SA	Isotopes: 15 – MI: 2 – T: 2
SC	SC	Stream	75.3747	4.8601	3775	PNN	Isotopes: 1 – MI: 1 – T: 1
Precip. 6	P6	Rainfall	75.3758	4.8297	4413	PC	Isotopes: 14 – MI: 2 – T: 2
Precip. 7	P7	Rainfall	75.3905	4.8586	3635	PNN	Isotopes: 25 – MI: 2 – T: 2
Precip. 8	P8	Rainfall	75.3650	4.8526	4128	LV	Isotopes: 13 – MI: 2 – T: 2
RL	RL	Lake	75.3739	4.8186	4675	NSI, PC, C2	Isotopes: 1 – MI: 1 – T: 1
CL	CL	Lake	75.3658	4.5853	4100	LV	Isotopes: 1 – MI: 1 – T: 1
GM	GM	Glacier	75.3727	4.8142	4764	NSI, PC, C2	Isotopes: 1 – MI: 1 – T: 1
CTW	CTW	Tap water	75.3650	4.8526	4128		Isotopes: 1 – MI: 1 – T: 1
VTW	VTW	Tap water	75.5198	4.8601	3775		Isotopes: 1 – MI: 1 – T: 1

* Mean catchment elevation
MI – Major Ions
T – Trace elements

Concerning the surface water sampling sites, the sampling point Stream 1 is located on a small creek that is draining the páramo predominantly at altitudes in between 4306 and 4947 m a.s.l., constituted by a small portion of the Conejeras glacier. This point gathers the highest part of the Claro River catchment. The sampling point Stream 2 collects waters resulting from the melting of the Conejeras glacier at altitudes between 4681 and 4947 m a.s.l. which belongs to the upper catchment area of a tributary creek which belongs to the Quebrada Juntas sub-basin and joins the Claro River 350 m upstream of the sampling point Stream 5. Stream 3 is in the Claro river and contains the water draining from altitudes between 3473 and 4947 m a.s.l. which includes also the water from Stream 1. This site is located close to a series of hot springs which probably flow towards Stream 3, 4 and SC. Stream 4 collects the surface water from the San Antonio sub-basin which is mainly representing a small patch of the Andean Forest ecosystem at altitudes between 3084 and 3276 m a.s.l. SC belongs to a stream draining a sub-basin of sub-páramo. Finally, Stream 5, located in the Claro river channel, is the outlet and collects the water from the whole basin, including the ones of the sampling points SC, Stream 1, 2, 3 and 4, it spans from 2702 to 4947 m a.s.l. GM was taken from the melting water of the Conejeras

glacier and VTW from the tap water of the Villamaría municipality, where the end users of the water from the basin are.

The rainfall collector Precip. 6 was located next to the meteorological station “Páramo de Conejeras”, Precip. 7 and Precip. 8 were in the backyards of “La Cueva hut” and “El Cisne hut”, respectively (Figure 8 and Figure 9).

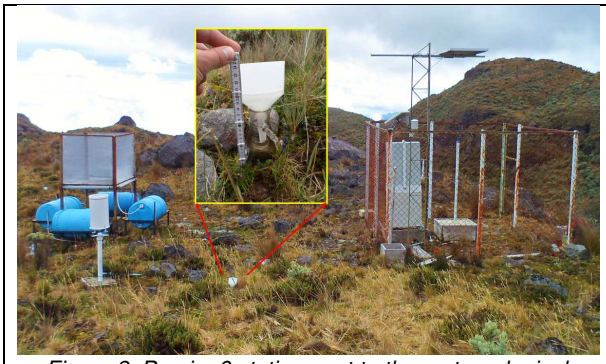

Figure 8: Precip. 6 station next to the meteorological station Páramo de Conejeras.

Figure 9: Collector Erlenmeyer used to store the precipitation in Precip. 8 next to the Cisne hut.

3.3 Stable isotopes

A total of 152 samples were analyzed: 140 from the first campaign and 12 from the second. During the first 5 months of the sampling, the rainfall collectors samples were put liquid vaseline in to avoid evaporation, but a possible contamination of the water was suspected by the laboratory and therefore this method was suspended. The surface water samples were collected directly from the streams or lakes by using a beaker to fill up the bottles (Figure 10). The rainfall samplers consisted of an Erlenmeyer of 500 ml for Precip. 6 and a glass beaker of 500 ml for Precip. 7 and 8, all accounted with a funnel with coarse porosity filter plate which was intended to prevent evaporation as well. The collector in Precip. 6 was partially broken between January 31 and May 18, 2018, therefore, possible leakages might have occurred in the sample of May 18, 2018. These collectors were placed and stabilized on the ground. A possible obstruction of the rainfall input by surrounding grass might have been happened during the sampling. The samples were stored in amber or plastic bottles depending on the availability, sealed with black tape (only in the second campaign) labeled and transported to the laboratory in Bogotá and Darmstadt.

The samples of the first campaign were analyzed in the Stable Isotopes laboratory of the SGC. The samples taken between January 2017 and February 2018 were analyzed with an “Off Axis Integrated Cavity Output Spectroscopy (OA - ICOS)” Los Gatos Research Laser Spectrometer (DTL 100) with autosampler injection. The stable isotope values are calibrated against VSMOW2 and SLAP2. The software employed to process the samples was “LIMS for lasers 2015 Version 10.096”. The standard deviation given by the laboratory is smaller than 2.0 ‰ and 0.30 ‰ for δ^2H and $\delta^{18}O$, respectively. The samples of the second campaign were analyzed in the Stable Isotopes laboratory of the Technische Universität of Darmstadt (TUD) with a Picarro L2130-i device. These samples were not included for seasonal analysis since their collectors presented signs of leaks during the collection period.

A comparative analysis between the isotope standards of the two laboratories involved in this project was developed. The TUD stable isotopes laboratory analyzed the isotope standards provided by the SGC of Colombia: W-35 Mar, W-36 Lago, W-37 DIWB and W-38 Nevado. The results were compared with the ones provided by the SGC laboratory. This comparison was carried out to find the deviation from isotopic values between campaign 1 and 2. The results are shown in the Table 3. The variation in the isotope standards ranges from 0.34 to 1.30 ‰ for $\delta^{18}O$ and from 0 to 0.3 ‰ for δ^2H. Standard deviations are lower than 0.27 in all the results.

Table 3: Results of the analysis of the SGC standards by the TUD.

Sample	Lab.	δ^2H (‰)	Std. Dev.	$\delta^{18}O$ (‰)	Std. Dev.
W-36 Lake	**TUD**	-35.40	0.39	-3.48	0.05
	SGC	-36.70	1.41	-3.48	0.27
W-37 DIWB*	**TUD**	-67.24	0.21	-9.95	0.03
	SGC	-66.90	1.57	-9.61	0.24
W-35 Sea	**TUD**	3.46	0.04	0.12	0.02
	SGC	2.80		0.31	
W-38 Glacier	**TUD**	-129.46	0.07	-17.44	0.02
	SGC	-128.80		-17.59	

*DIWB: Deionized water of Bogotá

All stable isotopes values and the deuterium excess (d-excess) or intercept, given in this study are expressed as δ values in per mil (‰) as first proposed by Dansgaard (1964) in the equation 1:

$$d = \delta D - 8\delta^{18}O \qquad (1)$$

For the estimation of the altitude effect in surface water the mean catchment altitude was calculated using ArcGIS. Two different approaches were considered to calculate the $\delta^{18}O$ variation across altitude in stream waters: in the first, only the samples from the months coinciding in all the stations were selected to reduce the bias given by the seasonality effect probably more expressed in some stations than in others, while in the second, all the samples were considered. In both, the gradient is drawn from the arithmetic average of the chosen values. The samples RL, CL, SC and GM belonging to the additional surface water of the second campaign are plotted but not considered for calculations. d-excess of the sample belonging to the August 13, 2018 in Stream 4 was discarded due to inconsistency of its results.

On the other hand, the altitude effect in precipitation samples considered all the samples taken for each station and their linear regression was calculated based on the precipitation-weighted means. Samples from the second campaign were discarded due to uncertainty in the precipitation amount. Therefore, different number of samples were taken into account due to the irregularity in the sampling for some stations, then, 13, 24 and 12 samples were considered for Precip. 6, 7 and 8, respectively. The altitude is always given in m a.s.l..

Isotope values and d-values for November 11, 15 and December 1 in Precip. 7 station were averaged to only one value and placed on the November 22 to facilitate the comparison in the seasonality effect plots.

3.4 Field parameters

Electrical conductivity, temperature of the water and pH where measured for all samples taken during the second campaign using a Multiparameter sensor (Orion star A329). The HCO_3^- (ppm) content was measured with a handheld alkalinity colorimeter for fresh water (Hanna HI 775) (Figure 11). Conductivity and pH for the samples Stream 3, 4 and 5 and VTW were measured in the laboratory.

Figure 10: Samples taken for major ions, trace elements and stable isotopes in Stream 1. In frames, group of samples once in the laboratory of the TU Darmstadt.

Figure 11: Measuring of physic-chemical parameters and sampling on the Conejeras glacier for the sample "Glacier melting – GM". In detail, colorimeter alkalinity meter and multiparameter for pH, conductivity and temperature.

Samples CTW, Stream 1 and 2 and VTW were additionally determined the HCO_3^- content in the laboratory by titration method; with 10, 5, 7.5 and 5 ml of sample, respectively, with HCl concentrated at 1 mmol/L. Furthermore, $CaCO_3$ values measured in the field for the samples P6, P7, P8, RL, CL, and GM with low pH and electrical conductivity were close or inside the accuracy range of the device (± 5 ppm), showing uncertainty in the results and causing an ion balance error higher than 5%. In consequence, these samples were measured the HCO_3^- by titration, with unsuccessful results. To cope with the high ion balance error, samples with positive error such CL, RL were added some of the HCO_3^- concentration necessary to equal the ions and cations sum to zero. On the other hand, samples with negative error such as GM, P6 and P8 were subtracted HCO_3^- to balance the charges in the same way. In the case of P7, despite all the HCO_3^- was subtracted, the sample continued with a negative error, reason why the initial HCO3- concentration was left.

Samples from the first campaign were not determined for these parameters due to a too less amount of water remaining after chemical analysis. Therefore, the HCO_3^- was calculated based on the missing value to equal the charges to zero.

3.5 Hydrochemistry

Fourteen samples for major ions and trace elements were collected during the second field campaign (rainy) and eight more were selected from the dry season of 2018. From the latter, samples S2, 3, 4, 5, P7 and 8 belong to March 2018, S1 to April and P6 to May 2018. For trace element analysis, samples were filtered through a 45 µm Polyvinylidene difluoride membrane during the sampling. Later, 100 µl of HNO_3 were added to the samples (H_2O diluted 1:2) to prevent cations to change the oxidation state. In the laboratory, 7 to 8 ml of sample were extracted, and 30 µl of HNO_3 were added for those of the first campaign which had not been acidified previously. Samples for major ions were filtered in the same way before analysis only if a big load of suspended sediments was observed. The analysis for major ions was performed in the laboratory of the TUD with a Metrohm 882 Compact IC Plus device. For trace elements, the Analytik Jena Plasma Quant MS Elite device for inductively coupled plasma mass spectrometry (ICP-MS) was used as well. For the ICP-MS, five multielement-standards were used: 2, 5, 10, 20, 50 and 100 ppb and four more internal standards of Sc 45; Y 89; In 115; Bi 209. Concentrations of HCO_3^- for the first campaign and for the samples RL, CL, P6, P8 and GM were calculated based on the missing value of anions necessary to equal the error of the ion balance to zero. On the latter, see details on the adjustments in chapter 3.4.

Comparisons between major ions and trace elements concentrations in precipitation and surface water sampled in the dry season of March 2018 and the rainy season of June 2019 were made. The mineralization of the major ion samples was calculated for the two periods by summing up the concentration of mmol/L of each element. Results were contrasted with the guideline values for drinking water quality of the World Health Organization (2018). This guidelines coincide in most of the parameters with the "Law 2115" of 2007 (MMADT-MPS, 2007) issued by the Ministry of Environment of Colombia in which the "permitted limits for drinking water" are set .

A historic record of ash emission from the Nevado del Ruiz Volcano was provided by the Sismologic and Vulcanologic Observatory of Manizales (Observatorio Vulcanológico y Sismológico de Manizales, OVSM) of the SGC. These events correspond to the ascent of lava domes (Servicio Geológico Colombiano, 2018a). The records have date and local time of emission, height of the ash column over the crater and direction of expulsion. A total of 313 ash emission events were registered from December 1, 2016 to June 25, 2019. Due to the position of the UCRB with respect to the volcano, only the events with ash emission direction to the south and the west were considered as potential influencers on the hydrochemistry of the waters, a total of 120 events were extracted.

3.6 Data processing

3.6.1. Weather records adjustment

Data of daily air temperature and precipitation from seven meteorological stations in the UCRB were obtained from IDEAM´s internal database. Several of the loggers in the stations have experienced technical problems since their installation (Morán-Tejeda et al. 2018). However, the majority showed to be continuous and complete. For the cases where long gaps in the parameter records were observed, an identification and correction or adjustment of the data series was carried out.

Anomalous temperature values (values around -25° C) in station Conejeras 2 were ignored since they were not consistent. Also, this station did not account with precipitation, therefore its records for 2017 were taken from PC and for 2018 from NSI due to their proximity. RC station was not measuring temperature; hence, the temperature was taken from SA and its precipitation from January 1, 2017 to November 11, 2017 was copied from SA station. The temperature of the sampling intervals was calculated by finding the average of the mean daily temperature values. This included the value of one day after the sampling of the previous sample and the day when the current sample was taken. Accumulated precipitation values were acquired by summing up the daily amounts for the period between samples.

Daily precipitation and air temperature data was obtained for the period January 1, 2017 to November 1, 2018 for stream water samples and May 5, 2017 to November 1, 2018 for precipitation samples. A hydrological year for generic seasonal comparisons was defined from June 1 to May 31 according to different studies by IDEAM and other researchers in Colombia (UPME and Universidad Nacional de Colombia 2000; IDEAM 2010a).

Relationships between δ^2H and d-excess of accumulated precipitation against mean daily temperature were evaluated for precipitation stations by establishing regressions lines where the dependent variables were represented in the Y axis.

3.6.2. Global Network of Isotopes in Precipitation (GNIP)

Data sets from the Global Network of Isotopes in Precipitation (GNIP) were obtained for the stations Apartadó (boundary between the Caribbean and Pacific region), Maicao (Caribbean region), Albania (Central Andes southwards of UCRB) and Bogotá (Eastern branch of the Andes). Their LMWL, monthly averages, long term and annual values were used to be compared with the data of Precip. 6, 7 and 8 belonging to the study site. Additionally, average of δ^{18}O values for the stations El Hato (Eastern branch

of the Andes near Bogotá), La Galvicia and Tona (Eastern branch of the Andes), La Maria (Central Andes) and El Tesoro (Caribbean region) were downloaded as well to compare against altitude. More details of the data set can be seen in the results chapter. Data were accessed on the June 15, 2019 at WMO/IAEA WISER database (https://nucleus.iaea.org/wiser/index.aspx). The location of the stations across Colombia is provided in the map of the Appendix 2.

3.6.3. Local Meteoric Water Lines (LMWL)

Linear regressions for surface water and LMWL´s for precipitation were calculated. For the first, the so called Ordinary Least Squares Regression (OLSR) has been widely used to determine the correlation between δ^2H and δ^{18}O in precipitation, however, it gives equal weight to all data points regardless of the precipitation amount. To reduce the effect of small precipitation samples and potential evaporation during sampling, the LMWL for precipitation was calculated based on the precipitation-weighted least square regression approach (PWLSR) (Hughes and Crawford, 2012).

The provided equations are taken originally from IAEA (1992), although they can be found and referenced in Hughes and Crawford (2012), Crawford et al. (2014) and Michelsen et al. (2015) as well.

The slope of the OLSR, the intercept and its standard deviation are given by the equation 2, 3 and 4, respectively:

$$a = \frac{\sum xy - \sum x \sum y/n}{\Sigma x^2 - (\Sigma x)^2/n} \quad (2)$$

$$b = \frac{\Sigma y}{n} - a\frac{\Sigma x}{n} = \bar{y} - a\bar{x} \quad (3)$$

$$\sigma_a = \frac{S_{y,x}}{\left(\sum x^2 - \frac{(\sum x)^2}{n}\right)^{0.5}} \quad (4)$$

Weighted mean values were calculated according to IAEA (1992) as in equation 5:

$$\bar{\delta}_w = \frac{\Sigma_{i=1}^{n} P_i \, \delta_i}{\Sigma_{i=1}^{n} P_i} \quad (5)$$

Where *Pi* and δi are the precipitation of the sampled period and its δ value.

The PWLSR is calculated as δ^2H = a δ^{18}O + b, where the values a and b in the line of best fit $y_i = ax_i + b$, are calculated as equation 6 and 7:

$$a = \frac{\sum_{i=1}^{n} p_i y_i x_i - \frac{\sum_{i=1}^{n} p_i x_i \sum_{i=1}^{n} p_i y_i}{\sum p_i}}{\sum_{i=1}^{n} p_i x_i^2 - \frac{(\sum_{i=1}^{n} p_i x_i)^2}{\sum p_i}} \quad (6)$$

$$b = \frac{\sum_{i=1}^{n} p_i y_i - a\sum_{i=1}^{n} p_i x_i}{\sum p_i} \quad (7)$$

All plots are presented with the Global Meteoric Water Line (GMWL) defined by (Craig, 1961) as in equation 8:

$$\delta^2 H = 8\delta^{18}\mathrm{O} + 10 \quad (8)$$

The parameters described above can be calculated by the free and open software LOCAL METEORIC WATER LINE FREEWARE (Crawford et al., 2014) based on Hughes and Crawford (2012) and IAEA (1992).

4. RESULTS

In the following sections, the results of the comparison between stable isotopes signatures and d-excess with meteorological parameters such as air temperature and precipitation are presented. The results obtained from the about 18 months of sampling in the study site (Appendix **3**) are also compared against data from GNIP of both local and regional studies. Detailed descriptions of the meteorological conditions are provided given the variability of the temperature and precipitation for each different station and the availability of high resolution temporal and spatial records which permit more comprehensive correlations. Although hydrochemistry is not the focus of this research, results of major ions (Appendix **4**) and trace elements concentrations (Appendix **5**) are also shown and described. Rare-earth elements analysis were performed within the framework of this research (Appendix **6**) even though they were not interpreted.

The overlap of the results with the geological map shows that all the stream samples are grouped in the unit Qto (ash, lapilli and pumice clasts) except by RL which probably lies on Qg (glacier deposits of lava). In consequence, Burbano and Figueroa (2015); González-Duque et al. (2015); Stewart et al., (2006); USGS, (2015), among others, concluded that there is a direct correlation between volcanic emissions (Appendix **7**) and hydrochemistry, thus, volcanic ash emissions events are compared with the sample campaign results. The integration of all the available data will allow further comparisons and interpretations and will give the opportunity to more inter-disciplinary discussions for future research to be developed.

4.1 Field parameters

Field parameters (temperature, pH, electrical conductivity and alkalinity) were measured during the second field campaign. Table 4 shows the parameters measured on surface water and precipitation. Temperature ranges from 0.5 in the stream water coming from the glacier melting to 13.6 °C in the Cisne lake. pH in stream water tend to be slightly basic, ranging from 7.16 to 8.00, excepting the glacier melting sample (5.8). The pH resulting in the outlet point of the watershed is 7.35 (Stream 5). Values in precipitation range from 4.54 to 5.63, similar to lakes (RL and CL). These values would be very close to the acid rain category, which according to Seinfeld and Pandis (2006) is when pH < 5.6. Samples P6 P7, P8, CL and RL from rainy season are around the acid rain limit.

Electrical conductivity values range from 10 to 230 µS/cm, being lower than 50 µS/cm in precipitation and lakes and in the samples of the upper part of the basin (GM, S1 and S2), sample in the outlet has 200 µS/cm. Streams below 4089 m a.s.l. present values over 140 µS/cm. Alkalinity, same as conductivity is low or inside the uncertainty of the device in surface water of the upper basin and precipitation samples while values can be higher than 40 ppm in samples lower than 4089 m a.s.l.

Table 4: Field parameters: temperature, pH, electrical conductivity and alkalinity measured in the field during the campaign between the 18 and the 21 June, 2019.

Sample	Type of water	Temperature (°C)	pH	Conductivity (µS/cm)	Alk (mg/L $CaCO_3$) *
Stream 1	Stream	4.9	7.70	26.0	11
Stream 2	Stream	1.3	7.43	14.0	4
Stream 3	Stream	NM	7.27	200	40
Stream 4	Stream	NM	7.16	146.9	43
Stream 5	Stream	NM	7.35	200.3	34
SC	Stream	8.3	8.00	230.2	39
Precip. 6	Rainfall	9.0	5.63	18.8	3
Precip. 7	Rainfall	10.5	4.54	36.3	4

Precip. 8	Rainfall	10.4	5.61	19.6	3
RL	Lake	4.2	5.40	10.5	NM
CL	Lake	13.6	5.38	26.9	0
GM	Glacier	0.5	5.81	22.8	8
CTW	Tap water	8.9	6.74	32.5	NM
VTW	Tap water	NM	7.04	104.4	NM

NM – not measured but recalculated later.
*Values as measured in the field. However, values were adjusted due to uncertainty of the device.

4.2 Stable isotopes

A total of 152 samples were collected: 52 (34%) of the samples were rain and 100 (66%) were surface water containing streams, glacier water and lakes. For the entire dataset, isotope values for precipitation range from -19.89 to -2.41 ‰ and -150.4 to -5.2 ‰ for $\delta^{18}O$ and $\delta^{2}H$, respectively and d-excess values range from -5 to 24 ‰. In surface water, values vary from -23.77 to -8.57 ‰ and -165.4 to -61.7 ‰ for $\delta^{18}O$ and $\delta^{2}H$, respectively, and d-excess values range from -11 to 26 ‰.

4.2.1. Seasonality effect

Plots comparing $\delta^{2}H$, $\delta^{18}O$, d-excess, air temperature and precipitation over the entire sampling period for precipitation and surface water samples are presented in this chapter. The graphs for precipitation display the isotope concentration of periods ranging from the next day of a sampling date till the next taken sample date. On the other hand, the graphs for surface water are showing the results for snapshot samples that only represent the isotope concentration in a punctual spot and for the corresponding date.

Figure 12 shows precipitation and temperature data taken from “Páramo de Conejeras” meteorological station compared with isotope values of station Precip. 6. The chart suggests that there are no real dry periods but a general decrease of days with rain and amounts per event throughout the year. The dry season extends from July to March with a short period of precipitation in October to November. Higher values appear in the period May to June 2017 and April to August 2018. Mean daily air temperature are between 2 and 6 °C along the year and the coldest month is January. The coldest temperatures were registered in January, March and July.

Isotope values vary between -19.89 and -9.49 ‰ and between -150.4 to -61.9 ‰ for $\delta^{18}O$ and $\delta^{2}H$, respectively, and the precipitation-weighted mean d-excess is 12 ‰ (5 ‰ in January and 18 ‰ in July, both 2018). Lowest values of isotopes are present in May, after a very wet period beginning at the end of March. Higher values coincide with partially dry periods of August 2017 and February and September 2018. Sampling periods tend to be comparable except for the sample of May 2018 whose collection period was around 3.5 months.

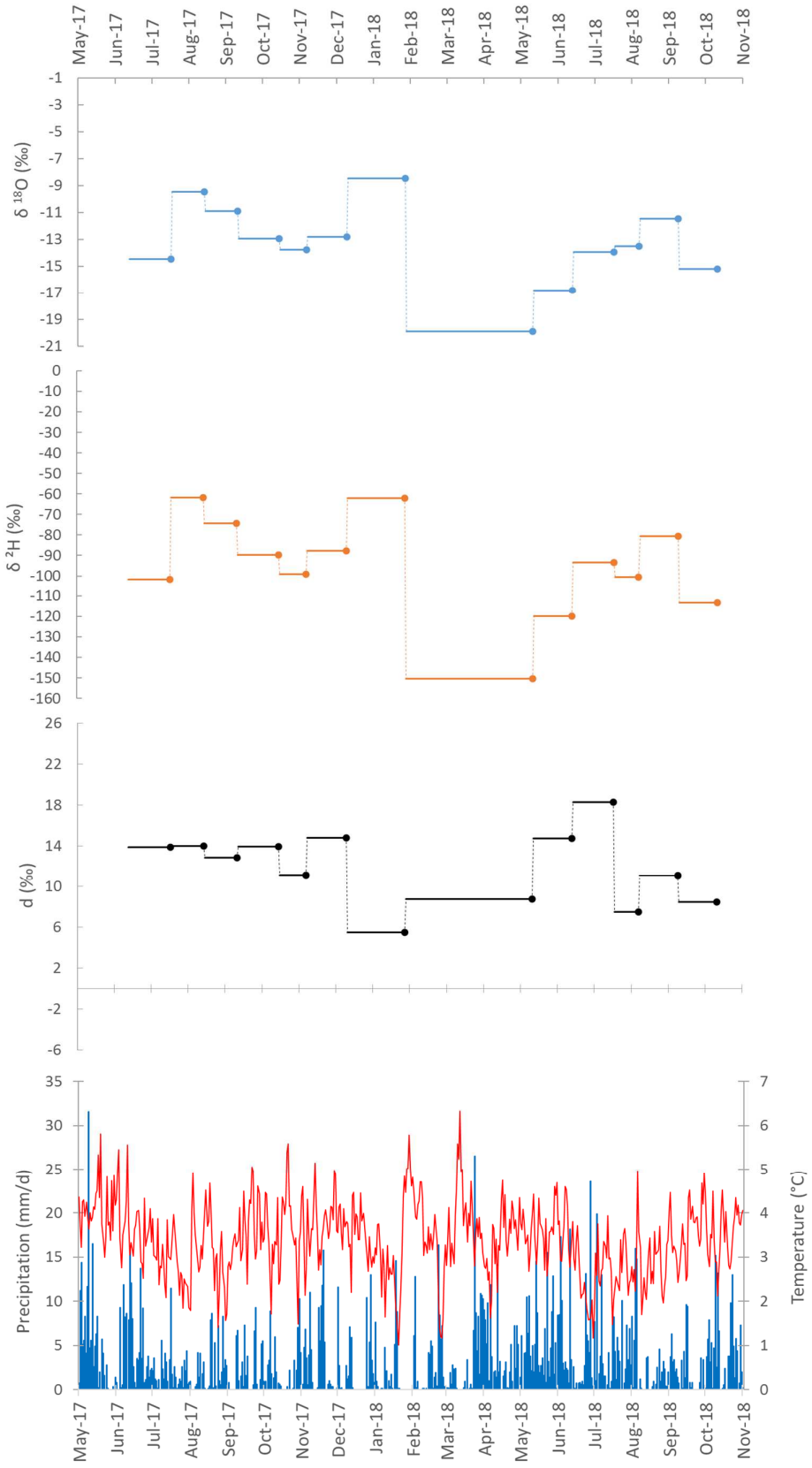

Figure 12: Variation of the δ^2H, $\delta^{18}O$ and d-excess values in station Precip. 6 compared with daily accumulated precipitation and daily mean air temperature values for the period 01.05.2017 to 01.11.2018.

In Figure 13, variation of the δ^2H, $\delta^{18}O$ and d-excess values in station Precip. 7 is shown against the "PNN" meteorological station records. Precipitation shows clear tendencies of rainy periods in May 2017, between April and August 2018 and scattered rainfall in September to October 2017. The driest months are January, February and August. Mean daily air temperature remains around 8 and 10 °C, extreme values above 11.5 °C were recorded in May to June 2017 and 2018. Coldest periods were in January and February 2018 with temperatures around 6°C. The period between April 14 and May 19 was not recorded.

Isotope values vary between -19.00 ‰ and -2.41 ‰ and between -140.9 ‰ and -5.2 ‰ for $\delta^{18}O$ and δ^2H, respectively, and a precipitation-weighted mean of d-excess is 9 ‰ with unweighted values of -5 in May and 18 ‰ in February. Most negative values of isotopes are clearly appearing in June both years: in 2017, four days after daily precipitations of 12 and 13 mm / day and in 2018, after a period of sustained rainfall over the month. On the other hand, most positive ones coincide with dry periods of August 2017 and February and March 2018 commonly with low accumulated precipitation values (<10 mm). Unweighted values vary between the lowest d-excess value of -5 ‰ in the hot days of June 2017 and the highest value of 18 ‰ in the cold month of February and October 2018.

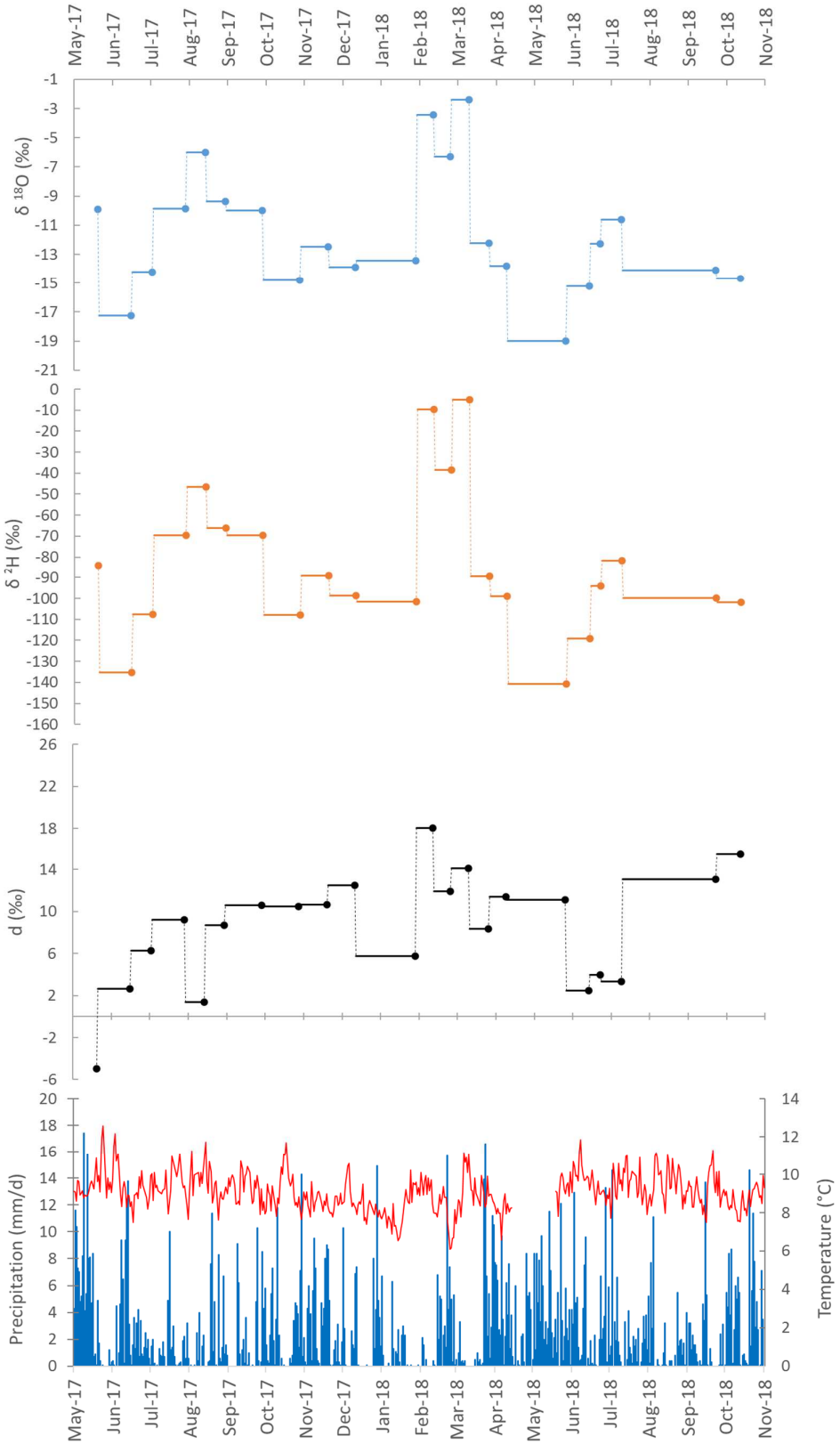

Figure 13: Variation of the δ^2H, $\delta^{18}O$ and d-excess values in Precip. 7 station compared with daily accumulated precipitation and daily mean air temperature values for the period 01.05.2017 to 01.11.2018.

Variation of the δ^2H, $\delta^{18}O$ and d-excess values of station Precip. 8 are shown in the Figure 14. The meteorological station “Laguna Verde” presents a marked seasonality contrast between the rainy period (June to August) of 2018 and the one in 2017 where the latter extends no longer than July followed by a dry time until November, accounting with sporadic rain events. Mean daily air temperatures are between around 3 to 5 °C. Colder periods are during July and August of both years and warmer periods for May, September to January 2017 and September to November 2018. High temperatures were recorded during the dry periods: May and November 2017 and February and March 2018.

Isotope values vary between -19.42 ‰ and -6.75 and between -147.2 ‰ and -38.3 for $\delta^{18}O$ and δ^2H, respectively, and a precipitation-weighted mean of d-excess is 10 ‰ with unweighted values of -1 ‰ in November 2017 and 24 ‰ in February 2018. Lowest values of isotopes are clearly appearing in May while highest match with dry periods of March 2018. Depleted isotope values are registered after a wet period in April 2018. Other rainy months during the whole sampling campaign such November 2017 and June to August 2018 did not present depleted isotope values as low as May 2018 despite the highest amount of rain.

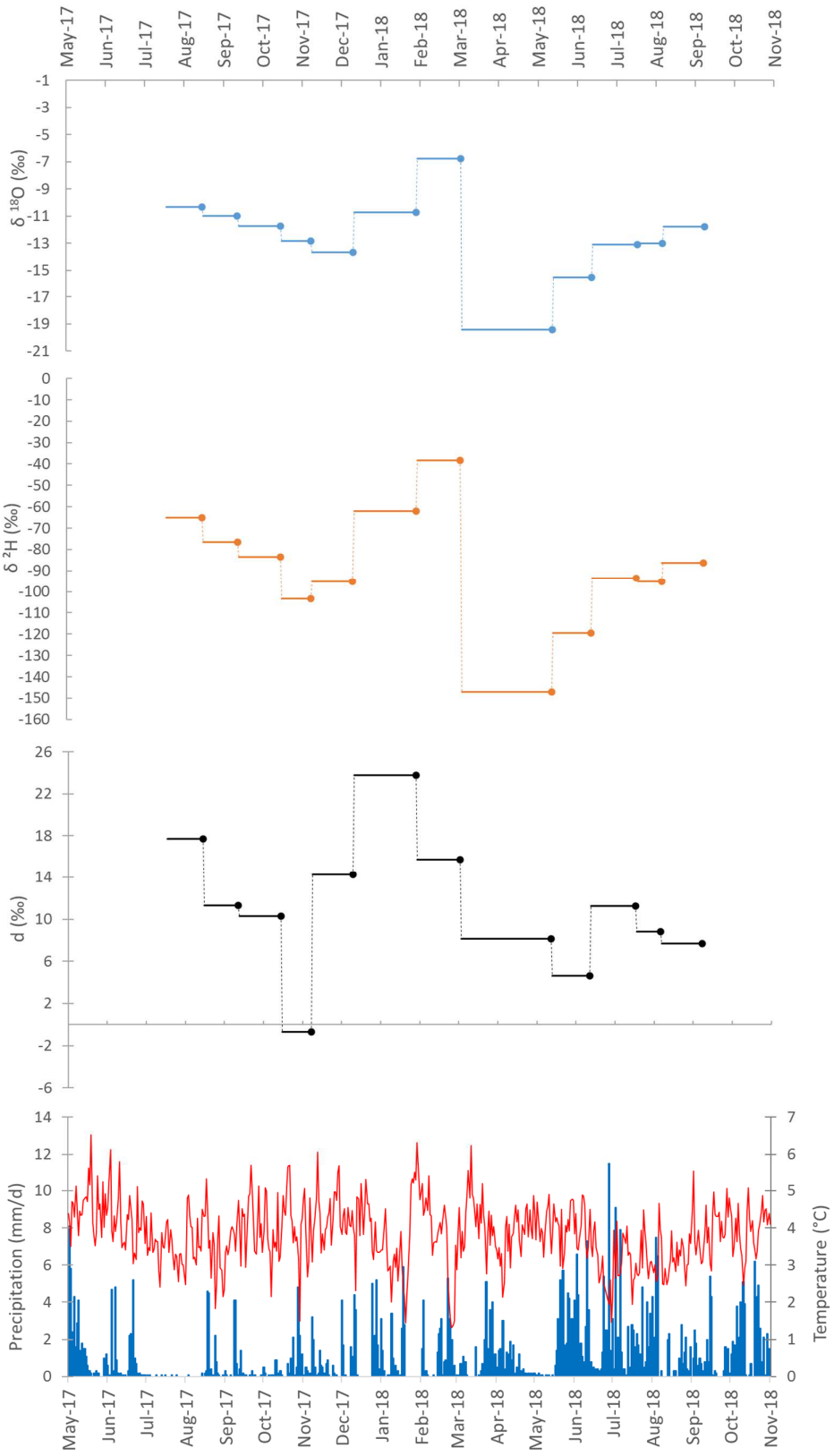

Figure 14: Variation of the δ^2H, $\delta^{18}O$ and d-excess values in station Precip. 8 compared with daily accumulated precipitation and daily mean air temperature values for the period 01.05.2017 to 01.11.2018.

Variation of the δ^2H, $\delta^{18}O$ and d-excess values in station Stream 1 are shown in Figure 15. Two clear rainy seasons are evident from around March to July 2017 and March to August 2018. Air temperatures range between 2 and 5 °C with higher records in May and October (2017) and February and September (2018). Lowest values of $\delta^{18}O$ and δ^2H are -21.85 and -150.5 ‰ in May 2017, respectively. These latter, occur in a snapshot sample seven days later than the highest rainfall event of the whole evaluated period (31.6 mm). Highest values are -10.8 ‰ and -84.9 ‰ in March 2017 and 2018, respectively for $\delta^{18}O$ and δ^2H which in turn are included in the driest period of the year.

Isotopic concentrations remain strongly constant for the period August to December 2017, time when the precipitation continues approximately without large variations. d-excess presents an abrupt change from -4 to 24 ‰ in the period April to May 2017. The positive peak coincides with the most negative value of δ^2H and $\delta^{18}O$. Inverse tendency between d-excess and isotopic signatures is also visible for the period April to May 2018. d-excess also remains constant between June and October 2017 although its most negative (-3 ‰) value is in January and March 2017 and the most positive (24 and 25 ‰) is in June and November 2017 matching with the dry and wet seasons, respectively.

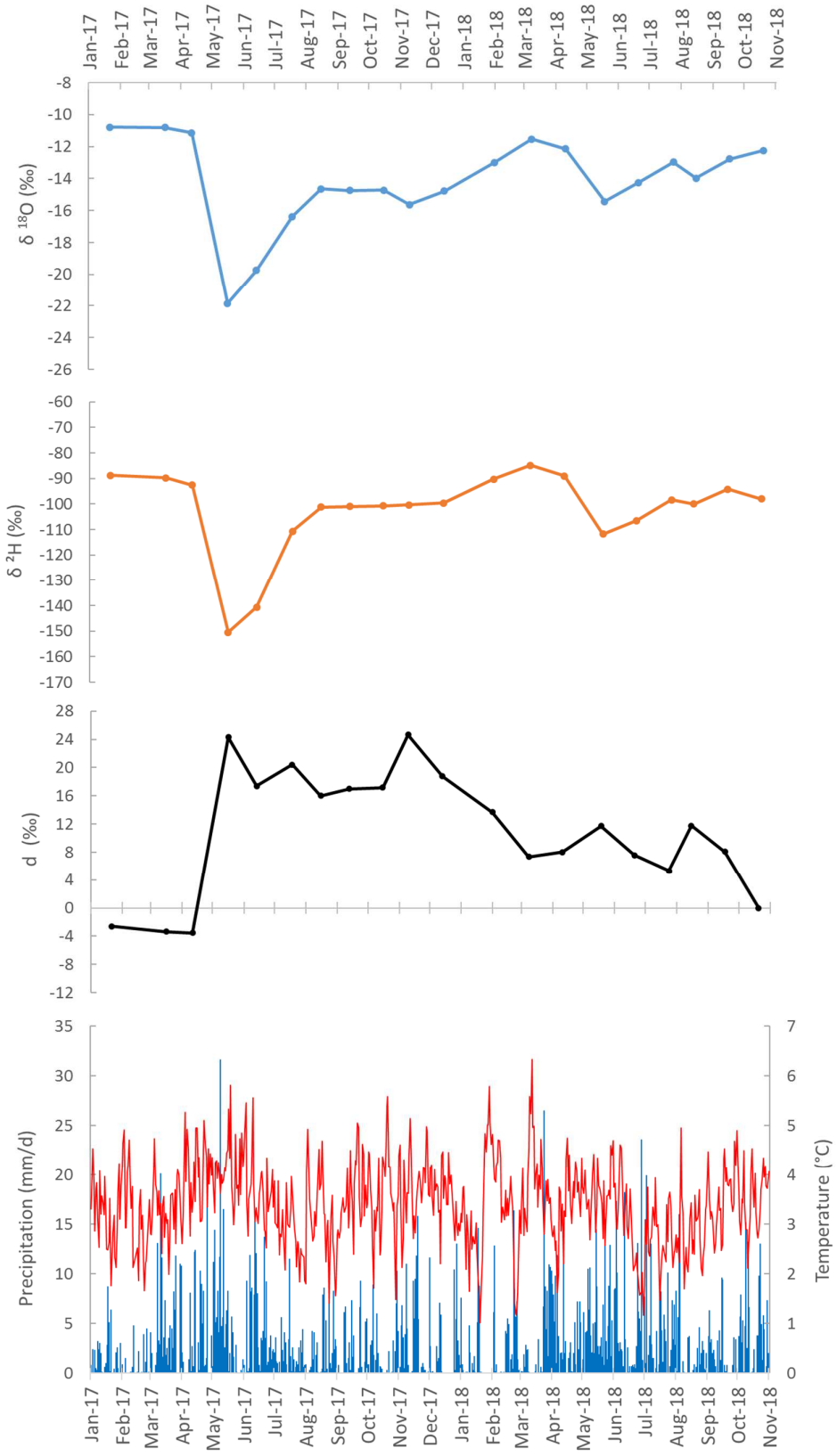

Figure 15: Variation of the δ^2H, $\delta^{18}O$ and d-excess values in station Stream 1 compared with daily accumulated precipitation and daily mean air temperature values for the period 01.01.2017 to 01.11.2018.

Variation of the $\delta^{2}H$, $\delta^{18}O$ and d-excess values in station Stream 2 are presented in Figure 16. Precipitation records of 2017 were taken from PC station, 1.4 km away and 267 m lower from the sampling point, therefore there might be bias in the correlation between the weather conditions of this year with the isotopic signature. Rainy season spans from March to July 2017 and from April to August 2018. There is no defined dry period but one with less precipitation from July 2017 to April 2018 presenting short rainy intervals in November 2017 and February 2018. Temperature indicates ranges between 0 and 2 °C with maximum peaks in February of both years and minimum values in January, February and August.

The most negative $\delta^{18}O$ and $\delta^{2}H$ values were measured for May (2017 and 2018) with -23.77 and - 165.4 ‰, respectively. These extreme values have a correspondence of one week later with the same high rainfall event of 2017 described for Stream 1 and with a continuous rainy period in 2018. The most positive values are observed in January, August, March and July with the highest peak in January 2017 with a value of -8.57 ‰ for $\delta^{18}O$ and -79.4 ‰ for $\delta^{2}H$. During the previous days to this sample, the precipitation did not surpass the 2.3 mm / day, reaffirming as one of the driest period of the year. d-excess values range from -11 (dry period) to 25 ‰ (rainy period).

Samples RL and GM taken 200 m downstream and 243 m upstream from the sampling site Stream 2 in June 2019, presented values of -14.84 and -14.84 ‰ of $\delta^{18}O$ and -105.9 and -111.9 ‰ of $\delta^{2}H$, respectively. GM correlates with alike values of Stream 1 and 2 of June 2018.

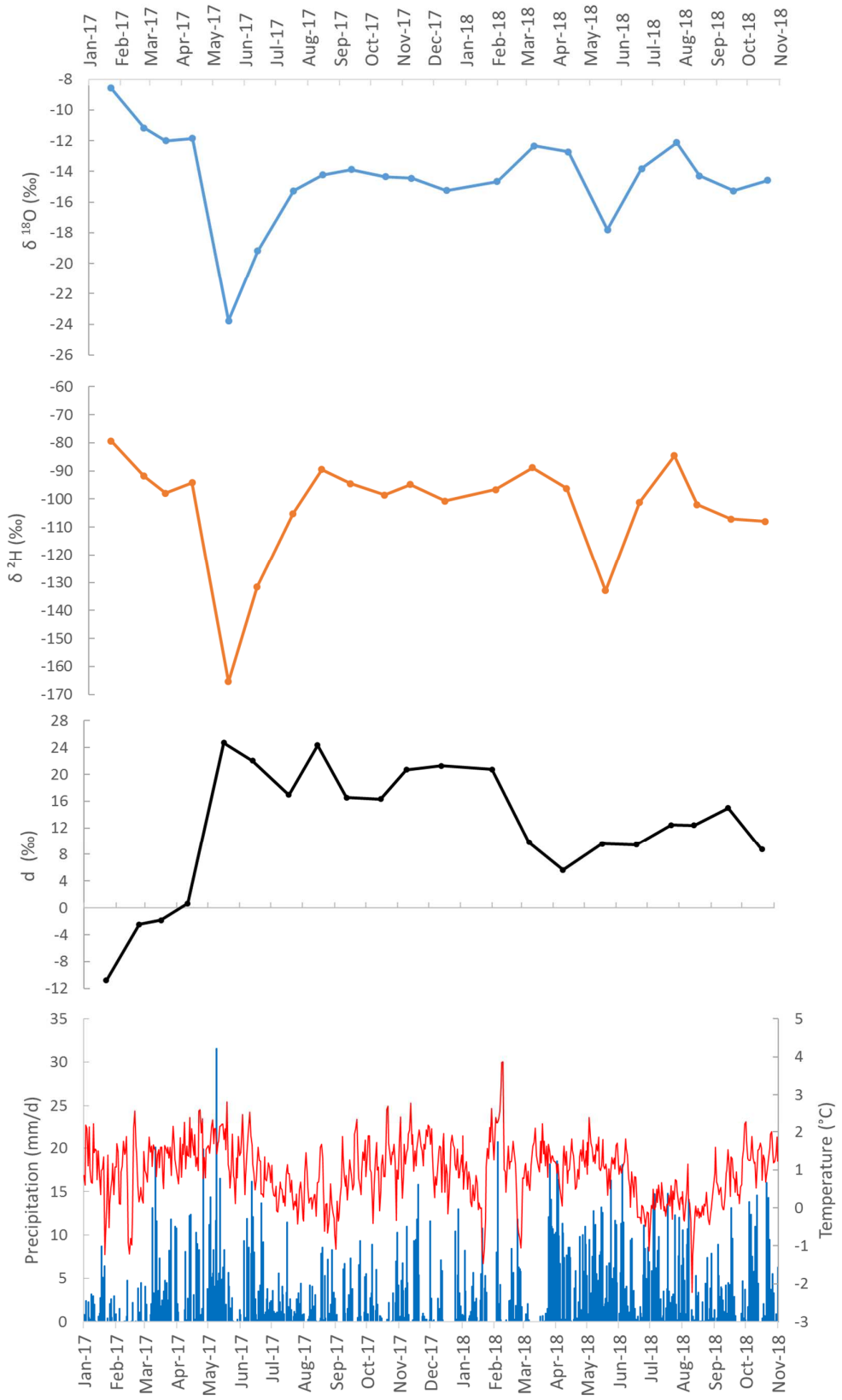

Figure 16:Variation of the δ^2H, $\delta^{18}O$ and d-excess values in station Stream 2 compared with daily accumulated precipitation and daily mean air temperature values for the period 01.01.2017 to 01.11.2018.

Variation of the δ^2H, $\delta^{18}O$ and d-excess values in station Stream 3 are shown in Figure 17. Isotope values of δ^2H and $\delta^{18}O$ remain with little contrast through the sampling period where values show variations that are lower than 3 ‰ and 12 ‰, respectively. Lowest values were measured in May though, when the rainiest time of the year takes place. Highest values are present in January, March and September 2017 during a dry season characterized by constant rain events. The sample "SC" taken in June 2019 from upstream the station Stream 3 indicates a value of -14.74 ‰ for $\delta^{18}O$ and - 106.6 for δ^2H, which is close to the value for S3 in June of the previous year. Expected positive δ^2H and $\delta^{18}O$ values for the typical dry period between December and March were not visible for this station in none of the two analyzed years.

Furthermore, the sample "CL" taken from a lake 325 m away from Precip. 8 and upstream of SC and Stream 3 showed values of -11.92 ‰ for $\delta^{18}O$ and -94.0 ‰ for δ^2H. These values would be comparable with the meteorological records of "Laguna Verde" station. On the other hand, d-excess shows a progressive and continuous increase from 6 ‰ in January to 20 ‰ in May.

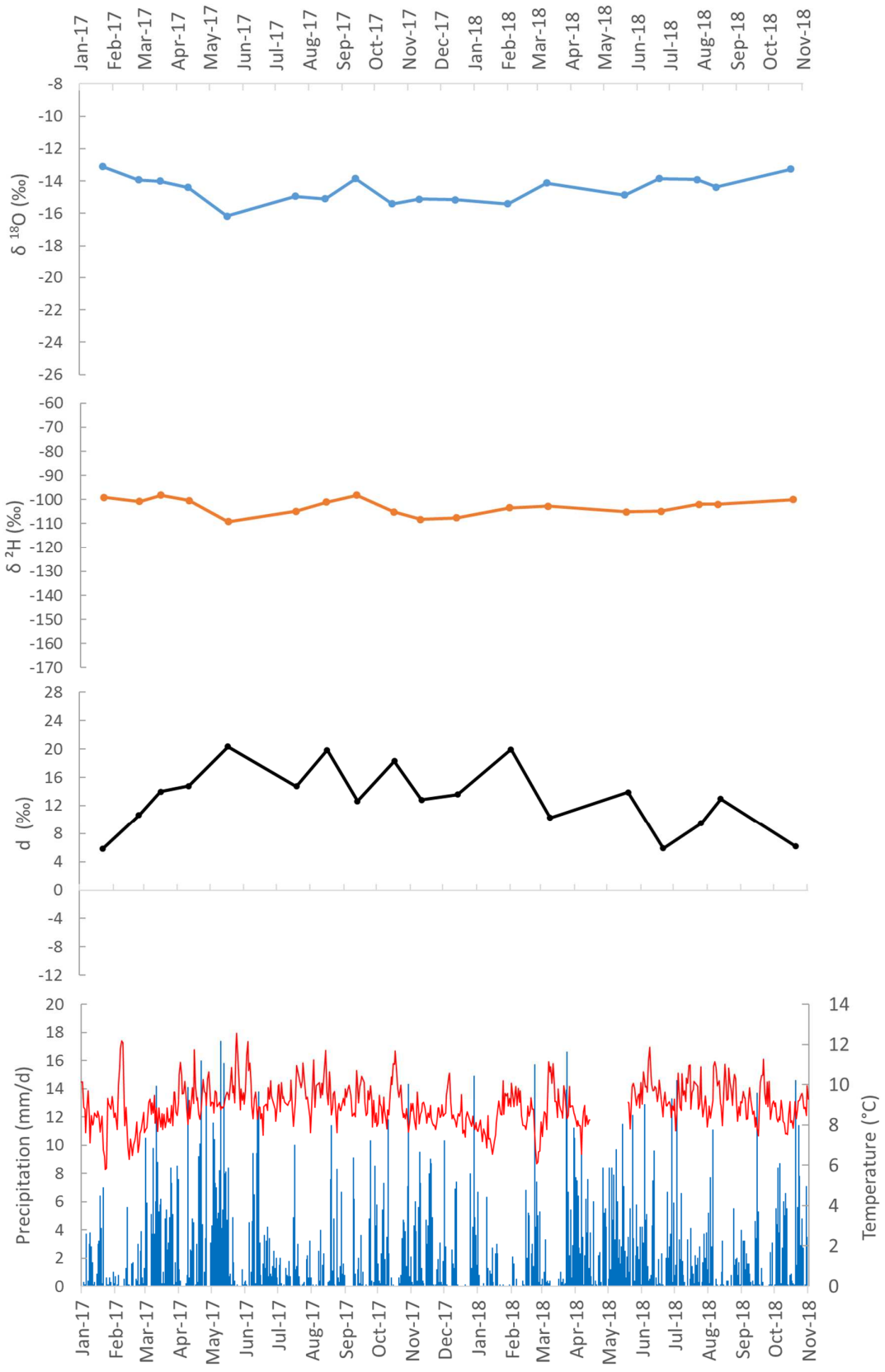

Figure 17: Variation of the δ^2H, $\delta^{18}O$ and d-excess values in station Stream 3 compared with daily accumulated precipitation and daily mean air temperature values for the period 01.01.2017 to 01.11.2018.

Variation of the $\delta^{2}H$, $\delta^{18}O$ and d-excess values in station Stream 4 are presented in Figure 18. Records of station San Antonio indicate a rainy season from March to June, October to December 2017 and April to May 2018. The mean daily air temperature ranges from 9 to 15 °C although there is a sudden fall from June to September 2018 when the average is around 10° C. The coldest month was January and the hottest June and September. In general, the temperature of 2018 was in average warmer than in 2017. Values for the sample of August 2018 were discarded due to its inconsistency.

$\delta^{18}O$ and $\delta^{2}H$ values varies slightly over time, keeping values around -14 ‰ and -98 ‰, respectively. No clear strong patterns of variation through meteorological parameters are identified. However, more positive values of isotopes are observed in dry months such as January to March (2017) and August to October (2018). Despite that March is generally a dry month, and enriched isotope values would be expected, during the March 2018 there was a short rainy period that caused a depletion up to -13.34 and -99.6 ‰ for $\delta^{18}O$ and $\delta^{2}H$, respectively.

d-excess presents the lower values during the period August and December (1 ‰) while the highest are from January to April (22 ‰).

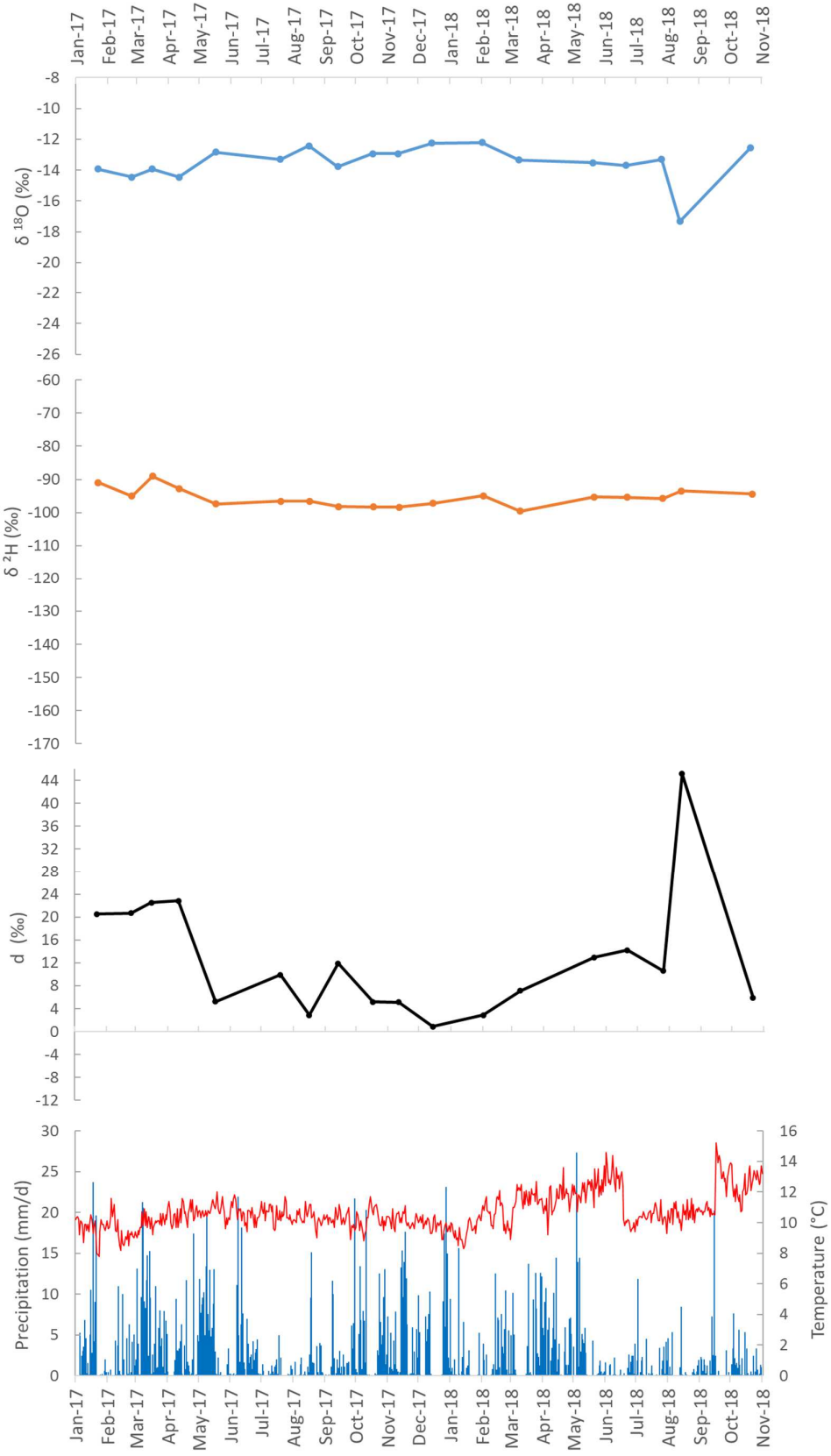

Figure 18: Variation of the δ^2H, $\delta^{18}O$ and d-excess values in station Stream 4 compared with daily accumulated precipitation and daily mean air temperature values for the period 01.01.2017 to 01.11.2018.

Variation of the $\delta^{2}H$, $\delta^{18}O$ and d-excess values at station Stream 5 is presented in Figure 19. Meteorological parameters are mostly complemented from San Antonio station. $\delta^{18}O$ and $\delta^{2}H$ values show low variation, from -89.87 to -100.28 ‰ and -12.6 to -15.1 ‰, respectively, except for the sample of February 2018, which presents extreme more positive anomalies (-8.66 and -61.8 ‰). This sample corresponds with a very dry period in the beginning of the 2018, which additionally contrast with the surrounding samples belonging to rainy periods. The most negative isotope values are in the rainy period of March 2017. The ranges in this station match with the ones in Stream 4. d-excess show a decrease from 26 ‰ (February to March) to 3 ‰ (May to August) which does not seem to correspond to any clear tendency in the temperature or the precipitation.

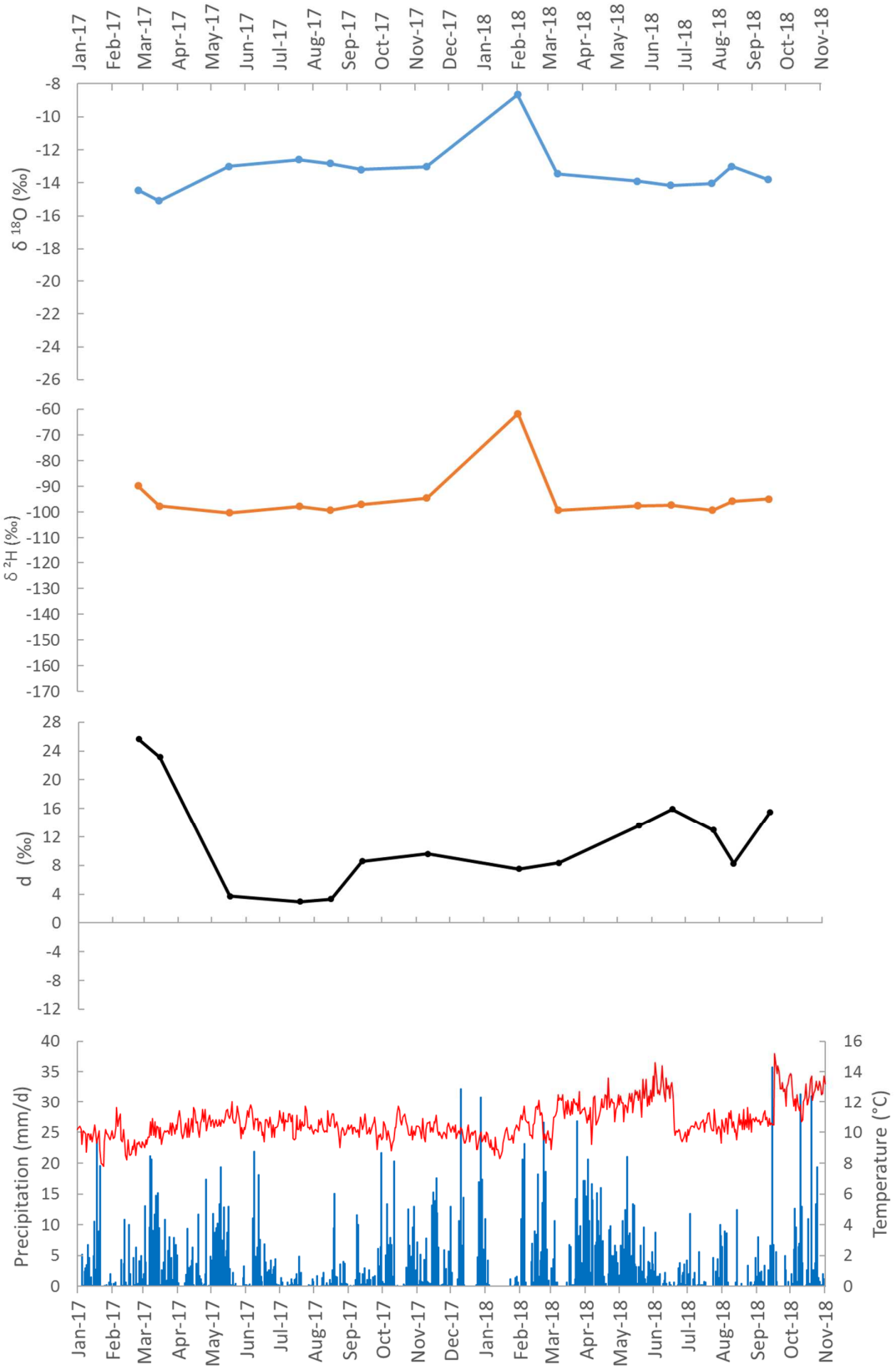

Figure 19: Variation of the $\delta^{2}H$, $\delta^{18}O$ and d-excess values in station Stream 5 compared with daily accumulated precipitation and daily mean air temperature values for the period 01.01.2017 to 01.11.2018.

A comparison of the seasonal variability in $\delta^{18}O$ average values between Bogotá (1971 to 2016) located at 2600 m a.s.l. and the measured precipitation samples in the stations of the study area (2017 to 2018) is presented in Figure 20. The comparison is conducted for one hydrological year ranging from June to May. This correlation aim at contrasting the available isotopic data for each month at the study site (Central Colombian Andes) with the monthly means of a long-term period at Bogotá (Eastern Colombian Andes). Tendencies follow a bi-modal behavior well synchronized with the regional weather patterns (similar in Bogotá as in the UCRB), varying on a seasonal basis (Rodríguez, 2004). Generally, the maxima occur between January and March for Bogotá and February and March for P 6, 7 and 8. A secondary peak is reached in August in all the assessed stations. The $\delta^{18}O$ decreases towards their minimum in the period May to June with a secondary peak centered in November. Precip. 6 station shows the peak for February one month in advance with respect to the other stations. Values of Bogotá present higher $\delta^{18}O$ when compared to the P6 and P8 of the UCRB.

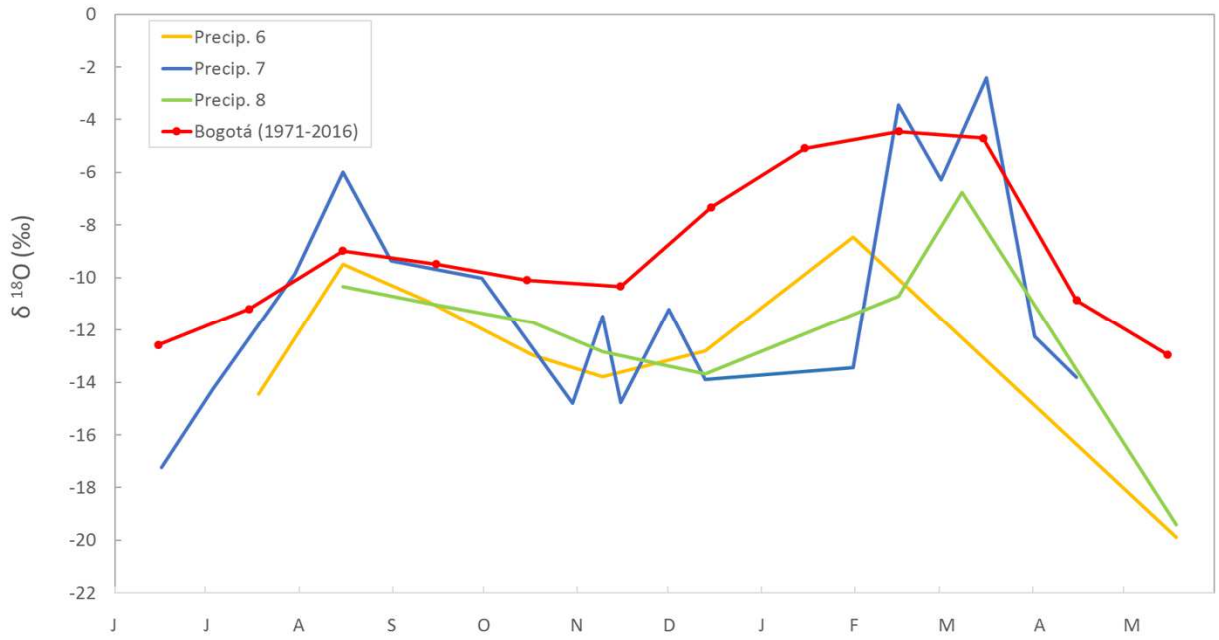

Figure 20: $\delta^{18}O$ behavior in the precipitation stations (6, 7 and 8) of the study area over one hydrological year (June to May) compared with monthly average $\delta^{18}O$ values of Bogotá (Eastern Cordillera) for the period 1971 – 2016. Data accessed from (IAEA, 2019)

4.2.2. Altitude effect

Altitude effect for precipitation is shown in Figure 21. All the precipitation samples collected are plotted and the gradient line is a linear regression calculated based on the precipitation-weighted mean (PWM) values of each station. Consequently, different number of samples were taken into account for each station due to the irregularity in the sampling, then, 13, 24 and 12 samples were considered for Precip. 6, 7 and 8, respectively. Considering the three stations, the $\delta^{18}O$ weighted mean in the two lower stations is around -13.2 ‰, where P7 is even more negative than P8, causing a non-continuous gradient, leading to an inverse gradient between P7 and P8. Precipitation-weighted mean for P6 is -15.08 ‰. On the whole, a variation of -0.36 ‰ of $\delta^{18}O$ / 100 m was determined with a R^2 value of 0.5, stating a moderate positive correlation between the line and the points.

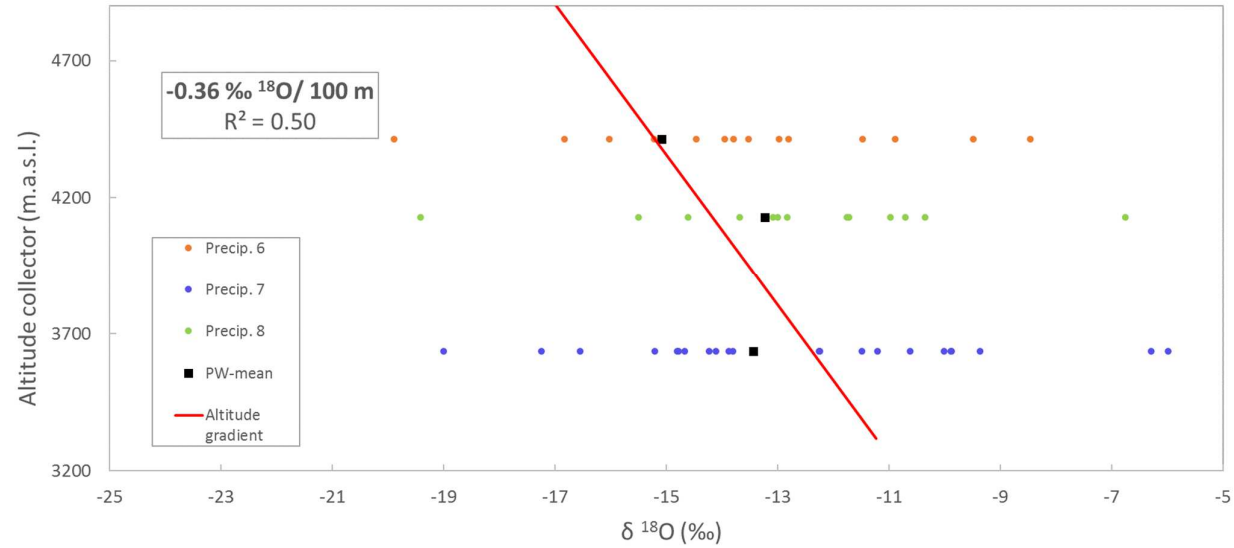

Figure 21: $\delta^{18}O$ altitude gradient for the total of the precipitation samples. Gradient line calculated based on the precipitation-weighted mean value of each station (black square).

An altitude effect for stream water is shown in Figure 22. All the collected samples are represented in the plot but the ones of the second campaign are not considered for calculations. Range of $\delta^{18}O$ spread generally increases with altitude (see 4.2.1) towards lower values.

A gradient of -0.14 ‰ / 100 m was calculated for the average of all the stream samples taken in each station, the R^2= 0.5 indicates a moderate positive correlation. On the other hand, a gradient of -0.18 ‰ / 100 m was calculated based on the arithmetic average of only the months coinciding in the 5 stations (in total 12 samples for each station between February 2017 and September 2018) to try to eliminate the seasonality effects, R^2 value is however 0.62.

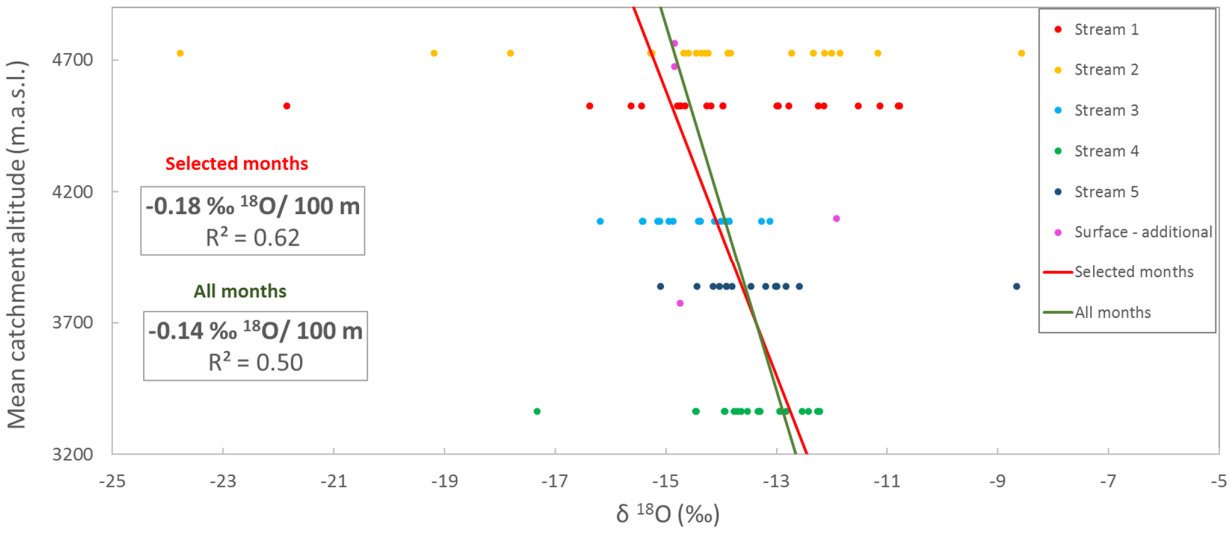

Figure 22: $\delta^{18}O$ altitude gradient for all the surface water samples. Red line shows the gradient considering the samples whose month coincided in all the stations. Green line shows the gradient with all the sampled months. The lines are drawn based on the arithmetic means.

A comparison between precipitation-weighted $\delta^{18}O$ values for stations located at different altitudes of Colombia is presented in Figure 23. Table 5 shows main information of the selected stations. More depleted ^{18}O values are observed as the altitude (meter above the sea level) increases. The pattern

follows a discontinuous linear tendency from 0 to approximately 4700 m a.s.l. with a breaking point in a fringe between 2000 and 2500 m a.s.l.. In the western part of the country, the $\delta^{18}O$ values lie below the linear regression and show more negative (< -12 ‰) values than in the east (> -12 ‰). This occurs even when the altitudes in the east are higher and therefore a more depleted value would be expected. The ^{18}O consequently, are less depleted for the samples located in the mountainous areas of the Eastern branch of the Andes (La Galvicia, Bogotá, Tona and El Hato) when compared to the stations located at the Western branch of the Andes (La Maria and Albania). From this observation, it can be noticed that two different slopes can be drawn: one from the sea level to about 2500 m a.s.l., and the second, a lower one from 2100 upwards.

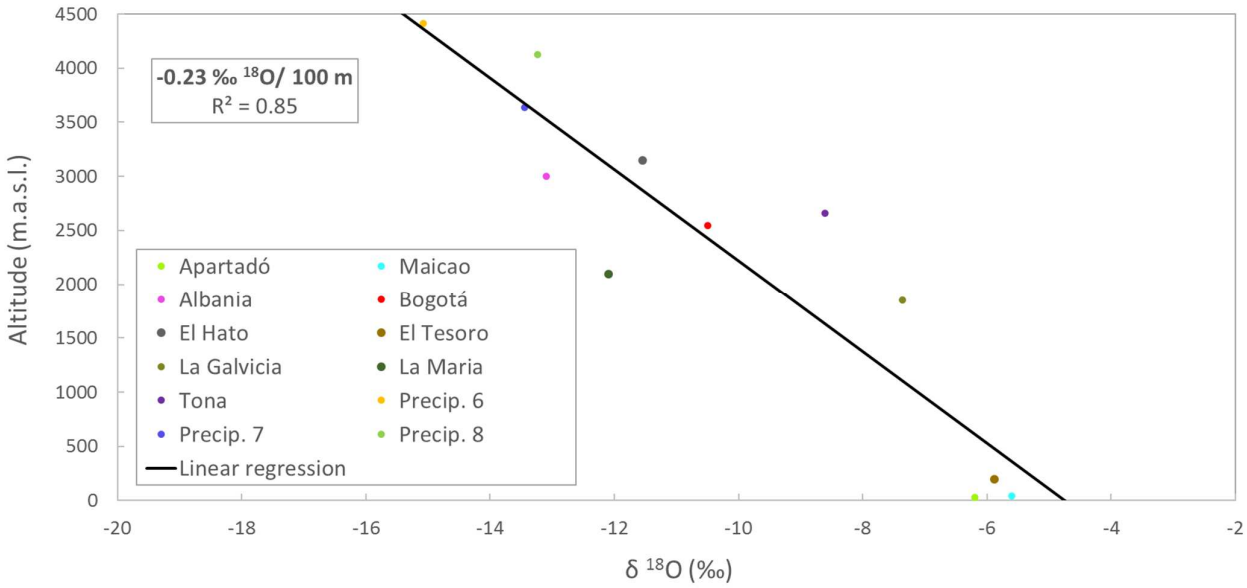

Figure 23: Relationship between $\delta^{18}O$ and altitude for the different stations in the country.

Table 5: $\delta^{18}O$ values for several stations along the country including this study. Source: GNIP 2019.

Region	Altitude	δ 18O (‰) W. Mean	year	n	Source
Apartadó (Tunelapa)	30	-6.2	2013 - 2016	3	GNIP
Maicao	45	-5.6	2004	5	
Bogotá	2547	-10.5	1971 - 2006	19	
Albania (Cali)	3000	-13.1	2003	10	
El Hato	3150	-11.55	1999	11	
El Tesoro	198	-5.88	2002 - 2016	9	
La Galvicia	1848	-7.36	2005	10	
La Maria	2100	-12.09	2003	9	
Tona	2660	-8.61	2005	13	
Precip. 6	4413	-15.08	2017 - 2018	2	This study
Precip. 7	3635	-13.44	2017 - 2019	2	
Precip. 8	4128	-13.23	2017 - 2020	2	

Other gradients of $\delta^{18}O$ in tropical regions agree with the gradients found here in this study. In two transects in Ecuador, a value of -0.17 ‰ / 100 m was found (García et al., 1997); -0.25 ‰ / 100 m for the entire Colombia (Rodríguez, 2004); -0.18 ‰ / 100 m for multiple sites of the Eastern Andes in Colombia (Saylor et al., 2009) and several more gradients that can be observed in Table 7.

4.2.3. Amount effect

The amount effect is described as the relationship between the amount of precipitation and the δ values (Clark and Fritz, 1997). The correlation indicates that strong precipitation events may be extremely depleted in ^{18}O and ^{2}H which is explained by the interaction of rainwater with the atmosphere, where the light isotopes exchange faster with vapor while falling down, being higher in light rains and drizzle (IAEA, 2000). In consequence, the amount effect is more evident in dry regions where the heavy isotopes are more enriched (Clark and Fritz, 1997).

Plots comparing the accumulated precipitation for each sampling period versus δ^2H and d-excess, respectively, are presented for the three precipitation sampling sites in Appendix **8**, Appendix **9**, Appendix **10** and Appendix **11**. However, these comparisons are not describing the amount effect precisely since the samples are collected during several rainfall events through the time, therefore the signature of the isotope composition reflects a mixture of light and strong rain events. R^2 are generally lower than 0.6 and the low correlation is evident.

Mean daily air temperature versus δ^2H and d-excess values present a broad scattering and does not show a clear correlation. Temperature remains highly constant through the year, with variations that do not surpass 2 °C in any of the stations.

4.2.4. Local Meteoric Water Line (LMWL)

Relationships of $\delta^{18}O$ vs. δ^2H with their LMWL´s for the station Precip. 6, 7 and 8 are presented in Figure 24, Figure 25 and Figure 26, respectively. The equations for such lines are:

- $\delta^2H = 8.22\ \delta^{18}O + 15.1$, $R^2=0.98$;
- $\delta^2H = 8.02\ \delta^{18}O + 9.6$, $R^2=0.98$; and
- $\delta^2H = 8.94\ \delta^{18}O + 22.8$, $R^2=0.97$

Which are falling close to the GMWL except for Precip. 8 which shows the intercept point in 22 and a slope higher than 10, standard value proposed by Craig, (1961).

The lowest δ values account for the samples with highest accumulated precipitation in Precip. 6 and 7 although in Precip. 8 this value corresponds to an average accumulated precipitation sample located in the middle of the plot. The precipitation-weighted means for Precip. 6 are $\delta^{18}O_w = -15.08$ ‰ and $\delta^2H_w = -108.9$ ‰; for Precip. 7 are $\delta^{18}O_w = -13.44$ ‰ and $\delta^2H_w = -98.1$ ‰ and for Precip. 8 are $\delta^{18}O_w = -13.23$ ‰ and $\delta^2H_w = -95.5$ ‰. P7 and P8 values are close and P6 values are more negative probably caused by the increased effect of altitude.

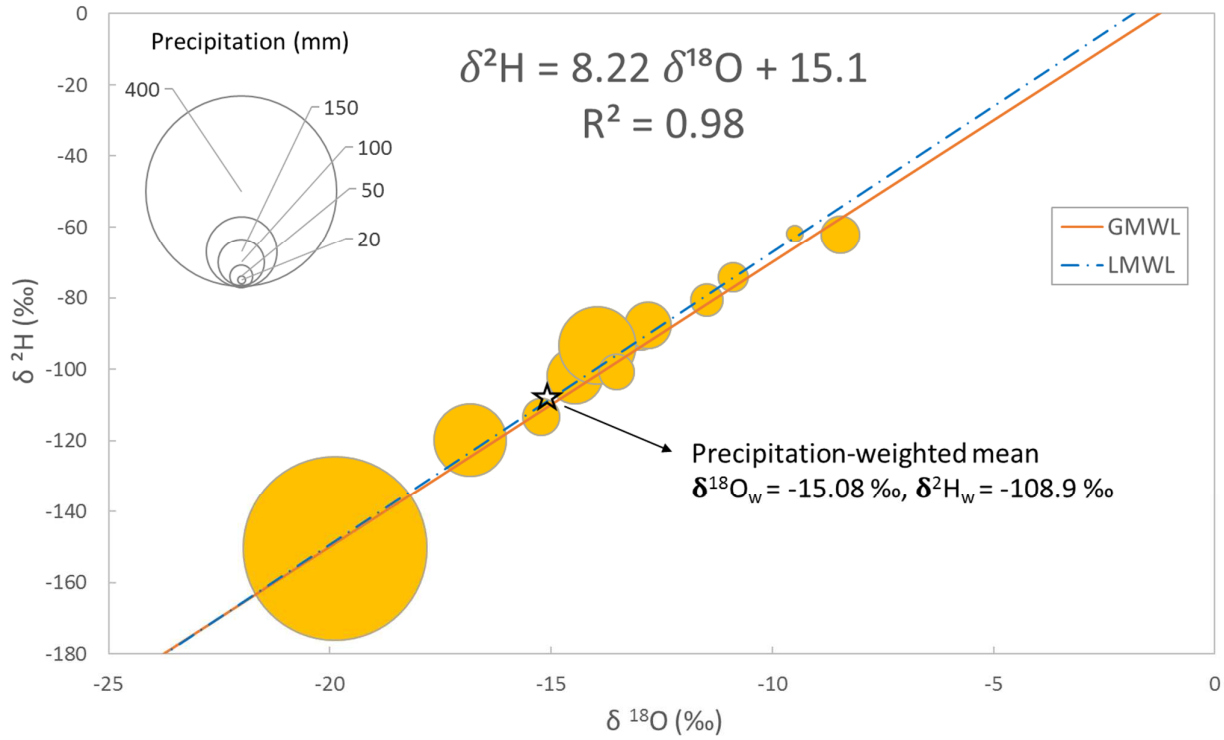

Figure 24: $\delta^{18}O$-$\delta^{2}H$ relationship for samples in Precip. 6 in conjunction with accumulated precipitation amount. LMWL drawn from PWLSR; precipitation-weighted means for $\delta^{18}O$ and $\delta^{2}H$ for the entire sampling period.

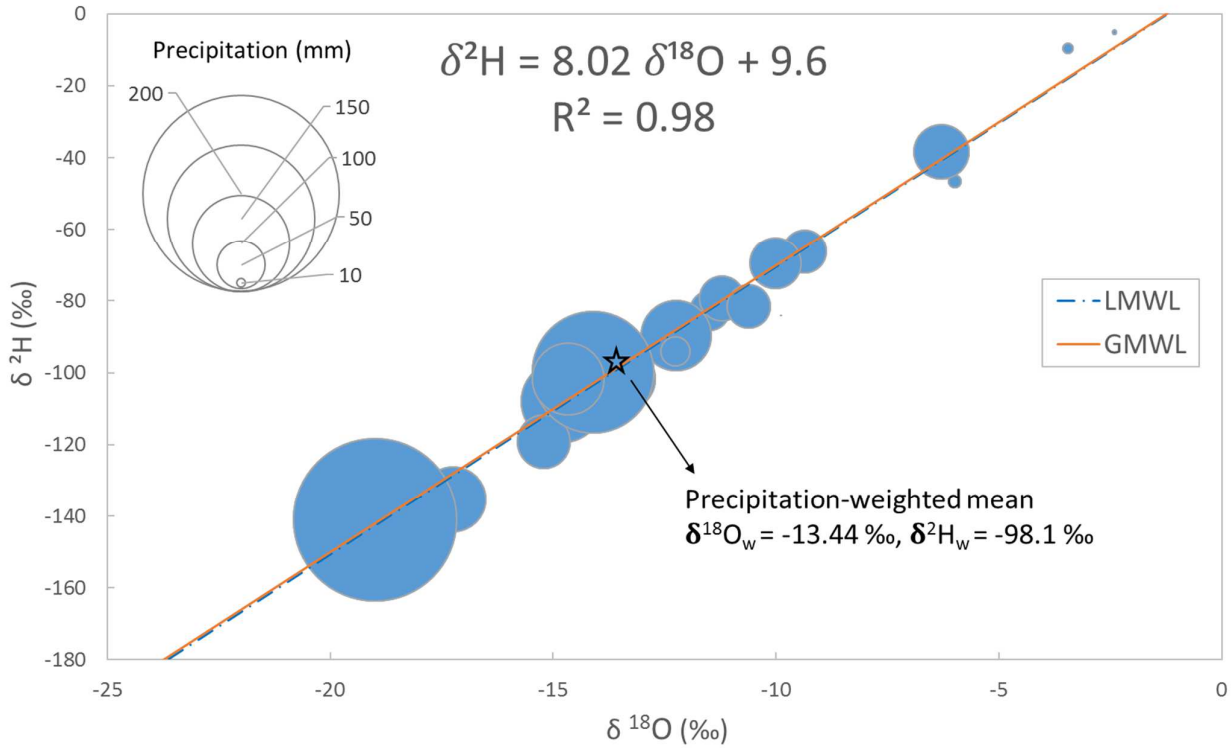

Figure 25: $\delta^{18}O$-$\delta^{2}H$ relationship for samples in Precip. 7 in conjunction with accumulated precipitation amount. LMWL drawn from PWLSR; precipitation-weighted means for $\delta^{18}O$ and $\delta^{2}H$ for the entire sampling period.

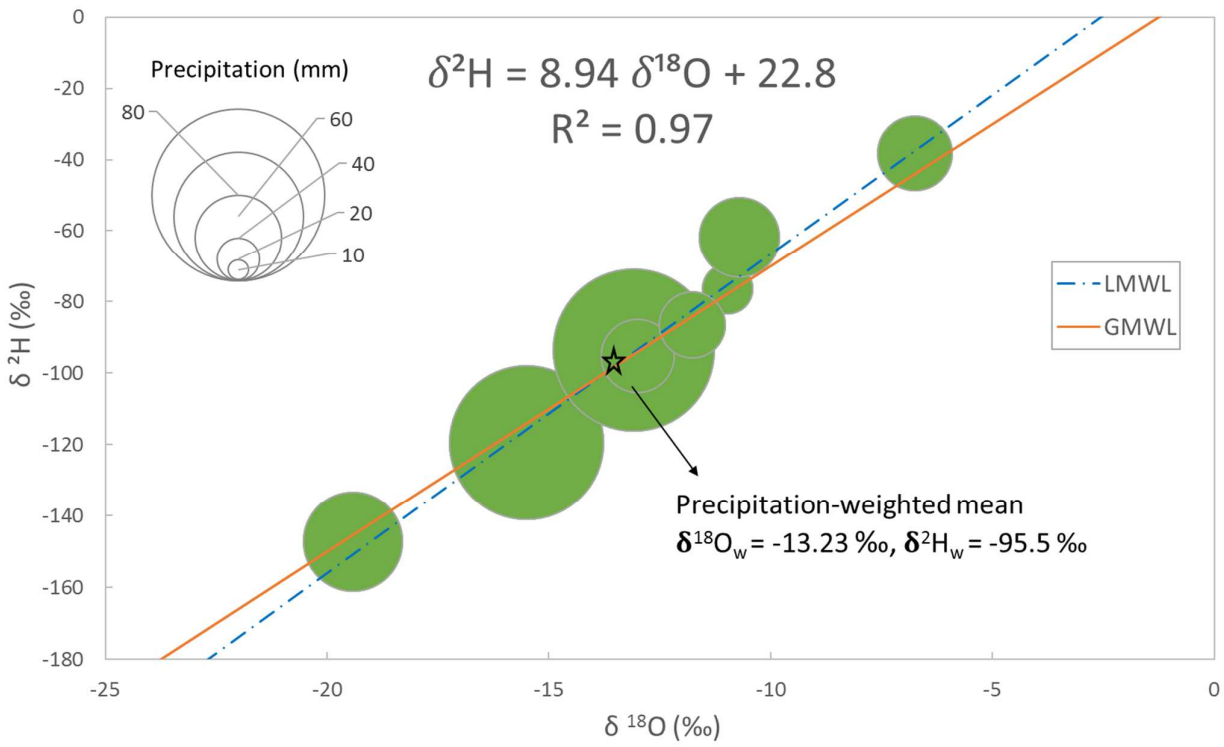

Figure 26: $\delta^{18}O$-δ^2H relationship for samples in Precip. 8 in conjunction with accumulated precipitation amount. LMWL drawn from PWLSR; precipitation-weighted means for $\delta^{18}O$ and δ^2H for the entire sampling period.

The totality of the precipitation samples for the UCRB are plotted in the Figure 27. Surface water samples are shown for comparison. The equation for the LMWL was $\delta^2H = 8.13\ \delta^{18}O + 12.5$, R^2=0.98, drawn based on the PWLSR method. The absolute isotopic values can be observed along the GMWL and LMWL. The location of the isotopic values show a wide scattering, especially in Precip. 7 where the range for $\delta^{18}O$ extends from -2.41 to -19 ‰ and for δ^2H from -5.2 to -140.9 ‰. However, the most negative values belong to Precip. 6 and 8 with $\delta^{18}O$ of -19.89 and -19.42 ‰, respectively and with δ^2H values of -150.4 and -147.2 ‰. Most positive values coincide in all the stations for the dry periods of the year corresponding to January, March and August. On the other hand, lowest isotope values correspond to the rainiest months May and June.

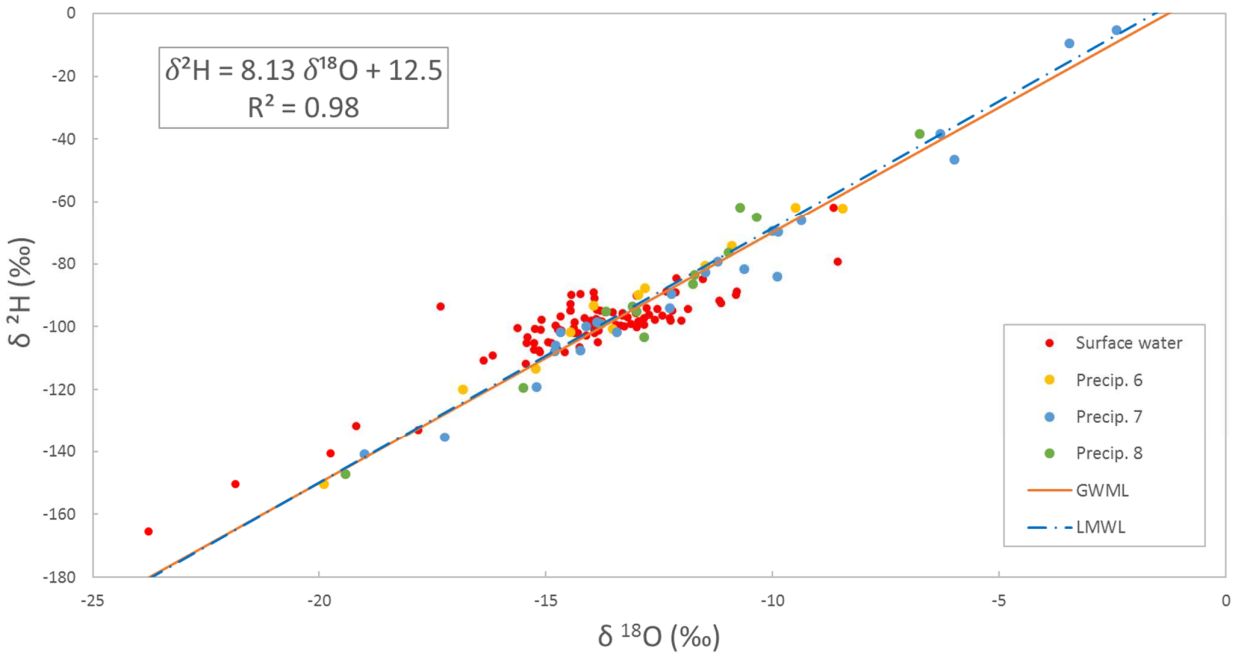

Figure 27: $\delta^{18}O$-$\delta^{2}H$ relationship for the total of the samples. In red, surface water samples of the study area. LMWL based on the precipitation weighted isotopic values.

A comparison of long term LMWL´s between locations in different geographical areas of Colombia and Precip. 6, 7 and 8 was developed to understand the variation of the isotopic signature with the altitude and the continental effect. The data used for this comparison are presented in the Table 6 and plotted in Figure 28. Values were obtained from GNIP (IAEA, 2019). Long records were only available for Bogotá and the other locations correspond to short-term projects not longer than 3 years. The station Albania only displays the period 2003 to 2004, Maicao 2002 to 2004, Apartadó 2013 to 2016 and Bogotá consider the average of a period between 1971 to 2016. Points show the monthly average values for each station. The slopes for the whole lines remain similar (from 7.95 to 8.22) to that one of the GMWL except for Precip. 8 whose slope is 8.94. The intersection point is however highly contrasting in this latter station as well (22.82), only comparable with Precip. 6 (15.08) and quite distant from the rest of the stations. Precipitation-weighted $\delta^{2}H$ and $\delta^{18}O$ values follow an altitudinal pattern where the most negative values are in samples that are located in the high mountains above 2500 m a.s.l. reaching the lowest value in Precip. 6 with -108.9 ‰ and the highest in Maicao with -36.8 ‰ for $\delta^{2}H$. Locations of the referenced studies are shown in the map of Appendix **2**.

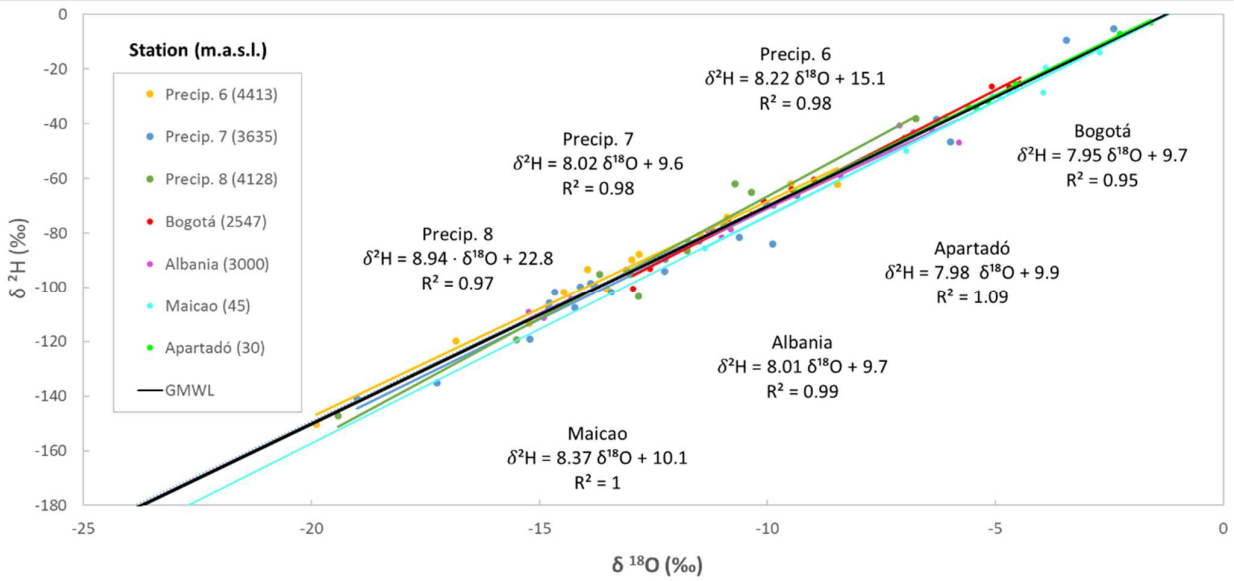

Figure 28: Compilation of LMWL´s (based on PWLSR method) for the individual precipitation stations of the study area and for four more regions of Colombia showing the average value of the months as points. Data obtained from GNIP (IAEA, 2019).

Table 6: LMWL for locations across Colombia and for the three precipitation stations in the study area with information on altitude and precipitation weighted isotope values. Source: GNIP 2019 and this study.

Region	Latitude	Longitude	Altitude	LMWL (PWLSR)	δ²H[‰] W.Mean	δ¹⁸O[‰] W.Mean	Period
Apartadó	7.7898	-76.6508	30	$\delta^2H = 7.98\ \delta^{18}O + 9.9$	-39.8	-6.2	2013 – 2016
Maicao	11.3726	-72.2474	45	$\delta^2H = 8.37\ \delta^{18}O + 10.1$	-36.8	-5.6	2002 – 2004
Bogotá	4.7000	-74.1300	2547	$\delta^2H = 7.95\ \delta^{18}O + 9.7$	-74.0	-10.5	1971 -2016
Albania -Cali	3.4405	-76.0017	3000	$\delta^2H = 8.01\ \delta^{18}O + 9.7$	-95.4	-13.1	2003 – 2004
Precip. 6	4.8297	-75.3758	4413	$\delta^2H = 8.22\ \delta^{18}O + 15.1$	-108.9 (13)	-15.1	2017-2018
Precip. 7	4.8586	-75.3905	3635	$\delta^2H = 8.02\ \delta^{18}O + 9.6$	-98.1 (24)	-13.4	
Precip. 8	4.8526	-75.3650	4128	$\delta^2H = 8.94\ \delta^{18}O + 22.8$	-95.5 (12)	-13.2	

A compilation of LMWL´s equations, altitude gradients for $\delta^{18}O$ and $\delta^{2}H$ and d-excess in the tropical America was compiled to understand which driving factors might influence the behavior of the isotopic signature in a regional way (Table 7). The location of each station is provided in the map of Appendix **1**.

Table 7: LMWL´s, d-excess and altitude effect of $\delta^{18}O$ and $\delta^{2}H$ from various sites in Latin America.

Region/Site/altitude (m a.s.l.)	LMWL	‰ ²H/ 100 m	‰ ¹⁸O/ 100 m m a.s.l.	*d* - (‰)	Reference
Colombia, national LMWL	$\delta^2H = 8.03\ \delta^{18}O + 9.6$ ‰	2	0.25		(Rodríguez, 2004)
Colombia, Eastern Andes, Tota Lake (3015)	$\delta^2H = 8.84\ \delta^{18}O + 19$ ‰				(Mariño-Martinez et al., 2018)
Colombia, Eastern Andes (multiple sites)	$\delta^2H = 8.02\ \delta^{18}O + 12.1$ ‰	1.46	0.18	12	(Saylor et al., 2009)
Colombia, Central Andes, Pereira Aquifer			0.1		(CARDER, 2007)
Colombia, Western Andes, Santa Fé de Antioquia, 500 – 2200	$\delta^2H = 7.99\ \delta^{18}O + 9.4$ ‰	0.47	0.07		(Vélez and Rhenals, 2008)
Colombia, Cauca basin	$\delta^2H = 8.10\ \delta^{18}O + 12.5$ ‰		0.21		(Betancur and Palacio, 2007)
Colombia, Aquifers of Cauca river (1500 – 2500)	$\delta^2H = 8.30\ \delta^{18}O + 13.5$ ‰				(Betancur and Palacio, 2007)
Colombia, Cienaga system, Caribbean	$\delta^2H = 8.02\ \delta^{18}O + 9.9$ ‰				(Santa et al., 2008)

Bolivia, Andes transect	$\delta^2H = 8.01\ \delta^{18}O + 15.0$ ‰		0.16 (Cochabamba transect)	17.8 (> 4000) 16.4 (1000 - 4000) 9.5 (< 1000)	(Gonfiantini et al., 2001) [1]
Ecuador, eastern slope of Andes	$\delta^2H = 8.32\ \delta^{18}O + 18.5$ ‰			15.4	(Esquivel-Hernández et al., 2019) [2]
Ecuador, western slope of Andes, 3400 – 3900	$\delta^2H = 8.04\ \delta^{18}O + 16.0$ ‰		0.5		(G. Mosquera et al., 2013) [3]
Equatorial Andes, northern Andes			0.5 (> 3000) 0.2 (< 3000)		(Rozanski and Araguas, 1995) [4]
Ecuador, Eastern Andes, 1700 – 3155	$\delta^2H = 8.31\ \delta^{18}O + 14.5$ ‰	–1.12	0.22		(Windhorst et al., 2013) [5]
Andes at 33°latitude, southern Andes			0.6 (< 1500) 0.2 (> 1500)		(Rozanski and Araguas, 1995)
Guatemala and Belize, Central America	$\delta^2H = 8.00\ \delta^{18}O + 8.7$ ‰		0.19 - 0.24		(Lachniet and Patterson, 2009) [6]
San Salvador, Central America	$\delta^2H = 8.10\ \delta^{18}O + 10.9$ ‰				(Lachniet and Patterson, 2009) [7]
Costa Rica, Pacific Coast	$\delta^2H = 7.60\ \delta^{18}O + 7.9$ ‰				(Sánchez-Murillo et al., 2013) [8]
Costa Rica, Caribbean slope	$\delta^2H = 6.97\ \delta^{18}O + 4.9$ ‰				(Sánchez-Murillo et al., 2013) [9]
Costa Rica, Central Valley	$\delta^2H = 7.94\ \delta^{18}O + 10.4$ ‰				(Sánchez-Murillo et al., 2013) [10]
Costa Rica, Páramo Chirripó, 3400	$\delta^2H = 8.07\ \delta^{18}O + 10.9$ ‰				(Esquivel-Hernández et al., 2019) [11]
Costa Rica, the entire country	$\delta^2H = 7.61\ \delta^{18}O + 7.4$ ‰				(Sánchez-Murillo et al., 2013)

Super index in the reference column indicate the location in map of Appendix 1.

4.2.5. Linear Regression for surface water

A linear regression was calculated for the surface water samples in Figure 29. The function described follows the equation $\delta^2H = 5.31\ \delta^{18}O - 25.8$ ‰, R^2=0.79. δ^2H values range from -165.4 to -61.8 ‰ with a mean value of -100.3 ‰. $\delta^{18}O$ values range from -23.77 to -8.57 ‰ with a mean value of -14.01 ‰. Samples at the rainy and warmest season (May to June) are extremely negative and the most enriched ones occur at the dry season (January and February) for stations S1 and S2, located in the highest part of the UCRB. For the stations located downstream, below 4100 m a.s.l. the dispersion is minimal and the samples tend to remain grouped even when the weather conditions are changing.

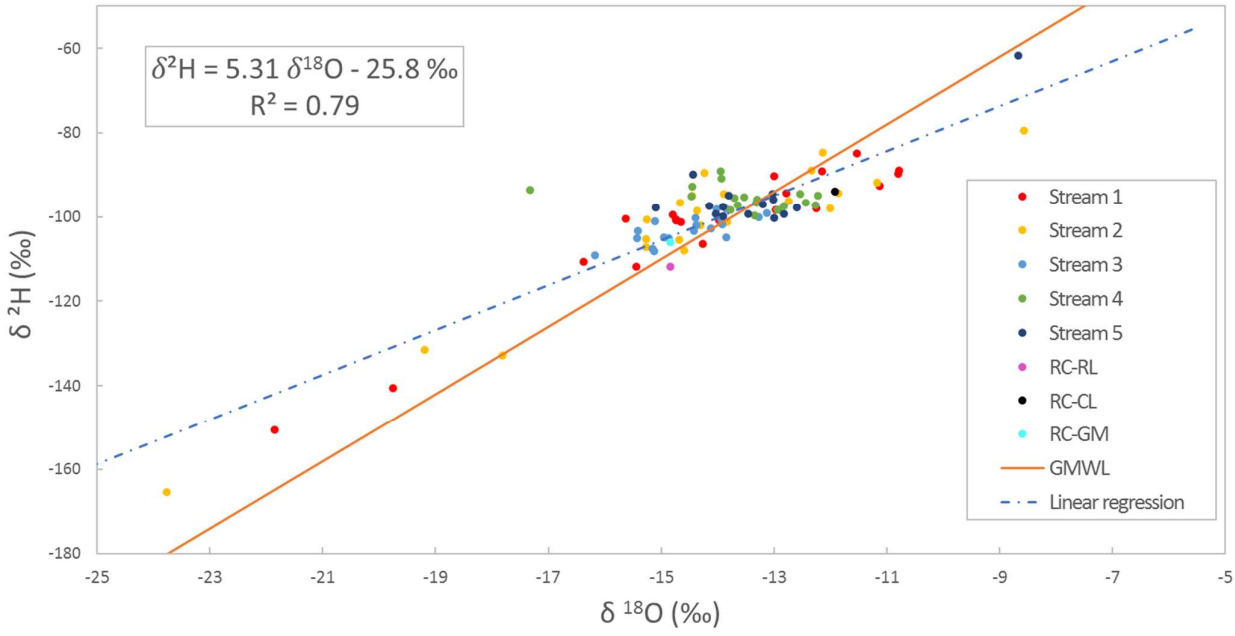

Figure 29: Linear relationship between $\delta^{18}O$-δ^2H for all surface water samples. The different stations are coded by colors as shown in the legend.

4.2.6. Deuterium excess in precipitation

The d-excess expresses the deviation of the isotopic composition in a local water sample from the expected behavior of the GMWL (Gonfiantini, 1998).

A relationship between d-excess versus altitude is shown for precipitation samples in Figure 30. Two linear correlations are presented: the first drawn on the precipitation-weighted d-excess values and the second without weighting by amount. Both regressions exhibit an increase of d-excess as the altitude increases. The highest value of d-excess is in February for P8 (24 ‰) and the lowest is in May for P7 (-5 ‰). Precipitation-weighted means of d-excess are 12 ‰, 9 ‰ and 10 ‰ for P6, P7 and P8 respectively. The variation of d-excess is higher in Precip. 8 and 7 with a range of 23 ‰, followed by Precip. 6 where values are more grouped.

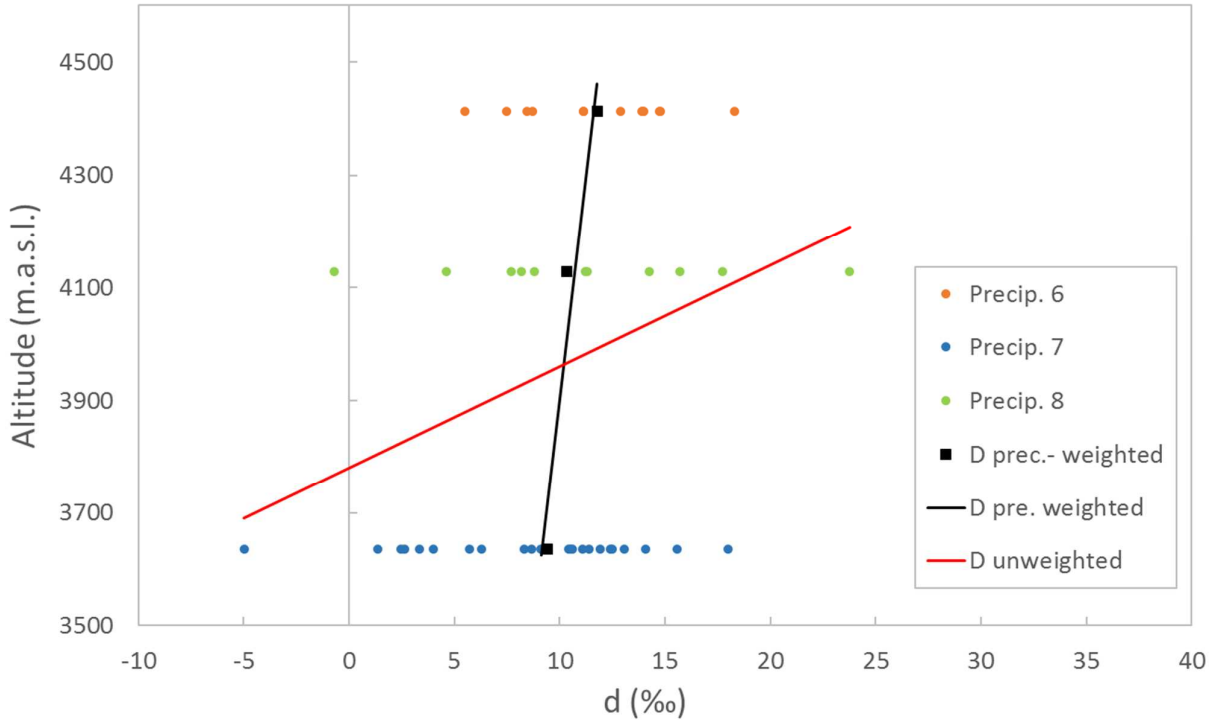

Figure 30: Relationship between d-excess and altitude for the precipitation samples.

4.3 Hydrochemistry

4.3.1. Major Ions

Comparison of the major ions concentrations in surface water for rainy and dry season are shown in Figure 31 and for precipitation in Figure 32. Only Na^+, K^+, Mg^{2+}, Ca^{2+}, Cl^-, SO_4^{2-}, HCO_3^- are considered since the other ions are contained in negligible percentages. In the Figure 33 and Appendix **12**, data are presented in 100 % stacked columns (values in mmol/L) taking into account all the ions. Ion concentrations are higher in the dry season, ratios compared between seasons range from 1:1.1 to 1:3.2.

Ions concentrations are characterized by: 1) increasing in the surface samples of the lower part of the basin as well as in SC sample contrasted with the ones upstream, 2) presenting concentrations in the same order of magnitude in surface samples from the upper watershed than in precipitation samples, around 1, 0.5, 0.3, 1 and 2 mg/L for Na^+, K^+, Mg^{2+} and Ca^{2+} and SO_4^{2-} in the dry period, respectively, 3) the relative percentages of cations follow the order $Ca^{2+} > Mg^{2+} > Na^+ > K^+$ in the stream samples of the

northern part of the watershed while in the southern the $Na^+ > Mg^{2+}$, and 4) presenting values below the recommended guidelines proposed by Law 2115 and World Health Organization (2018). There is an increase of the ion mineralization in dry season compared to rainy season, as presented more intensely in S1, S2 and in the precipitation samples. Li^+ and Sr^{2+} are only appearing in stream water of the lower basin.

Despite the conductivity in GM (22 µS/cm) is higher than in S2 (14 µS/cm), ions concentration are at least 7.7 times higher in S2. Na (0.77 mg/L), K (0.25 mg/L) and Ca (0.30 mg/L) are the most remarkable ions. Na^+, Mg^{2+}, Ca^{2+} and SO_4^{2-} are enriched in precipitation samples of dry season while for surface samples these values remain similar in percentage. Ion values for VTW are lower than S5 but in general higher than in CTW although it presents SO_4^{2-} and HCO_3^- in high content, 23.2 and 27.6 mg/L, respectively. The highest concentrations of NH_4^+ are present in the rainfall of the dry season with values around 0.3 mg/L.

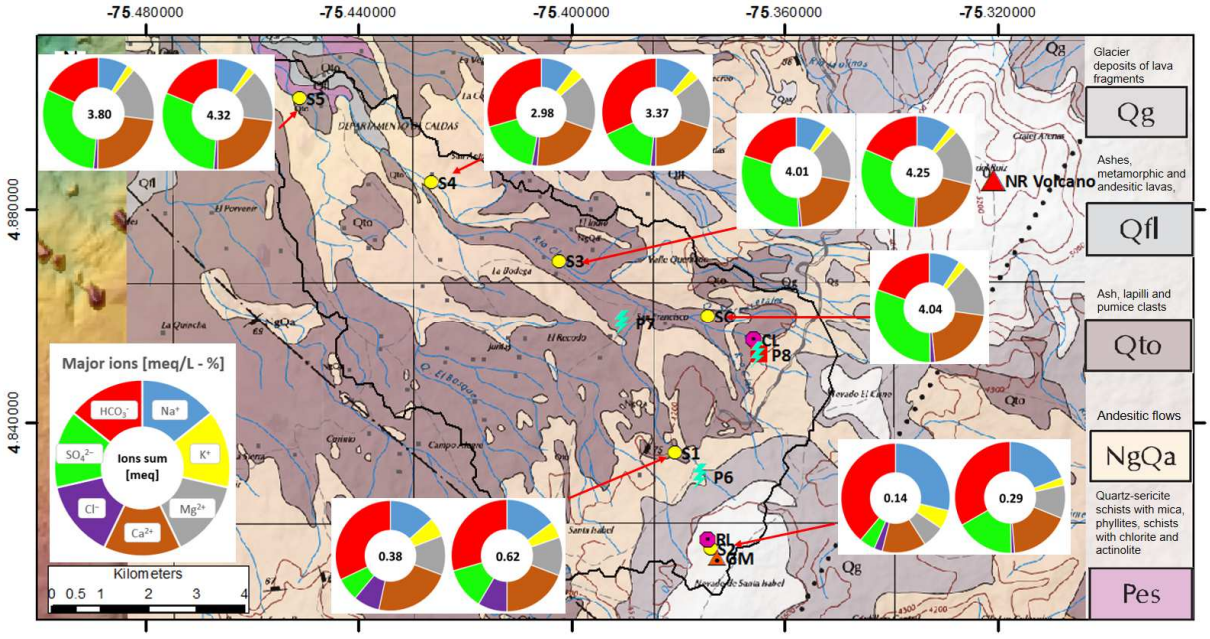

Figure 31: Concentration of major ions in surface water for rainy (left pie) and dry (right pie) seasons. Sample SC is also shown although it accounts only with rainy season.

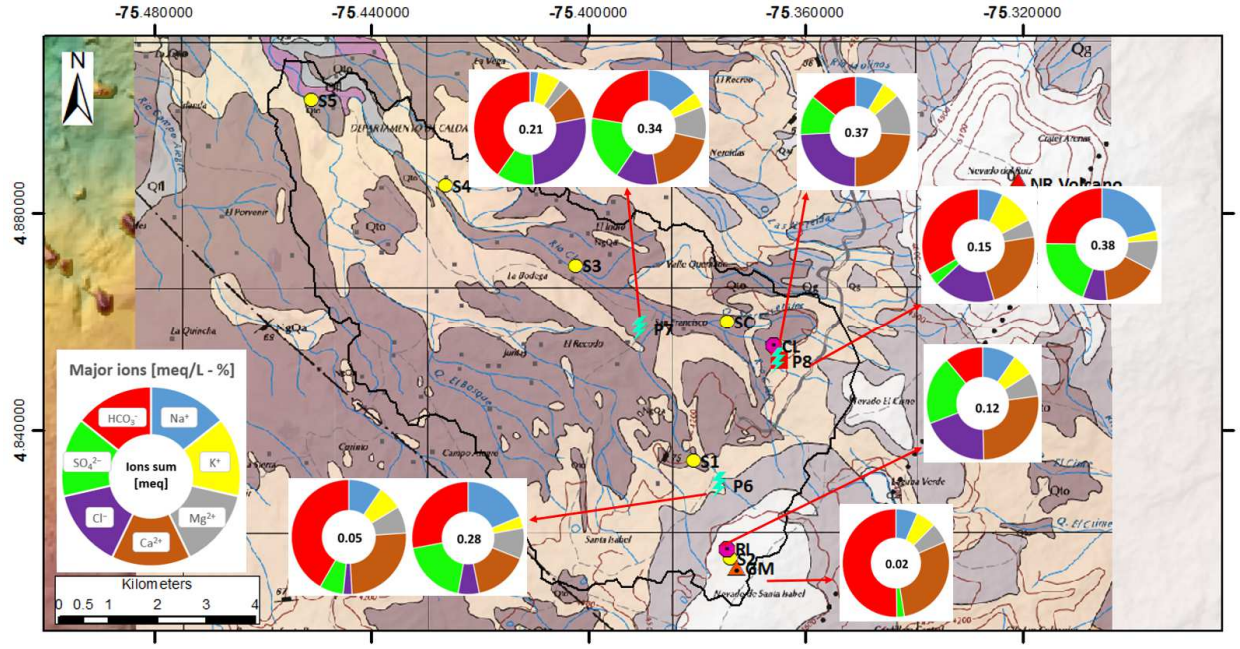

Figure 32: Concentration of major ions in precipitation samples for rainy (left pie) and dry (right pie) seasons. Samples from lakes (CL and RL) and glacier melting (GM) are also shown although they account only with rainy season.

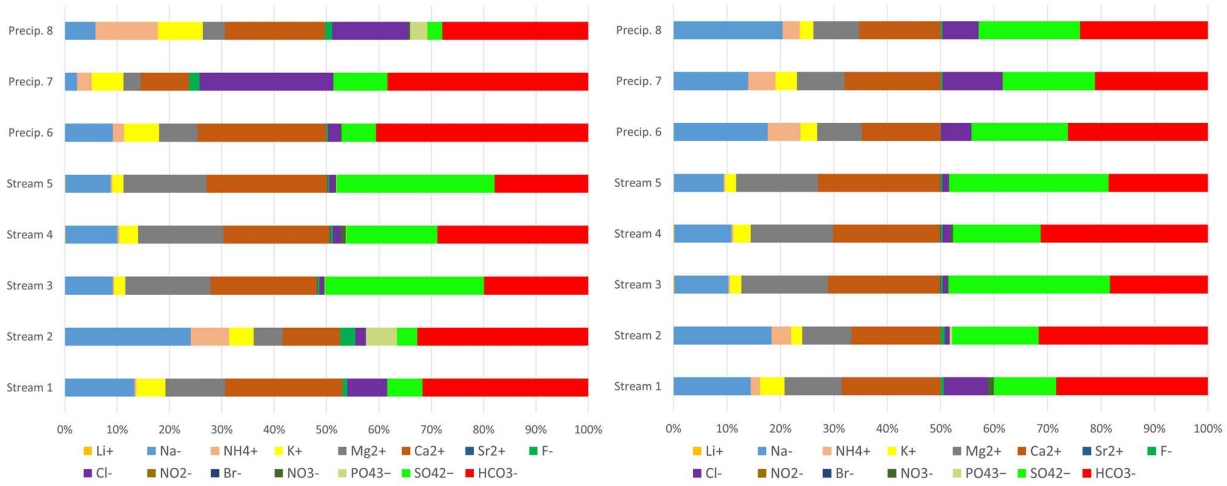

Figure 33: Major ions distribution (mmol/L) for the samples taken in rainy season (left) and dry season (right)

Piper diagrams for surface and rain water were drawn for rainy and dry season (Figure 34). In general, samples in rainy season have cations percentages between 40 and 60 % of Ca^{2+}, except for sample S2 whose value is 24 %. Percentages of $K^+ + Na^+$ range from 20 % (VTW), and 20 to 30 % (S3, S5, CTW, GM and SC) to 63 % (S2). Mg^{2+} spans from around 12 % (S2, P8 and GM) to 33 in the surface sample S4.

As for the anions, HCO_3^- reaches up to 96 % and 84 % in GM and S2, respectively and decreases to 22 % in RL. SO_4^{2-} appears variably depending on the position in the watershed, increasing in percentage downstream for samples such as SC, S3 and S5 with values of 59 %, 59 % and 61 %. The lowest values are seen in GM and precipitation samples. Percentages around 34 to 48 % of Cl^- are present in the lakes and P7 with lowest values in surface water and GM.

On the other hand, surface water samples from the lower part of the watershed (S3, S4 and S5) show a predominance of Ca^{2+}, Mg^{2+} and SO_4^{2-} and low values of Cl^-, $K^+ + Na^+$ and HCO_3^- for dry season.

Precipitation samples belong to the facies of Ca^{2+} - HCO_3^- in rainy season and to a more mixed group in dry season. Lakes were analyzed only for rainy season and show affinity with Ca^{2+} - SO_4^{2-} waters. Stream water does not show a defined pattern, since it is spread in the diagram in rainy season, where the samples lay on the boundary between Ca^{2+} - SO_4^{2-} water and Ca^{2+} - HCO_3^-, however, in dry period they group inside a mixed-type of water.

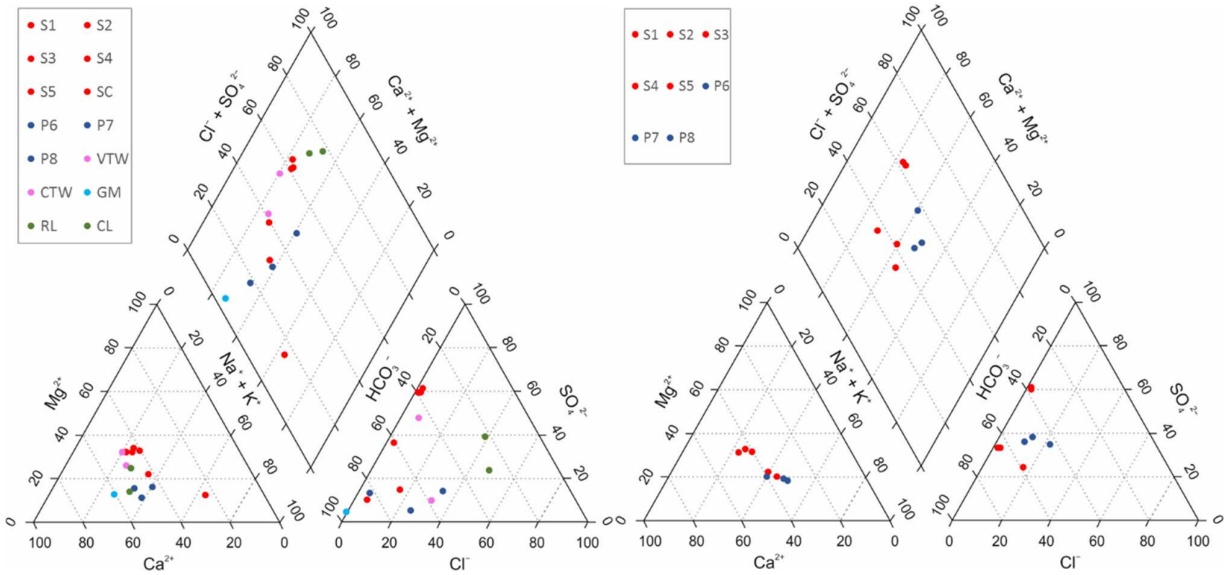

Figure 34: Piper diagram with the distribution of the types of water for the samples taken in rainy season (left) and dry season (right).

4.3.2. Trace elements

Trace elements results are presented in Figure 35 and Figure 36, concentrations are given in µg/L. Al concentration exceeds the permitted values of Law 2115 and the median value set by WHO (200 µg/L in both) in the sample of the lake CL. Anomalies of Al are present in S2 (175 µg/L) in rainy and dry season and in the lakes CL and RL (218 and 78.4 µg/L). Precipitation in P7 accounts with an unusual 69 µg/L in rainy season only in the second campaign, while in the first is barely 2 µg/L. GM and S2 differ in Al concentration by 170 µg/L. In general, Al (same samples evaluated in both seasons) in wet and dry season accounts with 161 and 328 µg/L in total, respectively, concentrating most of the amount in sample S2.

Ti has an anomaly in S2 for both campaigns: 5.3 and 4.7 µg/L, widely differing from the background values of the rest of the samples corresponding to less than 1 µg/L. V is only occurring in stream water samples in concentrations ranging from 4 to 6 µg/L. Rainfall in P7 and P8 account with anomalies of Mn of 12 and 19 µg/L in rainy season and 19 and 57 µg/L in dry season. Lake sample CL has the higher Mn value of the rainy season samples with 50 µg/L.

Higher values of Fe are found in the tap water of the Cisne hut -CTW-, S2, S5 and CL with 56.8, 43.7, 50.2 and 72.4 µg/L in the rainy season and only in S2 of dry season with 30.2 µg/L. Ni is especially higher in VTW, CL and S1 (dry) with 1.9, 1.6 and 2.1 µg/L, respectively. Cu is higher in both samples of tap water: 3.9 and 1.3 µg/L and in P8 (dry) 9.9 µg/L. Zn shows anomalies for rainy and dry season in P7 (11.2 and 20.6 µg/L) and P8 (5.7 and 34 µg/L) and CL (12.8 µg/L) respect to values lower than 3 µg/L in the other samples. As is higher in stream water of the northern part of the watershed with values between 2.7 and 4.4 µg/L compared with lower values for the other samples (less than 0.6 µg/L). S3 presents the 50 % of the As concentration found in all the analyzed samples coinciding in the first and

second campaign. Se is only found in VTW and in S3 from rainy season as well as in all the samples of the dry season in concentrations of 0.34 µg/L in average, increasing downstream. Ag, Cd, Sn and Tl tend to be below the detection limit or in concentrations lower than 0.05 µg/L in average.

The highest Sb concentration is 0.72 µg/L in VTW. Pb is higher in P7 and P8 (rainy season), with 0.15 and 0.25 µg/L, respectively, and P8 (dry season) with 0.65 µg/L. Ba levels are higher in both tap water samples and SC as well as in S3, S4 and S5 (in wet and dry season) than in the rest of the samples, 12 and 17 µg/L in average, respectively. Ba increases downstream from S1 to S4, excepting S2. In dry season the concentration is higher than 60 % of the total mineralization in S3, 4 and 5. U was identified only in surface waters and its concentrations increased gradually downstream from S1 to S4, decreasing in S5. Average concentrations were 0.03 µg/L for all the samples, being S4 (rainy) the highest with 0.15 µg/L.

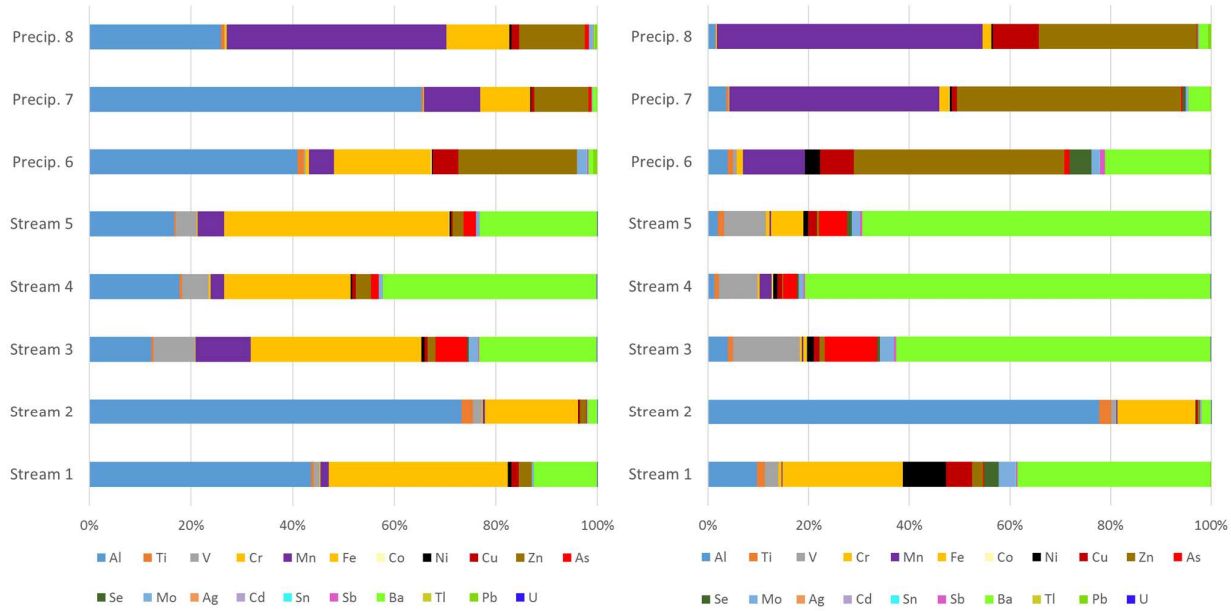

Figure 35: Concentration of trace elements (µg/L) for the samples taken during the rainy period (left) (June 2019) and dry period (right) (March to April 2018).

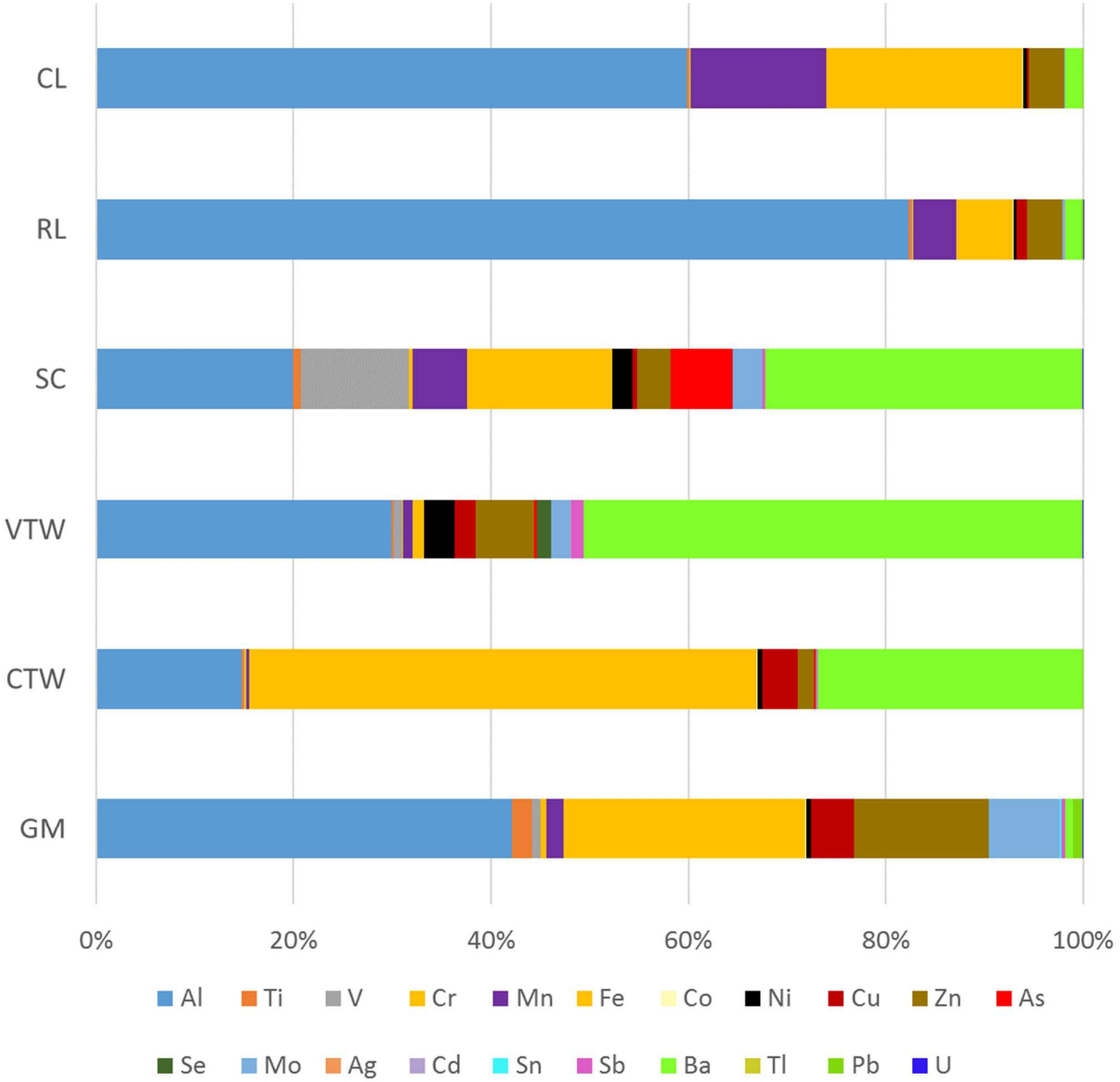

Figure 36: Concentration of trace elements (µg/L) for the complementary samples (glacier, lakes and tap water) taken during the second campaign (June 2019).

All in all, stream samples S3, S4 and S5 are the most enriched in trace elements. Furthermore, rainfall shows enrichment of Mn, Zn and Pb and S2 exhibits an enrichment of Al, Ti, V, Cr and Fe not coherent with the assumed source water (glacier melting). In precipitation samples from dry period Mn, Cu, Ba and Zn dominate more than the 90 % of the total mineralization. On the other hand, for the dry period, Ba and V show more than 80 % of the total mineralization in samples from the lower watershed (S3, 4 and 5). In the same period, samples from the upper watershed (S1 and 2) are dominated by the presence of Fe and Al with the input of high concentrations of Ba in S1.

Tap water in the municipality can contain relatively enrichment of some elements such Ni, Cu, Se, Mo, Sb and Ba. Tap water in “El Cisne hut” is enriched in Fe, Cu and Ba. The chemistry in tap water is dominated by Al and Ba in VTW and by Al, Ba and Fe in CTW. Water in lakes (CL and RL) are similar in composition despite of the different locations. Their most predominant ions are Al, Mn, Fe, Zn and

Ba. At last, CL is the most mineralized water presenting high anomalies in almost all the trace elements. In general, all the elements are present in concentrations much lower than the maximum permitted by WHO and Law 2115.

4.3.3. Volcanic ash fall

Events of volcanic emissions from the NRV are shown in the Figure 37. Only events that could have potentially reached the study area are presented. Data on the height of the ash over the volcano top is provided as well. A total of 120 events are counted from December 1, 2016 to June 17, 2019. Period of higher activity are between December 2016 and May 2017 with 79% of the considered events. A second and a third short volcanic activity periods registered between November 2017 and September 2018 and April to June 2019 were recorded respectively.

The emissions of September 4 and 5, 2018 were petrographically analyzed by the SGC. An approximate amount of 43.750 m^3 of material over 350 km^2 (including the lower part of the UCRB) was calculated to have been expulsed during these two days. The minerals found in the analysis were: plagioclase, pyroxen, lithic fragments, biotite and glass (Servicio Geológico Colombiano, 2018a). According to (USGS, 2015) and (Stewart et al., 2006), volcanic ashes can decrease the pH due to its acidic composition. At last, ashes contain soluble coats on its surface that are composed mainly by Ca, Na, K, Mg, Al, Cl, S and F and eventually enriched with droplets of H_2SO_4 and HCl (USGS, 2015).

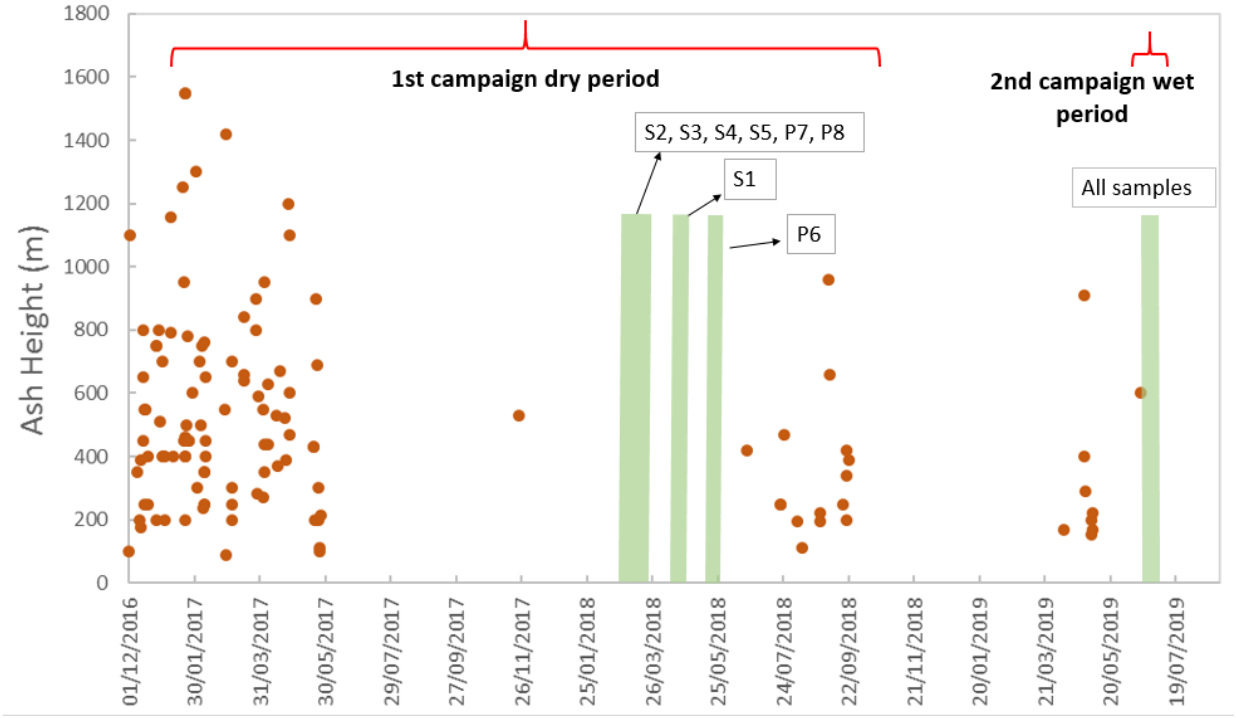

Figure 37: Volcanic ash emission events recorded for the period 01.12.2016 to 30.06.2019 indicating the height of the emission over the volcano top. Shaded lines indicate the date when the samples were sampled in both dry and wet periods.

5. DISCUSSION

5.1 Comparison between standards of labs

The comparative analysis of isotope standards between the laboratory of the SGC and the TUD allowed to contrast the results between the two campaigns. Deviation in the results between the two laboratories were almost negligible. It seems that, the change of equipment and analysis procedure do not give a major imprint on the results values. As long as the sampling method and the store of the samples have not altered the quality of the samples, the results here presented are reliable.

5.2 Methodology

The lack of temporal regularity in the sampling for isotopes posed challenging obstacles in the interpretation of the data. Sampling intervals spanned from one week to five months, aspect that on the one hand, increased the uncertainty on the calculation of the precipitation-weighted mean values, and on the other hand, amplified the possible causes of evaporation and the susceptibility of the collectors to damage. On the same aspect, the type and placement of the samplers involved several presumable constraints, (i) obstructions of the precipitation entrance, (ii) enhancement of the evaporation, (iii) pollution of the samples and (iv) breaking of the collectors.

A more precise availability on the location of the geological units, fumaroles, hot springs and bodies of water in the UCRB would have allowed more detailed interpretations on the correlation between isotope concentration, meteorological conditions and hydrochemistry.

The ion balance error of several of the samples chemically analyzed that was in some cases positive and in others negative, might be explained by two different processes. First, for the anion deficit, unmeasured organic species such as acetate, oxalate and formate already reported as typical in tropical and subtropical rainwaters (Mello and Almeida, 2004; Honório et al. 2010) might have occurred. Second, the low mineralization (conductivities below 40 µS/cm) demand a higher resolution of the devices to calculate the ions. In the case of this study, the handheld alkalinity colorimeter used in the field to calculate carbon species had a precision range of ±5 ppm. This uncertainty gets significant (> 100% for samples with $CaCO_3$ lower than 5 ppm) in samples where the HCO_3^- are between this range and in consequence, the ion balance error increases.

It is important to indicate that, as in this study, the values of HCO_3^- found by Honório et al., (2010) were close to the detection limit. Finally, some observations to the chromatograms of the major ions permitted to recognize unidentified peaks which remain as a question but that may have played a role in the balance of the charges during the calculations.

5.3 In-situ parameters

The pH values in surface water (except GM) are generally more alkaline than in precipitation. This change in the pH indicates an alkalization process given by the interaction between soil-rock and precipitation. Higher values of $CaCO_3$ only in the stream samples of the northern part of the basin, which are close to the thermal springs suggest that this anion comes from hot springs and not from the single interaction with superficial soil layers. The hypothesis given by (Arango et al., 1970) about the presence of $CaCO_3$ affecting the waters circulating in the hydrothermal systems would support this idea. On this regard, there are antecedents to support the hypothesis here stated. Investigations on a thermal spring neighboring the UCRB, registered in 2015 an average pH fluctuating between 7.5 and 8.3 and electrical conductivities of 3000 to 8000 µS/cm (Servicio Geológico Colombiano, 2016) and in 2016 registered between 5.6 and 6.8 (Servicio Geológico Colombiano, 2017). Nonetheless, pH values are in good agreement with the values of the streams influenced by the thermal waters.

The acidic value of GM, which has not had contact with the soil would suggest that the ice glacier is fed mainly by precipitation of snow. In line with this, it can be said that precipitation is acid and the pH in surface waters is neutral to alkaline due to interaction with $CaCO_3$ in the underlying geological units.

One of the remaining questions about the correlation between samples that is still due to be answered is on the inconsistency between GM and Stream 2 pH and conductivity. Although Stream 2 is barely 200 meters downstream GM, the pH changes from 5.8 to 7.4 and the conductivity, illogically decreases even when the mineralization is higher in S2. On this regard, it is fair to point out that Stream 2 presented an intense whiteish color not noticeable in GM, indicating the presence of chemical elements acquired in this short trajectory.

The pH in precipitation is acid and the conductivity values are lower than 40 µS/cm, same as in the lakes. This similarity could indicate that either the lakes are recharging from precipitation without prolongated interactions with the mineralogy of rocks surrounding or the recharge water comes from overflow on saturated soils. The electrical conductivity values lower than 40 µS/cm coincide with average values taken for the rainfall 45 km southeast of UCRB in Ibagué (< 20 µS/cm) (Ramírez Arcila and Ospina Zúñiga, 2014) and in another study site in the southern Colombian Andes (14 µS/cm) (Burbano and Figueroa, 2015). Acid rain values in the samples P6 and P7 are in line with the findings of González and Aristizábal (2012) and González-Duque et al. (2015) in the city of Manizales (4.9 in average). Acid values like these have been commonly attributed to the input of vehicular emissions and volcanic activity (USGS, 2015; Burbano and Figueroa, 2015). Both factors match to the geological setting of the study area and to the location close to a city considerably affected by fossil fuels emissions.

Finally, despite that the expected pH values for the waters in the watershed are acidic, as those ones measured in the lakes, precipitation, surface waters with low rock interaction and experiments of andesite ashes (Addabbo et al., 2015), the measurements taken, presented slightly alkaline pH and increase of the conductivity in stream samples influenced by the thermal activity.

Samples with short terrestrial transient times such GM, S1, S2 and lakes showed the similar behavior of precipitation due to the brief periods in contact with the underlying materials. Transient time is, in this way, affecting clearly the pH, the conductivity and the alkalinity as the water-soil-rock interaction occurs. All these described parameters, in addition, showed an increase downstream, demonstrating a hydraulic continuity of the flow.

5.4 Major ions

Major ions concentrations are higher in samples from dry season than in the ones of rainy season due to the interaction of several factors. First, the influence of much more volcanic ash emissions events occurred during the previous months to the sampling period. For the samples of the rainy season, the volcanic activity decreased, and in consequence, the influence of the aerosols which might have been washed out already. Second, dilution effects happened in the rainy season given by the amount of water available as runoff, decreasing relatively the ions concentration. Third, the discharge of the streams during wet periods is composed mainly by baseflow and runoff, while in dry periods it is constituted mostly by baseflow with longer soil-water interaction and therefore, dissolved ions (Osorio et al. 2003). Finally, the geological units, the presence of thermal springs, the volcanic ash fall and the drainage area, played an essential role in the modification of both concentration and composition of the analyzed waters.

Major ion percentages remained highly constant in stream samples of both seasons. However, geographically speaking, there are some contrasting behaviors to highlight. Stream samples located in the northern part of the basin showed higher ion concentrations and a different composition than the ones in the southern portion. The most likely explanation for this is, on one hand, the higher drainage area on the geological unit Qto (ash, lapilli and pumice clasts) in the north, and on the other hand, the closeness to the volcanic cone and the connection to the flows coming from it. These factors led the northern portion of the UCRB to have a higher amount of material available to be eroded both in-situ

and transported. It is worth to point out, that the precise location of the thermal springs and fumaroles was not georeferenced. However, according to Figure 4 and field observations, at least a thermal spring is located downstream SC and upstream S3 and S5.

The atypical higher concentration of SO_4^{2-} and Mg^{2+} in the stream samples SC and S3 are in line with the potential input of thermal springs already mapped by Arango et al., 1970. High concentrations of Cl^- in SC and CL as well as F^- in SC might be due to the presence of biotite and the input of HCl, HF and other compounds released by volcanic emissions or atmospheric aerosols with anthropogenic influence (Stewart et al., 2006; USGS, 2015; Burbano and Figueroa, 2015). This thermal spring also registered in 2016 a content of Na^+ and Ca^{2+} of 580 and 46 mg/L, respectively, and 1040, 170 and 150 mg/L of Cl^- , HCO_3 and SO_4, respectively (Servicio Geológico Colombiano, 2017). Despite that the Na^+ and Ca^{2+} values previously described for the spring are substantially larger than the concentrations in S3 and S5, it is still logic to consider their correlation since just a small input from the hot spring is occurring. To illustrate this effect, other studies in the Galeras Volcano (Colombian Central Andes) registered HCl, H_2S, SO_2, and HF in the fumaroles as well as SO_4 and Cl content in thermal waters and steam (Fischer et al., 1997).

Higher concentrations of elements such Mg, Ca, Na, K and the presence of Fe, Al, Ti, Ba, and F in the surface samples of the northern part of the watershed confirms the interaction between rainfall and surface water with the geological units. Minerals such biotite, hornblende, augite, muscovite and a wide range of plagioclases and potassic feldspars are among the typical minerals in the andesites, basaltic andesites, dacites, diorites and quartzdiorites outcropping in the area. Furthermore, the composition of volcanic ashes in the area (feldspar, hornblende, biotite, magnetite, augite, hypersthene and apatite (Lizcano et al. 2006) complement these chemical arrangement.

As for the southern and upper watershed stream water, the affinity of major ions percentages with precipitation samples indicates that runoff there comes from precipitation and has a short time of interaction with the soil. It is also clear the impact of baseflow/runoff proportion. The relative percentage of $Na^+ > Mg^{2+}$ in precipitation behaves inversely contrasted to the $Mg^{2+} > Na^+$ in stream samples of the northern part of the basin. Such weathering pattern in the cations had been already found by Osorio et al. (2003) in a neighboring region. This behavior indicates that the weathering of magnesium minerals (typical from the geological units) plays a higher role in the northern section than in the southern one.

Despite of the closeness between GM with RL (lake approx. 400 m downhill) and GM with S2 (approx. 200 m downstream), there is a considerable difference in the ion percentages based on the Piper diagrams. In the first case, the sum of Cl^- and SO_4^{2-} indicates at least a 40 % in RL compared with less than 8 % for GM. In the second case, it is observable the reduction in the percentages of $Ca^{2+}$and the increase of SO_4^{2-} and Na^+ in S2 respect to GM. This might indicate that part of the melted water from the glacier, infiltrates the soil and travels through it to emerge downstream (probably to S2 and RL). Based on this, it could be concluded a chemical interaction between infiltrated water and soils and pre-existent rocks in between GM and S2. The mineralogy of the underlying rocks would support this hypothesis since one of the most common types of minerals in the rocks of the area are sulphides, such as pyrite (FeS_2), which would be the source of the sulfates in the waters of RL and S2.

In the precipitation samples, some ions like Na^+, Mg^{2+}, SO_4^{2-} increased in the dry season. These anomalies could be caused by the input of volcanic ashes occurring in the sampling period or contribution of air masses coming from the industrial areas of the city of Manizales. In agreement with these hypotheses, Servicio Geológico Colombiano, (2016; 2017; 2018b) found that the expulsion of SO_2 remained fluctuating but constant in the NRV since at least 2012, with an average flux not less than 900 T/d from 2015 to 2018 and reaching even 22000 T/d in the end of 2017. González-Duque et al., 2015, concluded that high levels of SO_4^{2-} and PM_{10} in the atmosphere of Manizales (20 km to the northwest of UCRB) behaved inversely compared to precipitation amount and relative humidity. Such concentration was sometimes higher in rural areas nearby the NRV, where it was reduced in the air when rainfall occurred, and therefore they were attributed to volcanic emissions (Cuesta-Mosquera et al., 2018).

In line with the above mentioned, comparative studies of chemical composition in rainfall in other regions also concluded that concentrations of major ions in dry season were higher than in rainy season (Mello, 2001; Mimura et al., 2016; Wu et al., 2016)). Also, such concentrations vary widely from site to site. Studies in China, Brazil, Argentina and Saudi Arabia have found that chemical compositions and concentrations differ depending mostly on air mass source, soil-rocks composition, closeness to anthropogenic activities, sea level elevation and meteorological conditions, among other factors (Lavado, 1983; Michelsen et al., 2015; Wu et al., 2016; Mimura et al., 2016). Nonetheless, with the purpose to understand the origin of the chemical elements in the precipitation of the UCRB, a more comprehensive data set must be acquired. As for the precipitation samples taken in the rainy season, it must be pointed out that they were in the collectors for at least 6 months, which might have been affected the concentration of volcanic minerals inside it.

Since the largest geochemical impact and the incorporation of the chemical elements to the soil and the streams occurs after hours or days of contact between the ash and the water (Eslava, 1985) (Fernández-Turiel et al., 2012); the change in the hydrochemistry of the water in the basin might be explained either by the interaction of water with geological materials or by the volcanic events not considered in the analysis.

5.5 Trace elements

The concentration of trace elements in the precipitation was commonly higher in the wet season although difference is not conclusive. The findings of Honório et al. (2010) in the Amazonas Forest agree with this pattern. However, there is debate on a typical correlation between trace elements and precipitation. For instance, Mello (2001), Mello and Almeida, (2004) and Mimura et al., (2016) observed higher concentrations in the dry period. Others authors, discovered that the most elevated concentrations are in the first precipitation events after a dry period and decreased by dilution over the next rain events (Wetang and Wamalwa, 2015; Doria, 2017). On this aspect, the latter is unlikely to occur since a “typical dry” period does not occur in the UCRB but rather a decrease in the precipitation amount. In this sense, an over-concentration of trace elements in dry period would not be probable since a scavenging process may occur permanently.

Some samples, namely S2 and CL presented the highest trace elements concentrations of the study. In the case of CL, the enrichment might indicate a high evaporation rate. On the other hand, in S2, the enrichment seems to be explained by a contribution of groundwater where aluminosilicates are the most predominant material eroded. For precipitation samples such P7 (rainy) and P8 (dry), either volcanic emissions or aerosols from nearby urban areas might point out the answer. However, further research must be done to determine the sources.

High content of trace elements such As, Mb, V, Mn, Mo and Ba in S3 support the idea of thermal springs influence. High levels of H_3BO_3 found by Arango et al. (1970) in hot springs of the UCRB agree with the possible influence from thermal waters. Heavy metals such Fe, Ni, Cu, Mo and Sb in tap water suggest the occurrence of dissolution of minerals from the pipelines. Elements such Mn, Zn, Ba, Se, Br, B, Al, Si, Cd, Pb, As, Cu, Fe may appear from the leachate of volcanic ashes (Stewart et al., 2006) and the presence of PM_{10} in the air of natural and anthropogenic origin (Doria and Castillo, 2016). Furthermore, the high content of Al and Fe both in surface and precipitation water indicates two sources. For precipitation, the volcanic glass present in the atmosphere as aerosols of allophanic compounds contributed to the enrichment in Al. And for the surface waters, the same previously mentioned mineral present in the soil horizons commonly formed from volcanic ashes (Stewart et al., 2006; Lizcano et al., 2006).

The analysis of these hydrochemical data are very valuable to establish first approaches to the understanding of interaction between the volcanism, meteorology and hydrochemistry in the Central Andes of Colombia, even more necessary since all the major ions are inadequately sampled in dry and wet deposition in South America (Vet et al., 2014).

Despite of the influence of volcanic activity, agriculture, hydrothermal systems and cattle raising, the water in the UCRB is -based on the WHO and Law 2115 guidelines- *chemically* drinkable from the source. In line with this, the streams of the upper watershed are consumed in the "Cisne Hut" without any treatment. However, harmful biological agents can still be present where the anthropogenic influence may have impact on it. In this regard, Agudelo-Londoño et al. (2012) concluded that in a neighboring watershed, the risk of pollution by pharmaceutical agents applied to the livestock was "very high". At last, water in the outlet for the Villamaría municipality reflects the chemistry of the source and fulfills the requirements of the drinking water regulations.

Finally, a differentiation of the influence of volcanic ash fall on ion concentrations between precipitation and stream samples was not possible since the sampling periods did not correspond with punctual volcanic emissions to the direction of the watershed. However, influence is not discarded by emissions to other directions since the dynamics of the winds are complex at such altitudes.

5.6 Seasonality effect

The seasonal effect is described as the fluctuation of the stable isotope ratios as the result of temperature variation (Leibundgut et al. 2009) and (Clark and Fritz, 1997). However, the temperature variation in the UCRB along the year is lower than 5° C in stations of the same altitude. In consequence, the seasonal variation is exerted mainly by the variation in precipitation periods and thus, by the amount of rain and not by the temperature. Nonetheless, the overlapping of several effects is not discarded.

The results for $\delta^{2}H$ and $\delta^{18}O$ values show a high range of variation due to the difference in altitude, meteorological conditions and dates of sampling. In general, surface water presented more depleted values than precipitation. However, the discrete nature of the stream samples (snapshot) where specific extreme meteorological events might have occurred during the sampling day could have imposed a considerable imprint. Conversely, in precipitation samples, mixing of enriched and depleted rain events were surely collected. Coherently, heavy isotopes content in precipitation were more negative during the rainy season (May to June and October to November) than the dry season (January to March and August to September) due to the amount effect.

Seasonal variation of the heavy isotopes in the UCRB responded more to the change in rainfall amount than to the one of temperature. In agreement with this, Vimeux et al. (2005) found in Bolivia that local temperatures had minor influence on the stable isotopes composition. Example values like -0.58 ‰ $\delta^{18}O$ / °C (Lachniet and Patterson, 2009) and 1.13 to 1.64 $\delta^{18}O$ ‰ / °C (Vuille and Werner, 2005) gave an insight of the magnitude of the variation of $\delta^{18}O$ with temperature in the tropics. If as an example, taking the above-mentioned gradients, a rounded annual variation of 5° C would be considered for any station in the UCRB, as a consequence, a variation between of 2.9 and 8.2 ‰ $\delta^{18}O$ across the year would be expected. This expected theoretical variation is much lower than the one in the precipitation samples although within the ranges of the ones for stream water in the basin. In line with this, the low correlation with temperature is confirmed in this study by the fact that despite of a low variation of the temperature along the year, the isotope concentrations responded wide and clearly to the modification of the precipitation patterns. Snapshot examples strengthen this hypothesis. For instance, isotopes values in S1 in the month of May (wet period) are very contrasting in the two sampled years: while the precipitation was higher in 2017 than in 2018 for the same period, the temperature remained the same. This isotopic variation, independently from temperature is explained by giving the precipitation amount a key role in this variation.

On the surface water isotopes values, the effect of amount might also have exerted control since the minimal values matched with the increase of the stream discharge, typically appearing during the rainy months. On this respect, Saylor et al., (2009) concluded the same effect of precipitation on surface water in the Eastern Andes of Colombia. This behavior agrees with the findings of Gonfiantini et al., (2001) in Bolivia where typically, surface water presented more depleted heavy isotopes values than precipitation. Stream water samples in the highest stations (S1 and S2) are congruent with the seasonal influence. A clear example is the most depleted $\delta^{2}H$ and $\delta^{18}O$ values of all the research in May 16, 2017

where the registered values appeared one week after the heaviest rainfall event of the whole recorded period.

On the other hand, seasonal variation is masked in the stream stations S3, S4 and S5, which are simultaneously downstream the boundary between the Andean forest and the páramo (3900 m a.s.l.). This attenuation effect was already described by Gomez et al. (2015) in Bucaramanga (eastern Andes); a variation of only 2 ‰ in the extremes for stream water were found. The low isotope variation together with the more depleted values, might then be attributed to the role of the Andean forest canopy and the Cloud forest fringes in the increase of the evaporation. The extra evaporation might have caused a push of the isotope signals towards a homogenization of the O and H stable isotopes ratios. This vapor recycling effect has been observed in bigger scales as well, for instance in the Amazonas forest, where the evaporation is the dominant factor during the winter months (Salati et al. 1979). The effect above described might have been caused as well by several factors such as (i) buffering effect by groundwater input from upper recharge areas (ii) mixing and neutralization by thermal waters or (iii) mixing with surface water from upstream.

At last, d-excess also indicates a higher evaporation in stream water at lower topographies where the forest is located. These scenarios given by the d-excess will be developed later in the discussion.

Precipitation patterns in the Andean region of Colombia are similar in terms of distribution of the rain over the year. Rainy and dry seasons in Bogotá and the UCRB correspond in months and duration, presenting a bi-modal behavior. Most depleted isotopic values are found in the rainiest month of the year (June) and for the second rainy season (November) in both sites. During a hydrological year, $\delta^{18}O$ average values of Bogotá are higher than P8 and P6 of the UCRB. This difference might be explained by an altitude effect in the study area since the rainfall collectors surpassed the altitude of Bogotá by around 1500 (P8) and 1800 m (P6), causing the rainfall to be more depleted in heavy isotopes. Nonetheless, despite P7 collector is higher than Bogotá by 1000 m, its less depleted peaks during the dry seasons are more positive than the ones of Bogotá. Another explanation for the observed depletion displacement in the stations of the study site may be probably that the period of evaluation of only one year in the UCRB might have accented the influence of single extreme values when compared to the long-term records of Bogotá. Furthermore, the secondary lowest peak for $\delta^{18}O$ average in the UCRB was observed around November, contrasting by one month with the findings of Saylor et al., (2009) for the region of Bogotá, where this was located in October. Such time displacement, must be assessed to the light of the interaction of the ITCZ on the different locations of the sites.

5.7 Amount effect

According to Sturm et al. (2007), the amount effect in South America is dominant during rainy season. In the UCRB, even though higher values of accumulated precipitation presented more depleted values of $\delta^{2}H$ in accordance with the expected amount effect, the precipitation amounts are not exactly reporting individual events but their sum. A clear example is P6 where accumulated precipitation of 386 mm shows the most depleted $\delta^{2}H$ value, -150.4 ‰, remaining unclear if the cause is either because of the sample was describing a predominant rain event or because it was taken in the rainy season or because the precipitation accounts for 3.5 months. Despite of the obstacle to make comparisons, which must be dealt with a more systematic sampling at event scale, more depleted values can be observed in the rainiest months of the year indicating either a seasonal effect or an amount effect, but more likely the overlapping of both. Finally, a comprehensive analysis of the amount effect cannot be conducted since the samples are mixing different types of rain events (light and heavy).

5.8 Altitude effect

In the UCRB, the concentration of heavy isotopes decreases as altitude increases, which is coherent with the expected behavior given by the altitude effect (IAEA, 2000; Dansgaard, 1954). However, the $\delta^{18}O$-altitude correlation is not homogeneously linear neither for precipitation nor for stream water samples. This effect was already observed by Gonfiantini et al. (2001) who through model simulations

established that the altitude effect deviates from linearity when altitude increases. For example, contrasting gradients can be extracted when analyzed stream samples located below the 4100 m a.s.l. with the ones located upstream. The scattering occurring for these sites above 4100 m a.s.l. might be explained by (i) the precipitation amount influence given by a seasonal effect, (ii) the temperature vertical gradient and (iii) the initial relative humidity of the ascending masses.

The comparison of the altitude gradient based on the precipitation-weighted mean (PW-M) for the stations P6, P7 and P8 showed a non-linearity in the regression line. This was because of the presence of more enriched $\delta^{18}O$ values in P8 which pulled the PW-M towards zero causing a weak positive correlation expressed by an R^2 value of 0.5. This permits to interpret that there is a significant influence by the amount effect expressed in the large variation of the $\delta^{18}O$ range over time. Furthermore, the PW- M of P6 is the most depleted, which is coherent for the highest station. The altitude effect gradient of - 0.36 ‰ of $\delta^{18}O$ / 100 m is, however, higher than the reported by other studies in similar locations of the tropical regions such as -0.2 ‰ of $\delta^{18}O$ / 100 m (Cortes et al., 1997) and -0.22 ‰ of $\delta^{18}O$ / 100 m (Windhorst et al., 2013) but fits in the range of 0.1 to 0.6 ‰ of $\delta^{18}O$ / 100 m stated by Windhorst et al. (2013), -0.35 ‰ of $\delta^{18}O$ / 100 m (Sánchez-Murillo et al., 2013) or 0.4 to 0.6 ‰ of $\delta^{18}O$ / 100 m (Siegenthaler and Oeschger, 1980b).

Additionally, in coherence with the behavior for precipitation water. The correlation $\delta^{18}O$-altitude in stream water considering all the samples showed the same R^2 correlation coefficient (0.5) as precipitation. An attempt to improve the description of the altitude effect by omitting the $\delta^{18}O$ values of months which did not coincide for all the stream stations was successful. This correction improved the fit of the line to R^2=0.62 with a gradient of -0.18 ‰ of $\delta^{18}O$ / 100 m. It indicates a better correlation, although still not completely linear. This non-linearity seems to be due to the higher dispersion of the isotope values in the water located at high altitudes (S1 and S2) and closer to the glacier which is masking the altitude effect. These high-altitude stations are affected by the precipitation signature and therefore the amount effect compared to the lower ones (S3, S4 and S5) as well. Thus, overlapping effects (altitude and seasonal or amount) are more noticeable in the higher altitudes. The stream water shows an isotopic signature more like the rain (S2 and S1 vs P6) than that one of the stream water from lower altitudes (P7 vs S3). The non-linearity already discussed might be also a consequence of using the mean catchment elevation instead of the real altitude above the sea level. To cope with this, further calculations are recommended.

In lower altitudes (< 4100 m a.sl.), the mixture from water of the rest of the watershed and buffering effects caused probably by baseflow input are more observable. The variation of the $\delta^{18}O$-altitude correlation indicates a complexity in the hydrological cycle system. In the UCRB an orographic distillation process is clear since the $\delta^{18}O$ decreases more in lower topographies. This finding was already described by Sánchez-Murillo et al. (2013) in Costa Rica where a gradient of -0.2 ‰ of ^{18}O / 100 m was found in the inner mountainous valleys. Nonetheless, the non-systematic stable isotopes elevation relationships in the UCRB can be also attributed to what Rohrmann et al. (2014) called “convective storms”, typical in intermontane basins where convection dominates over adiabatic lifting of air masses. In this regard, further research must be done, since the complexity of the air circulation and the influence of the Chocó stream in the UCRB (Poveda et al. 2006) encourages to think of additional driving factors.

When $\delta^{18}O$-altitude correlations in more stations along Colombia are considered, two different gradients can be separated spatially and altitudinally. A boundary in the central branch of the Colombian Andes and in an altitude fringe between 2000 to 2500 m a.s.l. can be drawn. The eastern Andes showed more enriched $\delta^{18}O$ values than the western Andes, probably due to the influence of the air masses coming from nearby evaporation sources like the Caribbean Sea or the Amazon forest. On the other side, the variation in the altitude effect of ^{18}O was higher for samples located below the fringe 2000 to 2500 m a.s.l. and concurrently for stations located to the east of the Central Andes. For Rozanski and Araguas (1995), the change of the altitude gradient in the northern Andes occurred from 3000 m a.s.l. supporting the finding in this research although with a slight variation. In line with this, different sources of air masses for the eastern and the western Andes might be a coherent explanation for the divergent altitude effect of the study area. This proposed hypothesis is coherent with the IDEAM and UPME (2017) wind

direction models which locate the UCRB as a convergent point of all the wind sources all around the year. At last, a marked effect of continentality on the altitude effect was observed since the stations located close to the coast showed enriched isotope values.

In conclusion, the altitude effect for precipitation found in this study was in agreement with the one described for the entire Colombia by Rodríguez (2004) 0.25 ‰ / 100 m. The altitude effect of stream water matched to the ones found in two transects in Ecuador of -0.17 ‰ / 100 m (García et al., 1997), to -0.18 ‰ / 100 m for multiple sites of the Eastern Andes in Colombia (Saylor et al., 2009) and with several more gradients that can be observed in Table 7.

5.9 LMWL

LMWL´s for P6 and 8 showed intercepts widely deviated from 10 due to the evaporation effect. For P7, the line was close to the GMWL. The δ^2H and δ^{18}O values for the three precipitation stations are generally scattered and not homogeneously clustered due to the influence of seasonal effects. The most disperse values belong to the station P7 which has very enriched isotopic and very depleted values compared with the other two stations. Stream water values of the upper watershed appeared mostly in the middle of the graph due to homogenization of the isotopic content by buffering factors given by the mixing of different tributaries and probably the input of baseflow released over time. These values followed slightly the tendency of the precipitation though, depleted in rainy season and enriched in dry season. Outlier values and anomalies belong only to S1 and S2. Comparison of the lines in the UCRB with others of the country also showed a larger difference of the intercept value as the altitude increases.

The difference between the slopes in the LMWL´s and the surface water linear regression suggests that surface water isotope concentrations have been modified significantly by evaporation or mixing. Therefore, it is not clear if this evaporation occurred during rainfall or other processes (Kendall and Coplen, 2001). Also, not only the occurrence of distillation processes can cause this but also the characteristics of the precipitation and its various driving factors like the origin of air masses. The LMWL for the UCRB, $\delta^2H = 8.13\ \delta^{18}O + 12.5$, R^2=0.98, differs from the Colombian Meteoric Line proposed by Rodríguez (2004) $\delta^2H = 8\ \delta^{18}O + 9.6$, which is not extraordinary if it is considered that only precipitation from altitudes above 3600 m a.s.l. were taken.

Precipitation-weighted means of δ^2H and δ^{18}O of the study area are considerably more depleted when compared with other locations of the country, especially those ones close to the sea level. Values are only comparable with the station Albania (3000 m a.s.l.) located to the west of the Central branch of the Andes. Conversely, it is noticeable that despite of the altitude of Bogotá station (2600 m a.s.l.), the values of δ^{18}O would not match for the altitudes of the UCRB if the altitude gradient found in this research would be used to calculate it. Values of 16.98, 14.1 and 16.7 ‰ in δ^{18}O would be expected for P6, 7 and 8, respectively. These two facts give support to the non-linear behavior of the altitude effect in this part of the tropics as well as to the hypothesis of a different altitude gradient for the eastern Andes compared to the western ones, both found in this study.

5.10 Deuterium excess

High d-excess values generally indicate that more evaporated moisture has been added to the air mass (Gat, 1996) and low values are associated with waters fractionated by evaporation and/or high moisture content in the moisture source (IAEA, 2000; Kendall and Coplen, 2001).

Generally, high d-excess for precipitation in the UCRB occurs in dry months and low and negative values in rainy season. Temperature seems to play a minor role on the d-excess since the latter widely varies despite the low fluctuation of temperature through the year. Other parameters, such as relative humidity (RH) and precipitation source are more likely to affect the d-excess (Pfahl and Sodemann, 2014). For the first, IDEAM data shows that the RH during the year is lower in the dry season, the variation, nonetheless, is < 15 % between extreme values. This relation only confirms the expected

high values of d-excess for dry periods. Thus, the d-excess variation in the UCRB might suggest that high values are mainly a consequence of recycled moisture and secondarily of relative humidity changes. This phenomenon, had been described before in a similar tropical basin in Costa Rica by Sánchez-Murillo et al. (2017). There, the occurrence of high d-excess in dry periods with moisture recycling enhanced by local evapotranspiration and evaporated rainfall in rainy periods was observed.

The phenomenon above mentioned is in good agreement with the explained source of rain for each of the periods. During dry season, since air masses from the north do not bring humidity, rainfall must be produced by local cycles of evaporation and precipitation, generating a constant recycling. Evaporative sources can be from several lakes (Martinelli et al., 1996) whose requirement would be accomplished by the several ones present in the paramo ecosystem as well as the cloud forest and the Andean forest, known as important humidity generators. In practice, these approaches can be tested through long term isotope monitoring programs that allow to give hints for the influence of open bodies of water and land use on the evaporation processes as proposed by (Henderson-Sellers and McGuffie, 2006).

On the other hand, during rainy season, the waters are coming from the east (Amazonas and Atlantic) after several episodes of fractionation occurred in the trade winds (Vallet-Coulomb et al., 2008). Nevertheless, the influence on d-excess by local processes like soil evaporation (Jouzel et al., 2013), mixing sources and recycled air moisture (Froehlich et al. 2002) and finally sampling routine procedures are not discarded. As an example of the last aspect, low d-excess values for P6 occurred in dry periods except for the rainy month May, where a rupture of the flask and long periods of sampling presumably caused evaporation from the sampler. These two factors may have affected the evaporation rate of the precipitation samples once collected.

Altitude showed a slightly positive correlation with d-excess as already observed by (Koeniger et al. 2017) in Lebanon. This is logic for the air masses that reach the top of the mountain (5000 m a.s.l.) being the ones that underwent the most evaporative history and the highlighted effect of increase in wind velocity and subsequent change in evaporation regime (Clark and Fritz, 1997; Sánchez-Murillo et al., 2017). Additionally, the variation of d-excess in stream water is higher in the stations located at lower topographies than close to the glacier, maybe because of enhanced evaporation while flowing in the channel.

5.11 Thermal springs influence on stable isotopes

It is accepted that once the water is infiltrated in the soil, its isotopic composition does not vary unless there is geothermal influence (Panarello and Albero, 1981). The low variation in the isotope values along the year for the surface water in the sampling stations S3 and S5, might be explained, additionally to the reasons already provided, by a buffering effect given by the input of isotopically enriched thermal water from the hot springs upstream of these two stations. Hot spring waters are usually more enriched in ^{18}O than meteoric waters and the shift between them increases with temperature (Gonfiantini and Panichi, 1978; Hoefs, 2009). Concurrently, ^{2}H remains unchanged. In this sense, S3 and S5 which should have similar isotopic signatures to the depleted values of their rains, might have undergone a shift towards more positive values in the isotope signal, mitigating the temporal variation.

Likewise, Arango et al. (1970) found $\delta^{2}H$ and $\delta^{18}O$ values of -110.7 and -15.4 ‰, respectively, in a sample taken from a hot spring (3630 m.a.s.l.) upstream of S3 and S5 in the UCRB. However, this only measured value in the 70´s is even more depleted than the actual ones for the stream water. One explanation for this inconsistency, is that according to Clayton and Steyner (1975), most of the water from hot springs comes from local precipitation. This, in effect, indicates that the depleted hot spring value would depend on the initial conditions of the meteoric water in the sampling time, for now unknown.

Another way to illustrate the influence of thermal systems in the same volcanic arc of the NRV, are the findings by Fischer et al. (1997) in the Galeras Volcano, 450 km to the south of NRV. Here, he measured $\delta^{2}H$ and $\delta^{18}O$ values in thermal water discharges from -64 to -82 ‰ and -11.1 to -8.5 ‰, respectively. This means, more enriched values that certainly influence the stream water when mixing occurs.

In consequence, an influence on the isotopic composition of the stream water in Stream 3 and 5 sampling sites is expected from the hot springs waters. Surely, the fluctuation in the hydrothermal system temperatures (around 2° C) might cause an increase or decrease of the δ values of stable isotopes in the stream waters, although it is not known at what extent. Also, the isotope concentrations would be significantly influenced by the initial isotope signature of the precipitation. Finally, this proposed geothermal effect would explain additionally, the lower slope of the linear regression for stream water compared to the one of the GMWL (Figure 29). However, this influence must be further researched since the monitoring campaigns were not designed considering this factor, and on top of that, none sample from the hot spring was taken.

5.12 Volcanic emissions

Volcanic emissions had a clear influence on the hydrochemistry of the surface water of the watershed as discussed previously. As for the stable isotopes concentration in surface and precipitation water, no reliable comparisons between ash fall events and isotopes concentrations were possible. First, there was not certainty on whether the ash fell into the collector and second, a long-term and higher temporal resolution water sampling was not carried out to establish systematic correlations. However, it is clear that the volcanic activity has influenced the faster melting of the Conejeras glacier in the UCRB (Morán-Tejeda et al., 2018) and therefore there is an input of water with specific isotopic signatures as the glacier responds to the weather. On this regard, isotopic patterns in stream water more influenced by weather phenomenon like the ENSO would be expected due to the high relevance of the glacier on the hydrology of the watershed.

5.13 Wind direction

The stable isotopes concentration cannot be understood without looking at the wind circulation patterns from a regional perspective. For the UCRB, there is a high degree of complexity since it is influenced by winds from the Caribbean Sea, the Atlantic Ocean and the Pacific Ocean all around the year although in different intensities depending on the months. Additionally, there are more local phenomena such as the Chocó Stream, the inter-mountain precipitations caused by adiabatic heating and the input of recycled moisture from the Cloud forest, the Andean forest (2200 to 3500 m a.s.l.) and páramo ecosystems (3500 to 4500 m a.s.l., respectively) as well as the Amazon Forest.

If the monthly wind provenance maps provided by IDEAM and UPME (2017) are observed, it can be concluded that during the dry season of December, the winds come from the north (probably the Caribbean Sea) and the west (Pacific Ocean passing through the Chocó Jungle, one of the most humid places on earth). However, the mentioned winds are dry and therefore a small imprint from the sea must be evident. In line with this, the rain events of this dry period should describe the isotope signature of rains produced locally and therefore with a high imprint of moisture recycling. On the other hand, during the rainy season of May the winds come from the Pacific Ocean and the southeast. Conversely, these streams carry a big amount of humidity and therefore the isotope signature in the local rains must be showing the composition of the Atlantic Ocean modified by the recycling of the Amazon forest and the ascent of the Andes (both the eastern and the central branch).

Finally, despite the simplification of IAEA (2000) arguing that the precipitation in the crest of the Andes slopes results from the Atlantic and in lower elevations from the Pacific Ocean. This study concludes a higher complexity influencing the isotope and chemical signatures. All the hypotheses posed in this work are welcomed to be discussed and further researched. The importance of the study here conducted lies also on understanding the isotopes and the hydrochemistry as tools to take correct decisions for the water management of the catchment.

It is worth to emphasize that the foregoing paragraphs represent the first tentative interpretation of a systematic isotopic monitoring program in the high tropical Andes of Colombia. This certainly is subject to reinterpretation, verification and development in the light of further investigations and more specific data availability.

6. CONCLUSIONS

The study of the hydrochemistry and stable isotopes in precipitation and surface waters of the UCRB showed a complex interaction between local vulcanological, meteorological and geological factors. However, the geographical and topographical setting of the Central Andes as well as the ENSO position through the year, establish the regional scenario that shapes the water cycle in the study site.

Precipitation and surface water from the upper and southern section of the basin showed very low conductivity values (40 µS/cm), contrasting with surface water in the northern section. pH values in precipitation and lakes were acidic (< 5.7) probably by the influence of aerosols coming from the volcanic ash emissions of the NRV or the ascending of air masses coming from the city of Manizales (4.9 in average). However, the pH and conductivity increased progressively as the interaction between precipitation and the geological materials occurred. In the same way, the proximity to the NRV and the presence of a hot-spring enhanced the alkalization and the presence of dissolved ions in the surface water.

Major ions concentrations were higher in samples from dry season than in the ones of rainy season for both surface and precipitation. For the first, the influence of several factors such as (i) dilution caused by runoff availability, (ii) less number of volcanic emissions before the rainy season sampling, (iii) size of the drainage area, and (iv) input of baseflow with a higher load of elements in solution; explain these variations. For the second, only number (ii) can explain it. Furthermore, higher concentrations of elements such Mg, Ca, Na, K and the presence of Fe, Al, Ti, As, Mb, Mn, V, Ba, and F in the surface samples of the northern part of the watershed confirms the interaction between rainfall with the geological units and the presence of thermal springs. Minerals such biotite, hornblende, augite, muscovite and a wide range of plagioclases and potassic feldspars are among the typical minerals in the geological units outcropping in the area. Trace elements were found in higher concentrations in the lake CL and stream sample S2 due to a high evaporation rate and a contribution of groundwater where aluminosilicates were the most predominant material eroded. Finally, despite of the influence of volcanic activity, agriculture, hydrothermal systems and cattle raising, the water in the UCRB is -based on the WHO and Law 2115 guidelines- *chemically* drinkable from the source. The analysis of these hydrochemical data are very valuable to establish first approaches to the understanding of interaction between the volcanism, meteorology and hydrochemistry in the Central Andes of Colombia.

The results for δ^2H and δ^{18}O values showed a high range of variation in stream and precipitation due to the difference in altitude, meteorological conditions and seasons. In coherence with this, the seasonal variation of the stable isotopes concentration responded more to the change in rainfall periods and amounts than to the one of temperature. Heavy isotopes content in precipitation were clearly more negative during the rainy season (May to June and October to November) than the dry season (January to March and August to September) due to the amount effect. As for the stream stations, the seasonality effect followed the behavior of the precipitation samples only in the upper watershed. In the stations S3, S4 and S5, the seasonality was masked presumably due to several reasons, namely, (i) the role of the Andean forest canopy and the Cloud forest fringes in the increase of the evaporation, (ii) buffering effect by groundwater input recharged in upper areas (iii) mixing and neutralization by thermal waters, and (iii) mixing with surface water from upstream areas.

In the UCRB, the concentration of heavy isotopes decreased as altitude increases. An altitude effect gradient of -0.36 ‰ of δ^{18}O / 100 m was found for precipitation and of -0.18 ‰ of δ^{18}O / 100 m for surface water. However, the δ^{18}O-altitude correlation is not homogeneously linear for any of them due to the masking by the amount effect especially at higher altitudes. On the other hand, mixing of surface and groundwater along with local meteorological phenomena imprint might have also played a key role in the modification of the altitude gradient. Finally, based on the δ^{18}O-altitude correlations and the Precipitation-weighted means of δ^2H and δ^{18}O along Colombia, two different gradients can be separated spatially and altitudinally. The first, with a boundary in the central branch of the Colombian Andes dividing the western and the eastern part of the country, where the eastern is more enriched in δ^{18}O.

The second, with a boundary in the fringe between 2000 to 2500 m a.s.l. where the linearity of the altitude effect changes.

The LMWL for the UCRB, $\delta^2H = 8.13\ \delta^{18}O + 12.5$, $R^2=0.98$, differed from the Colombian Meteoric Line proposed by Rodríguez (2004) $\delta^2H = 8\ \delta^{18}O + 9.6$, which is not extraordinary if it is considered that only precipitation from altitudes above 3600 m a.s.l. were taken in this study. The difference between the slopes in the LMWL´s and the surface water linear regression suggested that surface water isotope concentrations have been modified significantly by evaporation or mixing.

Generally, high d-excess for precipitation occurred in dry months and low and negative values in rainy season. Thus, the d-excess variation might suggest that high values are mainly a consequence of recycled moisture and secondarily of relative humidity changes. During dry season, since air masses from the north do not bring humidity, rainfall must be produced by local cycles of evaporation and precipitation, generating a constant recycling. In contrast, during rainy season, the waters bring humidity from the east (Amazonas and Atlantic) after several episodes of fractionation occurred in the trade winds. Nevertheless, the influence on d-excess by local processes like soil evaporation, mixing sources, recycled air moisture and sampling routine procedures are not discarded. These hypotheses can be tested through long term isotope monitoring programs that allow to give hints about the influence of open bodies of water and land use on the evaporation processes.

Based on the analysis of the isotope signatures of the study area and others in Colombia and the tropical Americas, it is concluded that there is a high degree of meteorological complexity in the Colombian Central Andes. The effect of winds from the Caribbean Sea, the Atlantic Ocean and the Pacific Ocean all around the year; the presence of the vast Amazon Forest as evaporation source; the reported local phenomena so-called “Chocó Stream”; the inter-mountain precipitations caused by adiabatic heating; the input of recycled moisture from the Cloud forest, the Andean forest and the páramo ecosystems; and lastly the volcanic systems, constitute the interesting range of driving factors on the water cycle of the tropical Andes.

The present study provides a comprehensive analysis of the isotopic and chemical composition of surface and precipitation water in the Upper basin of the Claro River. The LMWL´s, altitude gradients and chemical composition could be used to set up a methodology for the “National Network of Isotopy” and the “Glaciers and High Mountain Ecosystems Monitoring Program” ran by IDEAM; to compare with hydrological and hydrogeological studies to continue understanding the water cycle in the region as well as to make decisions on the catchment management.

Thanks for reading…

7. APPENDIX

7.1 Appendix 1: Location of the study sites on stable isotopes referenced in this section across the tropical América.

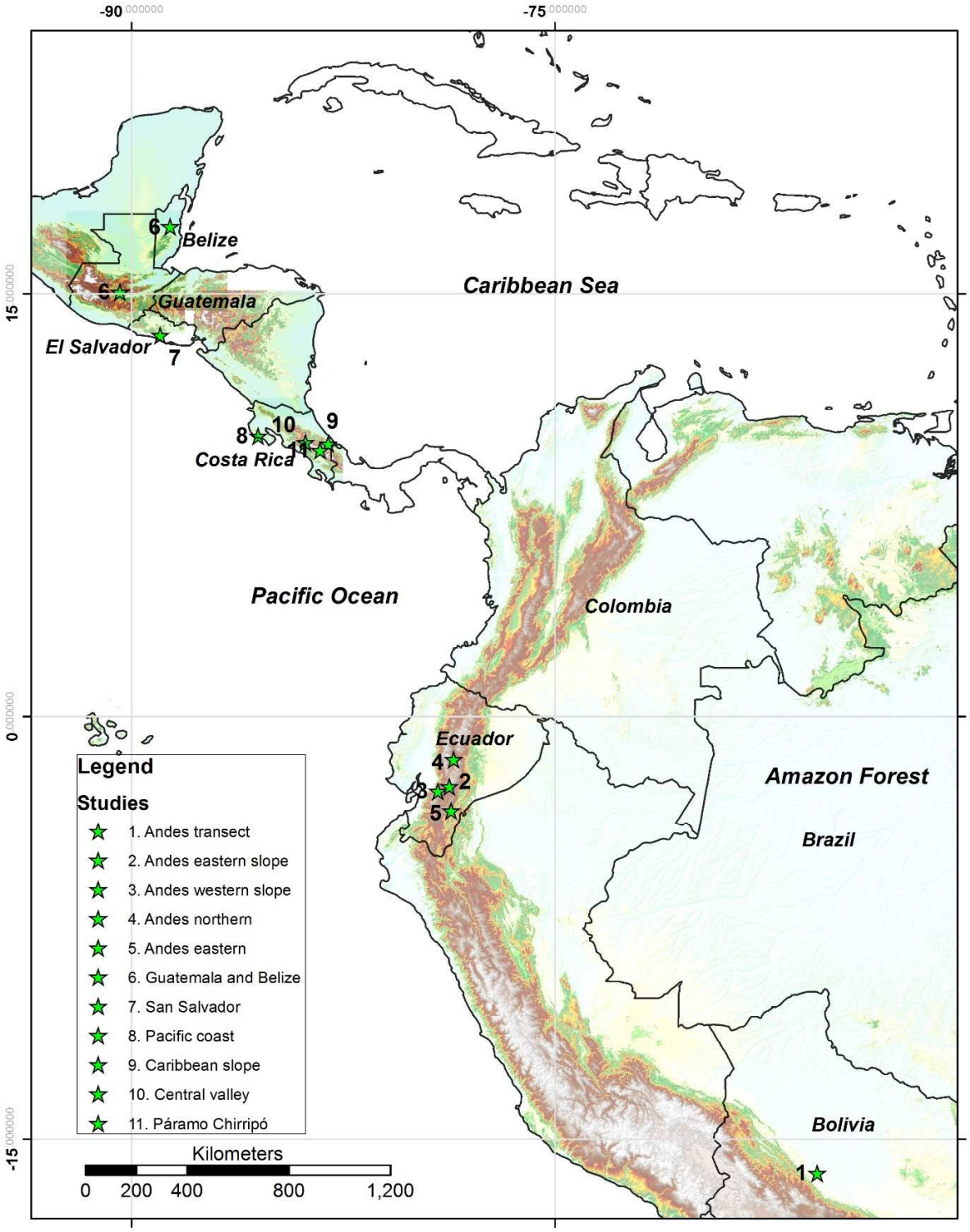

7.2 Appendix 2: Location of the study sites on stable isotopes across Colombia.

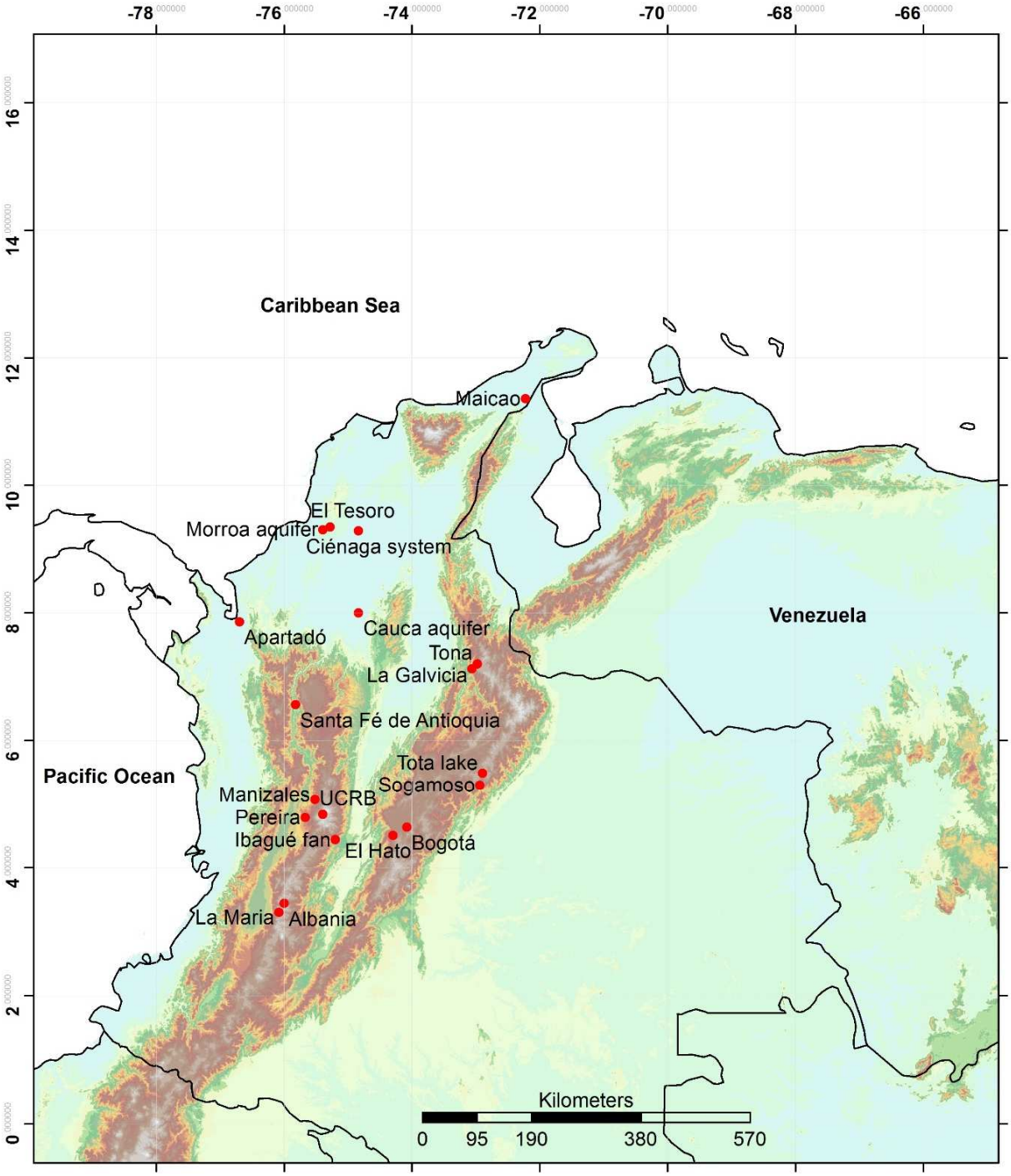

7.3 Appendix 3: δ^2H, $\delta^{18}O$ values for the totality of the precipitation and surface samples in the study site.

Location	Sampling date	δ18O (‰)	δ2H (‰)
Stream 1	21/01/2017	-10.78	-88.8
	16/03/2017	-10.80	-89.8
	11/04/2017	-11.13	-92.6
	16/05/2017	-21.85	-150.5
	13/06/2017	-19.75	-140.6
	18/07/2017	-16.38	-110.6
	15/08/2017	-14.65	-101.2
	12/09/2017	-14.74	-100.9
	15/10/2017	-14.73	-100.7
	09/11/2017	-15.63	-100.4
	13/12/2017	-14.79	-99.6
	31/01/2018	-12.99	-90.2
	08/03/2018	-11.53	-84.9
	10/04/2018	-12.14	-89.1
	18/05/2018	-15.44	-111.8
	20/06/2018	-14.26	-106.5
	24/07/2018	-12.97	-98.4
	15/08/2018	-13.97	-100.0
	17/09/2018	-12.78	-94.2
	20/10/2018	-12.25	-98.0
	19/06/2019	-13.97	-100.9
Stream 2	22/01/2017	-8.57	-79.4
	23/02/2017	-11.17	-91.8
	16/03/2017	-12.01	-97.9
	11/04/2017	-11.86	-94.2
	16/05/2017	-23.77	-165.5
	13/06/2017	-19.19	-131.5
	18/07/2017	-15.27	-105.2
	15/08/2017	-14.23	-89.5
	12/09/2017	-13.88	-94.5
	15/10/2017	-14.36	-98.6
	09/11/2017	-14.45	-94.9
	13/12/2017	-15.25	-100.7
	31/01/2018	-14.67	-96.6
	08/03/2018	-12.34	-88.9
	10/04/2018	-12.73	-96.2
	18/05/2018	-17.81	-132.9
	20/06/2018	-13.83	-101.2
	24/07/2018	-12.13	-84.6
	15/08/2018	-14.30	-102.0
	17/09/2018	-15.27	-107.2
	20/10/2018	-14.59	-108.0
	19/06/2019	-14.68	-105.5
Stream 3	22/01/2017	-13.12	-99.1
	24/02/2017	-13.93	-100.8
	16/03/2017	-14.01	-98.1
	11/04/2017	-14.39	-100.4
	17/05/2017	-16.18	-109.1
	19/07/2017	-14.95	-104.9
	16/08/2017	-15.11	-101.0
	13/09/2017	-13.85	-98.2

	17/10/2017	-15.42	-105.1
	11/11/2017	-15.13	-108.2
	14/12/2017	-15.15	-107.7
	01/02/2018	-15.41	-103.4
	09/03/2018	-14.12	-102.7
	20/05/2018	-14.87	-105.1
	21/06/2018	-13.85	-104.9
	26/07/2018	-13.92	-101.9
	13/08/2018	-14.37	-102.0
	21/10/2018	-13.27	-100.0
	21/06/2019	-14.42	-103.3
Stream 4	22/01/2017	-13.93	-90.9
	24/02/2017	-14.46	-95.0
	16/03/2017	-13.94	-89.0
	11/04/2017	-14.45	-92.8
	17/05/2017	-12.83	-97.4
	19/07/2017	-13.31	-96.6
	16/08/2017	-12.43	-96.6
	13/09/2017	-13.77	-98.3
	17/10/2017	-12.93	-98.3
	11/11/2017	-12.94	-98.4
	14/12/2017	-12.26	-97.2
	01/02/2018	-12.22	-94.9
	09/03/2018	-13.34	-99.6
	20/05/2018	-13.53	-95.3
	21/06/2018	-13.70	-95.4
	26/07/2018	-13.30	-95.8
	13/08/2018	-17.33	-93.5
	21/10/2018	-12.54	-94.4
	21/06/2019	-13.64	-97.2
Stream 5	24/02/2017	-14.44	-89.9
	15/03/2017	-15.10	-97.7
	17/05/2017	-13.00	-100.3
	19/07/2017	-12.59	-97.8
	16/08/2017	-12.83	-99.3
	13/09/2017	-13.20	-97.0
	11/11/2017	-13.02	-94.6
	01/02/2018	-8.66	-61.8
	09/03/2018	-13.46	-99.3
	20/05/2018	-13.90	-97.6
	19/06/2018	-14.15	-97.3
	26/07/2018	-14.03	-99.3
	13/08/2018	-13.01	-95.8
	15/09/2018	-13.80	-94.9
	21/06/2019	-13.91	-99.9
SC	20/06/2019	-14.74	-106.7
RC-RL	19/06/2019	-14.84	-111.9
RC-CL	20/06/2019	-11.92	-94.0
RC-GM	19/06/2019	-14.84	-106.0
Precipitation 6	18/07/2017	-14.46	-101.8
	15/08/2017	-9.49	-61.9
	12/09/2017	-10.89	-74.2
	17/10/2017	-12.97	-89.8
	09/11/2017	-13.79	-99.2
	13/12/2017	-12.81	-87.7
	31/01/2018	-8.46	-62.2
	18/05/2018	-19.89	-150.4
	20/06/2018	-16.83	-119.9

	25/07/2018	-13.95	-93.3
	15/08/2018	-13.52	-100.7
	17/09/2018	-11.48	-80.7
	20/10/2018	-15.22	-113.3
	19/06/2019	-16.02	-116.8
Precipitation 7	20/05/2017	-9.89	-84.1
	16/06/2017	-17.24	-135.3
	03/07/2017	-14.23	-107.6
	30/07/2017	-9.87	-69.7
	15/08/2017	-5.99	-46.6
	31/08/2017	-9.36	-66.2
	30/09/2017	-10.01	-69.5
	30/10/2017	-14.80	-107.9
	11/11/2017	-11.49	-82.8
	15/11/2017	-14.78	-105.9
	01/12/2017	-11.21	-79.3
	14/12/2017	-13.88	-98.6
	01/02/2018	-13.43	-101.7
	15/02/2018	-3.45	-9.6
	01/03/2018	-6.29	-38.4
	16/03/2018	-2.41	-5.2
	01/04/2018	-12.24	-89.6
	15/04/2018	-13.81	-99.1
	02/06/2018	-19.00	-140.9
	21/06/2018	-15.21	-119.2
	30/06/2018	-12.26	-94.1
	17/07/2018	-10.62	-81.6
	01/10/2018	-14.11	-99.8
	21/10/2018	-14.67	-101.8
	20/06/2019	-16.55	-124.9
Precipitation 8	16/08/2017	-10.35	-65.1
	13/09/2017	-10.97	-76.5
	17/10/2017	-11.72	-83.5
	10/11/2017	-12.83	-103.3
	13/12/2017	-13.68	-95.2
	01/02/2018	-10.71	-61.9
	08/03/2018	-6.75	-38.3
	19/05/2018	-19.42	-147.2
	19/06/2018	-15.50	-119.4
	25/07/2018	-13.09	-93.5
	14/08/2018	-13.00	-95.2
	16/09/2018	-11.76	-86.4
	20/06/2019	-14.61	-110.2

7.4 Appendix 4: Results of major ions analysis.

				results of Ion Chromatography [mg/L]														Titration
		EC at 25°C [µS/cm]	pH [-]	lithium (Li+)	sodium (Na+)	ammonia (NH4+)	potassium (K+)	magnesium (Mg2+)	calcium (Ca2+)	strontium (Sr2+)	fluoride (F−)	chloride (Cl−)	nitrite (NO2−)	bromide (Br−)	nitrate (NO3−)	phosphate (PO43−)	sulphate (SO42−)	bicarbonate (HCO3-)
2nd campaign - rainy season	RC-VTW	104.4	7.04	0.02	3.92	0.20	1.48	4.06	9.99	0.15	0.12	2.69			0.35		23.17	27.58
	RC-CTW	32.5	6.74		1.03	0.02	0.65	0.78	2.46		0.09	2.53			0.18		1.06	8.05
	Stream 1	26.01	7.7		1.16	0.03	0.82	0.53	1.70		0.07	1.02			0.01		1.22	7.32
	Stream 2	14.02	7.43		0.77	0.18	0.25	0.09	0.30		0.08	0.10				0.26	0.26	2.76
	Stream 3	200	7.27		8.46	0.20	3.37	7.93	16.37	0.20	0.25	1.12			0.43	0.17	58.52	48.77
	Stream 4	146.9	7.16	0.03	6.78	0.19	4.18	5.92	12.14	0.20	0.23	1.66			1.71	0.13	24.86	52.43
	Stream 5	200.3	7.35	0.03	7.54	0.20	3.21	7.33	17.52	0.17	0.22	1.59			0.40	0.09	55.09	41.46
	Precip. 6	18.86	5.63		0.10	0.02	0.12	0.04	0.23		0.00	0.04			0.01		0.15	
	Precip. 7	36.3	4.54		0.11	0.10	0.50	0.08	0.38		0.08	1.89					1.04	4.88
	Precip. 8	19.64	5.61		0.21	0.33	0.52	0.08	0.59		0.04	0.79			0.03	0.16	0.21	3.66
	RC-CL	26.9	5.38		0.70	0.05	0.72	0.54	1.73		0.15	3.05			0.01		2.01	
	RC-RL	10.5	5.4		0.26	0.05	0.29	0.10	0.62		0.05	0.79					1.08	
	RC-SC	230.2	8	0.04	8.38	0.20	3.91	7.49	17.00	0.15	0.37	1.96	0.01		0.19	0.25	58.68	47.55
	RC-GM	22.77	5.81		0.03	0.02	0.05	0.01	0.11								0.02	
1st campaign - dry season	Stream 1				2.07	0.193	1.111	0.81	2.313		0.065	1.81			0.447		3.503	
	Stream 2				1.215	0.19	0.239	0.322	0.968		0.04	0.098				0.041	2.247	
	Stream 3			0.037	9.899	0.206	3.635	8.353	17.907	0.184	0.269	1.291	0.02		0.562	0.077	61.629	
	Stream 4			0.033	8.312	0.203	4.249	6.329	13.516	0.208	0.228	1.77			1.011		26.556	
	Stream 5			0.035	9.195	0.186	3.531	8.065	19.77	0.178	0.229	1.744			0.409		61.885	
	Precip. 6				1.141	0.309	0.346	0.285	0.834		0.002	0.57					2.437	
	Precip. 7				1.086	0.311	0.531	0.365	1.221		0.02	1.35	0.007				2.795	
	Precip. 8				1.768	0.215	0.379	0.39	1.152		0.023	0.9					3.429	

7.5 Appendix 5: Results of trace elements analysis.

	results in ppb [µg/L]	Al27	Ti47	V51	Cr52	Mn55	Fe56	Co59	Ni60	Cu63	Zn66	As75	Se78	Mo95	Ag107	Cd111	Sn118	Sb121	Ba137	Tl205	Pb206/7/8	U238
2nd campaign - rainy season	RC-GM	4.29	0.21	0.09	0.06	0.17	2.50	0.01	0.05	0.44	1.39	0.00	<DL	0.74	<DL	<DL	0.02	0.04	0.07	<DL	0.10	0.01
	RC-CTW	16.22	0.25	0.11	0.24	0.30	56.81	0.02	0.56	3.95	1.84	0.18	<DL	0.18	<DL	<DL	<DL	0.02	29.68	<DL	0.04	<DL
	RC-VTW	17.88	0.15	0.48	0.05	0.61	0.67	0.02	1.86	1.26	3.52	0.21	0.84	1.14	<DL	0.08	0.01	0.72	30.21	<DL	0.03	0.02
	Stream 1	25.62	0.33	0.66	0.09	0.96	20.74	0.03	0.38	0.87	1.49	0.02	<DL	0.20	<DL	<DL	<DL	0.03	7.28	<DL	0.06	0.01
	Stream 2	175.05	5.35	4.11	0.49	1.07	43.69	0.02	0.12	0.91	2.81	0.39	<DL	0.36	<DL	0.01	0.01	0.07	4.27	<DL	0.12	0.02
	Stream 3	8.74	0.32	5.84	0.13	7.78	24.10	0.03	0.41	0.44	1.16	4.44	0.27	1.28	<DL	<DL	0.01	0.15	16.63	<DL	0.03	0.05
	Stream 4	16.42	0.44	4.92	0.36	2.45	23.04	0.03	0.33	0.65	2.74	1.40	<DL	0.61	<DL	0.01	0.01	0.11	39.00	<DL	0.03	0.15
	Stream 5	18.85	0.42	4.66	0.14	5.93	50.20	0.05	0.38	0.39	2.44	2.77	<DL	0.74	<DL	<DL	<DL	0.11	26.11	<DL	0.01	0.07
	Precip. 6	2.98	0.09	0.02	0.05	0.36	1.39	0.01	0.02	0.36	1.70	<DL	<DL	0.13	<DL	<DL	0.01	0.02	0.07	<DL	0.06	<DL
	Precip. 7	69.02	0.29	0.15	0.08	11.69	10.35	0.04	0.19	0.68	11.25	0.59	<DL	0.19	<DL	0.01	0.01	0.04	0.82	<DL	0.15	<DL
	Precip. 8	11.42	0.27	0.06	0.18	19.10	5.43	0.02	0.19	0.68	5.69	0.37	<DL	0.32	<DL	0.01	0.01	0.06	0.07	<DL	0.25	<DL
	RC-SC	10.23	0.40	5.61	0.21	2.79	7.54	0.02	1.02	0.29	1.70	3.22	<DL	1.54	<DL	<DL	0.01	0.16	16.45	<DL	0.01	0.03
	RC-RL	78.38	0.26	0.12	0.15	4.13	5.38	0.11	0.26	1.01	3.46	0.03	<DL	0.19	<DL	0.01	0.02	0.05	1.53	<DL	0.15	0.01
	RC-CL	218.55	0.71	0.33	0.38	50.03	72.41	0.31	1.64	0.81	12.79	0.20	<DL	0.20	<DL	0.01	0.01	0.04	6.51	<DL	0.10	<DL
1st campaign - dry season	Stream 1	2.35	0.38	0.65	0.13	0.05	5.78	0.01	2.08	1.24	0.53	0.04	0.72	0.80	<DL	<DL	0.01	0.08	9.25	0.01	0.04	<DL
	Stream 2	151.50	4.71	1.85	0.08	0.43	30.25	0.01	0.11	0.66	0.53	0.05	0.27	0.44	<DL	0.01	0.01	0.07	3.72	<DL	0.10	0.01
	Stream 3	1.75	0.48	5.93	0.20	0.14	0.30	0.01	0.59	0.52	0.47	4.72	0.20	1.25	<DL	<DL	<DL	0.20	28.05	<DL	0.03	0.02
	Stream 4	0.75	0.62	4.91	0.25	1.50	0.16	0.02	0.56	0.59	0.15	1.78	0.18	0.62	<DL	0.01	<DL	0.19	51.38	0.01	0.02	0.05
	Stream 5	1.08	0.66	4.49	0.37	0.20	3.48	0.01	0.47	0.96	0.22	3.04	0.54	0.87	<DL	0.01	0.01	0.20	37.59	<DL	0.03	0.04
	Precip. 6	0.37	0.10	0.07	0.12	1.17	<DL	<DL	0.29	0.64	3.98	0.10	0.42	0.14	<DL	<DL	0.01	0.10	1.97	<DL	0.04	<DL
	Precip. 7	1.65	0.20	0.07	0.05	19.28	0.94	0.01	0.22	0.46	20.61	0.13	0.32	0.11	<DL	0.03	0.01	0.09	2.01	0.01	0.06	<DL
	Precip. 8	1.53	0.15	0.02	0.15	57.27	1.85	0.03	0.38	9.88	33.95	0.15	0.08	0.08	<DL	0.02	0.06	0.11	1.96	0.01	0.65	<DL

7.6 Appendix 6: Results of rare-earth elements analysis.

REEs results in µg/L / ppb		139	140	141	146	147	151	160	159	163	165	166	169	174	175
	sample name	La139	Ce140	Pr141	Nd146	Sm147	Eu151	Gd160	Tb159	Dy163	Ho165	Er166	Tm169	Yb174	Lu175
2nd campaign - rainy season	RC-VTW	0.031	0.004	0.002	0.007	0.002	0.001	0.002	0.000	0.0011	0.0004	0.0009	0.0001	0.001	0.0001
	RC-CTW	0.039	0.0156	0.0033	0.0159	0.005	0.0011	0.0039	0.0005	0.003	0.001	0.0018	0.0002	0.0024	0.0004
	Stream 1	0.056	0.0444	0.0118	0.0556	0.014	0.0018	0.0126	0.0015	0.011	0.002	0.0076	0.001	0.0063	0.0011
	Stream 2	0.151	0.251	0.032	0.127	0.028	0.004	0.020	0.003	0.0126	0.0023	0.0064	0.0008	0.0051	0.0007
	Stream 3	0.025	0.006	0.001	0.006	0.002	0.001	0.002	0.000	0.001	0.0002	0.0009	0.0002	0.001	0.0002
	Stream 4	0.033	0.015	0.003	0.014	0.004	0.002	0.003	0.000	0.0027	0.0006	0.0018	0.0003	0.0026	0.0004
	Stream 5	0.037	0.0152	0.0029	0.0109	0.004	0.0011	0.0024	0.0004	0.003	0.001	0.002	0.0003	0.0017	0.0003
	Precip. 6	0.029	0.0043	0.0009	0.0032	0.001	0.0001	0.0006	0	0.000	0.000	0.0003	0	0.0003	0
	Precip. 7	0.039	0.029	0.0046	0.0195	0.006	0.0007	0.0033	0.0005	0.002	0.001	0.0016	0.0002	0.002	0.0002
	Precip. 8	0.045	0.046	0.006	0.020	0.005	0.000	0.005	0.001	0.003	0.0005	0.0012	0.0001	0.0006	0.0001
	RC-CL	0.067	0.093	0.014	0.061	0.012	0.002	0.011	0.001	0.006	0.001	0.004	0.001	0.004	0.0004
	RC-RL	0.056	0.055	0.009	0.043	0.009	0.001	0.008	0.001	0.005	0.0009	0.0025	0.0003	0.0026	0.0003
	RC-SC	0.036	0.029	0.004	0.015	0.003	0.001	0.004	0.000	0.002	0.000	0.001	0.000	0.001	0.0002
	RC-GM	0.023	0.016	0.002	0.008	0.003	0.000	0.002	0.000	0.0014	0.0002	0.0005	0.0001	0.0004	0
1st campaign - dry season	Stream 1	0.0454	0.0217	0.009	0.0396	0.0072	0.0014	0.0078	0.001	0.0061	0.0013	0.0042	0.0007	0.0048	0.0007
	Stream 2	0.1026	0.1573	0.0213	0.0814	0.0146	0.003	0.0152	0.0018	0.01	0.0017	0.0047	0.0008	0.0045	0.0006
	Stream 3	0.0258	0.0047	0.001	0.0054	0.0003	0.0013	0.0007	0.0002	0.0007	0.0001	0.0002	0.0001	0.0004	0
	Stream 4	0.03	0.015	0.002	0.0099	0.0013	0.0022	0.0017	0.0002	0.0007	0.0001	0.0008	0.0001	0.0005	0.0001
	Stream 5	0.0328	0.0091	0.0014	0.008	0.0011	0.0017	0.0018	0.0002	0.0007	0.0003	0.0011	0.0001	0.0007	0.0001
	Precip. 6	0.0141	0.0017	0.0002	0.0008	0.0002	0.0001	0.0002	0.0001	0	-0.0001	-0.0001	0	0	0
	Precip. 7	0.0278	0.0178	0.0014	0.0076	0.0017	0.0002	0.0013	0.0002	0.0008	0.0001	0.0003	0.0001	0.0003	0
	Precip. 8	0.0204	0.0156	0.0015	0.0072	0.0014	0.0003	0.0007	0.0001	0.0008	0.0001	0.0004	0.0001	0.0002	0

7.7 Appendix 7: Volcanic ash emission events from the period 01.12.2016 to 30.06.2019.

Date	Local time	Ash height (from Volcano top)	Direction
01/12/2016	6:17:32	100	SouthWest
02/12/2016	15:48:18	1100	West
09/12/2016	5:48:55	350	West
11/12/2016	8:28:06	200	West
12/12/2016	17:13:07	175	West-NorthWest
12/12/2016	5:30:58	390	West
14/12/2016	20:43:54	650	West
14/12/2016	16:24:33	800	West-SouthWest
14/12/2016	9:36:11	450	West
15/12/2016	4:26:51	250	West-NorthWest
15/12/2016	4:21:10	550	West-NorthWest
16/12/2016	16:29:21	550	SouthWest
18/12/2016	12:16:14	400	South-SouthWest
18/12/2016	8:13:51	250	South-SouthWest
26/12/2016	17:58:50	750	West
26/12/2016	17:58:21	750	West
26/12/2016	5:55:43	200	SouthWest
28/12/2016	6:44:24	800	South
29/12/2016	7:49:41	510	South
01/01/2017	11:21:24	700	West
01/01/2017	10:01:55	400	West
02/01/2017	8:13:28	400	West-SouthWest
03/01/2017	8:28:43	400	West
03/01/2017	7:41:37	200	West
08/01/2017	7:53:48	790	South-SouthWest
08/01/2017	7:44:26	1156	South-SouthWest
11/01/2017	18:07:16	400	SouthWest
19/01/2017	9:26:02	1250	West-SouthWest
21/01/2017	12:33:36	950	SouthWest
21/01/2017	12:20:11	450	SouthWest
22/01/2017	15:07:03	460	South-SouthWest

22/01/2017	9:55:43	200	SouthWest
22/01/2017	9:53:12	400	SouthWest
22/01/2017	7:56:47	400	SouthWest
22/01/2017	7:53:50	1550	SouthWest
22/01/2017	6:31:13	1550	SouthWest
23/01/2017	17:48:57	500	South-Southwest
24/01/2017	8:52:28	780	SouthWest
25/01/2017	18:33:33	450	West-SouthWest
25/01/2017	12:15:24	450	SouthWest
28/01/2017	7:03:11	600	West
31/01/2017	7:33:46	1300	SouthWest
02/02/2017	5:50:01	300	SouthWest
04/02/2017	13:06:30	700	West-NorthWest
05/02/2017	9:00:50	500	West-NorthWest
06/02/2017	16:46:29	750	West
07/02/2017	17:59:28	236	South-Southwest
08/02/2017	14:33:44	350	West
08/02/2017	14:33:44	350	SouthWest
08/02/2017	11:27:20	250	SouthWest
08/02/2017	7:00:44	760	SouthWest
08/02/2017	5:17:10	250	West
09/02/2017	10:42:49	450	SouthWest
09/02/2017	10:05:16	400	SouthWest
09/02/2017	5:48:37	650	SouthWest
27/02/2017	7:03:50	550	SouthWest
28/02/2017	8:17:18	1420	SouthWest
28/02/2017	6:17:10	90	SouthWest
05/03/2017	8:11:01	200	SouthWest
05/03/2017	8:01:44	250	SouthWest
05/03/2017	6:34:52	300	West-SouthWest
05/03/2017	6:02:24	700	West-SouthWest
16/03/2017	9:32:16	840	West-NorthWest
17/03/2017	18:26:49	660	West-NorthWest
17/03/2017	9:59:15	640	West-SouthWest
27/03/2017	11:01:08	800	SouthWest
28/03/2017	7:14:24	900	SouthWest
29/03/2017	5:49:11	282	South-SouthWest
30/03/2017	9:53:59	590	West-SouthWest
03/04/2017	18:51:45	550	West-NorthWest
03/04/2017	14:03:42	270	West
04/04/2017	9:15:42	350	West-NorthWest
04/04/2017	6:50:04	440	West-NorthWest
04/04/2017	6:10:45	950	West-NorthWest
07/04/2017	6:49:06	630	West-NorthWest
07/04/2017	1:24:11	440	West-NorthWest
15/04/2017	9:19:32	530	West-NorthWest
16/04/2017	6:43:18	370	West-NorthWest
19/04/2017	16:58:38	670	SouthWest
23/04/2017	6:25:17	520	SouthWest
24/04/2017	7:36:17	390	West-NorthWest
26/04/2017	17:48:01	1200	SouthWest
27/04/2017	18:21:29	470	West-NorthWest
27/04/2017	11:49:25	600	West-SouthWest
27/04/2017	9:51:21	1100	West-SouthWest
19/05/2017	7:25:24	430	West-SouthWest
19/05/2017	6:36:06	430	West-SouthWest
21/05/2017	5:48:21	200	West-SouthWest
22/05/2017	13:50:58	900	West

23/05/2017	11:48:35	690	SouthWest
24/05/2017	10:35:47	300	West
24/05/2017	7:59:56	200	West
25/05/2017	14:50:29	110	West
25/05/2017	14:48:10	100	West
26/05/2017	8:05:04	215	West-SouthWest
24/11/2017	6:51:23	530	West-SouthWest
21/06/2018	7:21:17	420	South-SouthWest
22/07/2018	9:02:52	250	West-NorthWest
22/07/2018	9:02:33	250	West-NorthWest
25/07/2018	6:57:24	469	West-NorthWest
06/08/2018	17:01:00	195	West-NorthWest
10/08/2018	21:38:36	113	West-NorthWest
27/08/2018	17:44:20	220	West-NorthWest
27/08/2018	9:04:32	195	SouthWest
04/09/2018	11:17:14	960	West-NorthWest
05/09/2018	18:04:57	660	West-NorthWest
17/09/2018	7:34:50	250	West-NorthWest
20/09/2018	16:09:20	200	West-NorthWest
20/09/2018	9:47:16	420	West
20/09/2018	6:43:08	340	West-NorthWest
22/09/2018	10:10:15	390	West-SouthWest
07/04/2019	5:50:00	170	West-NorthWest
26/04/2019	18:00:35	400	SouthWest
26/04/2019	3:36:27	910	SouthWest
27/04/2019	17:49:17	290	West-SouthWest
03/05/2019	14:33:00	200	West-NorthWest
03/05/2019	7:13:59	154	West
04/05/2019	17:14:12	220	West-NorthWest
04/05/2019	16:23:33	170	West-NorthWest
17/06/2019	5:52:45	600	SouthWest

7.8 *Appendix 8: Relationship between δ^2H values and accumulated precipitation for the precipitation stations Precip. 6, 7 and 8.*

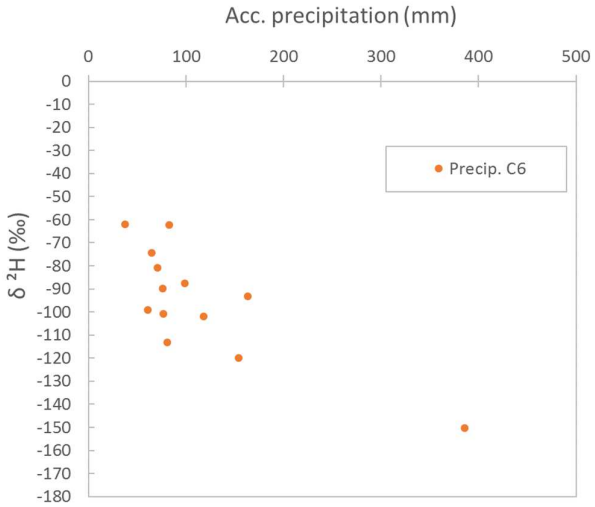

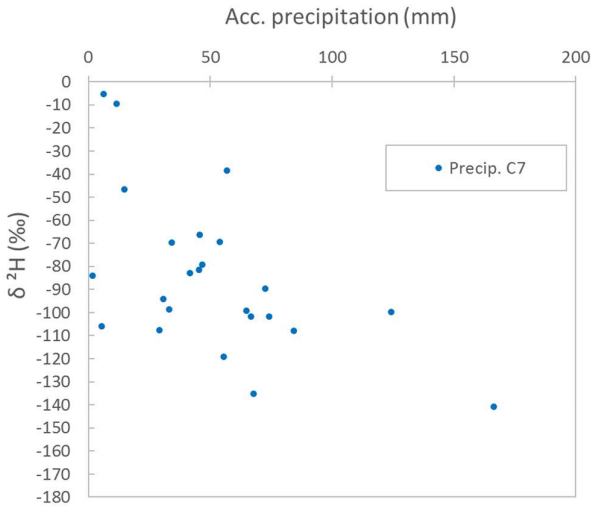

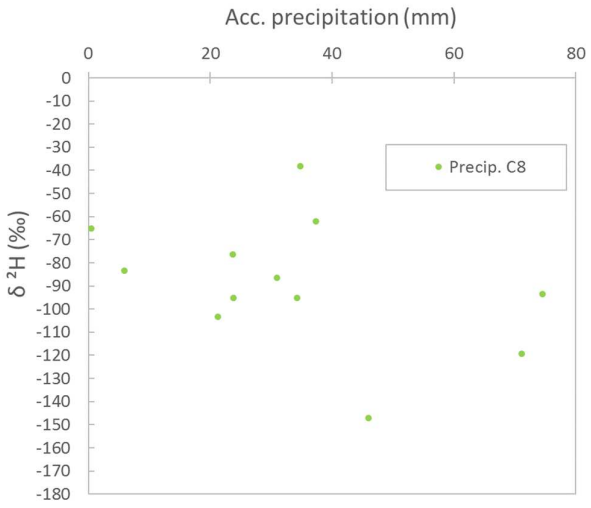

7.9 *Appendix 9: Relationship between d-excess values and accumulated precipitation for the precipitation stations Precip. 6, 7 and 8.*

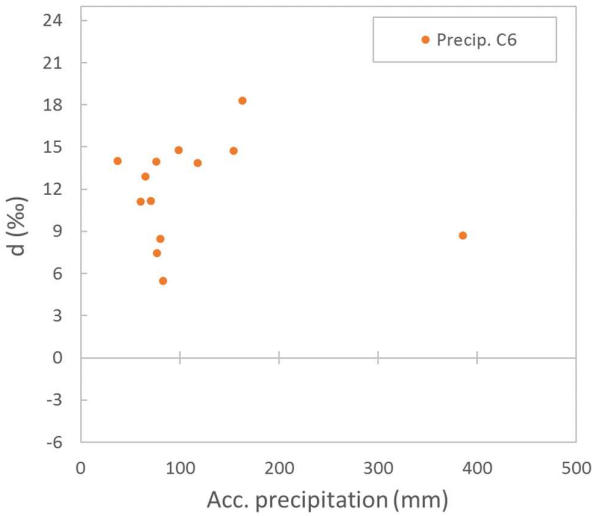

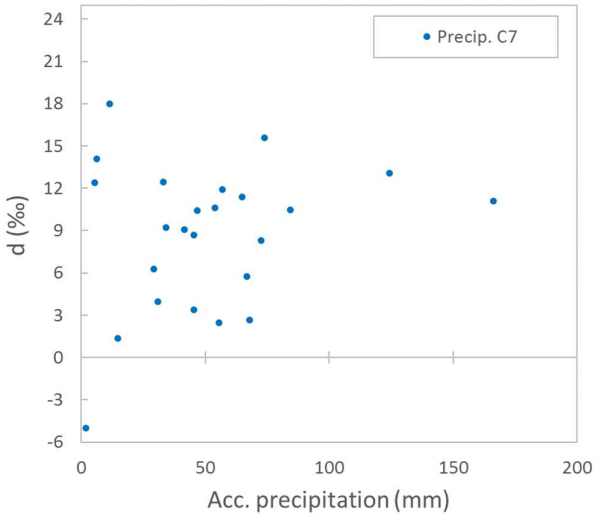

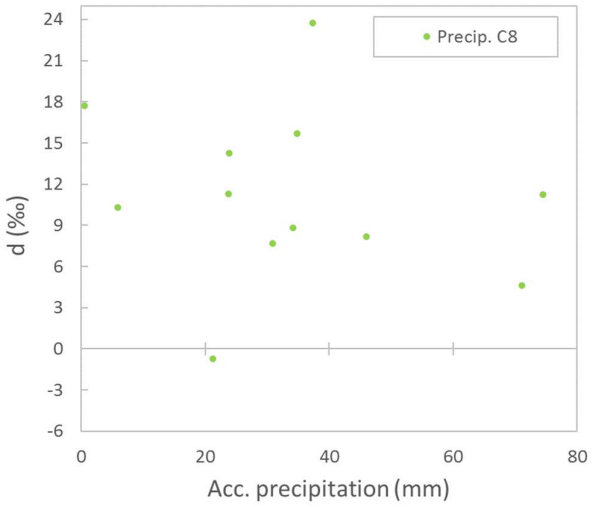

7.10 *Appendix 10: Relationship between δ^2H values and mean daily temperature (average for the sampling period) for the precipitation stations Precip. 6, 7 and 8.*

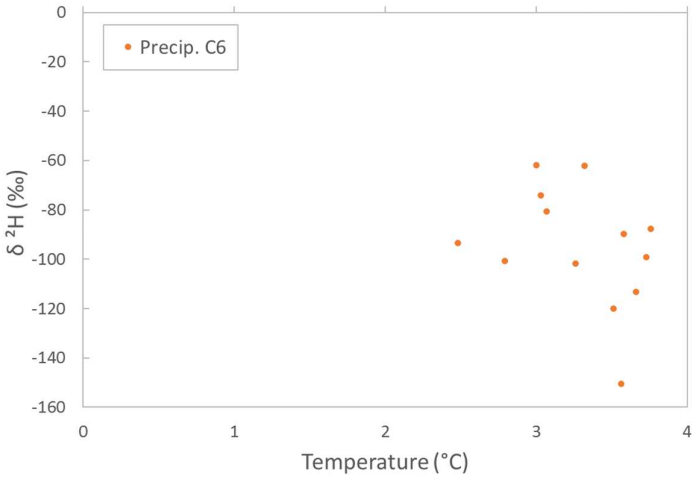

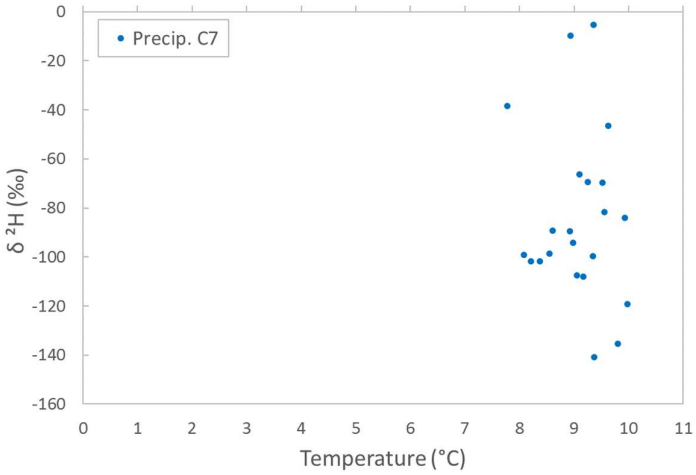

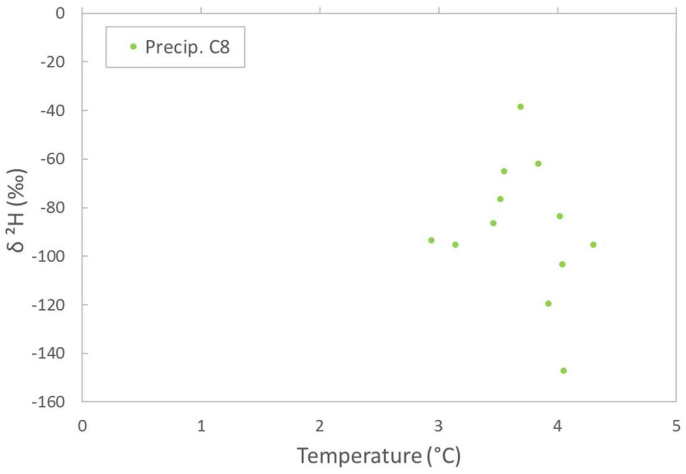

7.11 *Appendix 11: Relationship between d-excess values and mean daily temperature (average for the sampling period) for the precipitation stations Precip. 6, 7 and 8.*

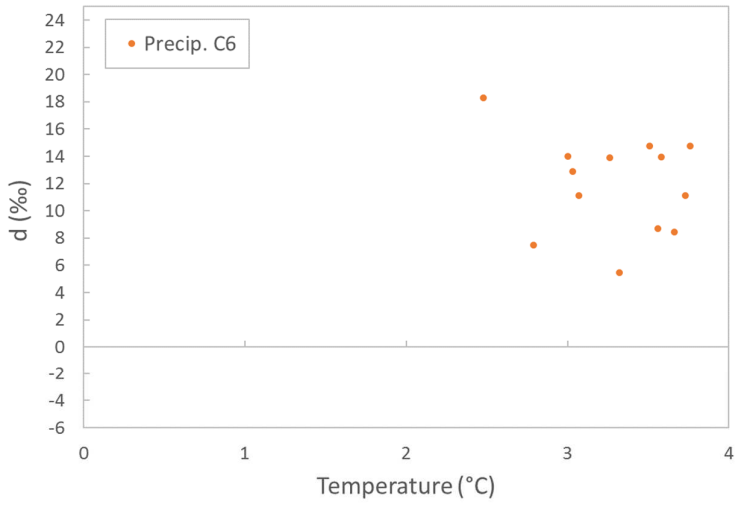

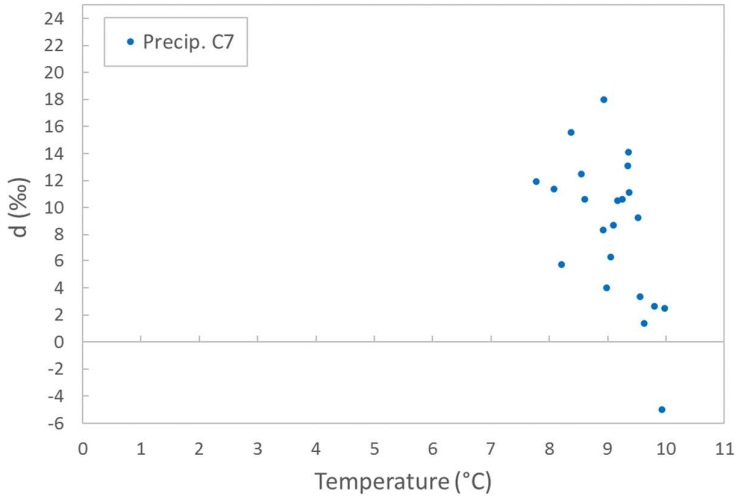

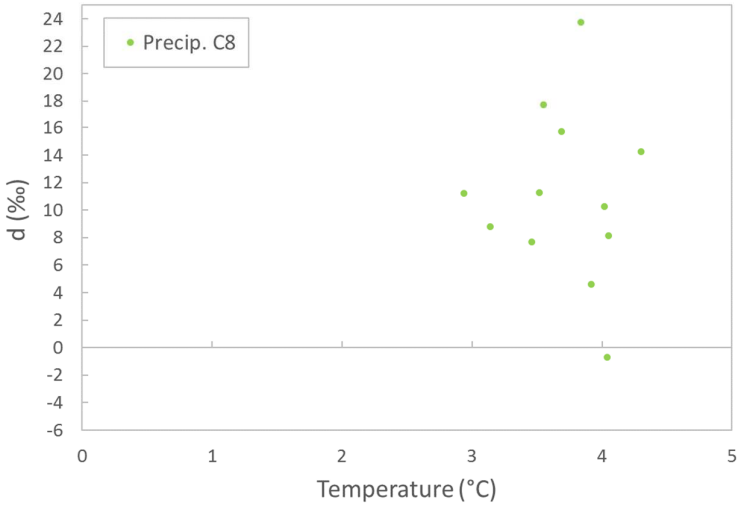

7.12 Appendix 12: Major ions concentration in lakes, glacier melting and tap water.

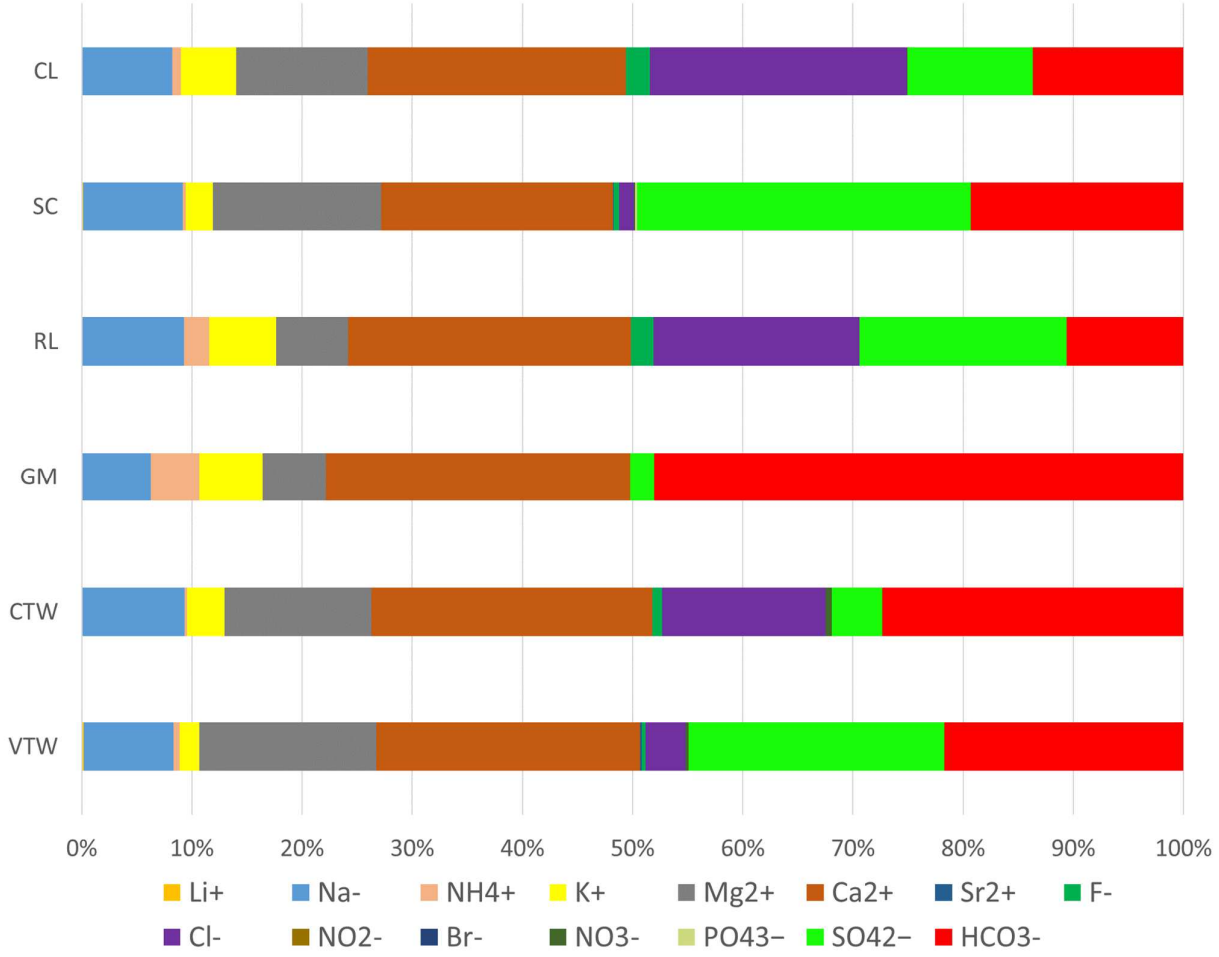

8. REFERENCES

1. Addabbo, M. D., Sulpizio, R., Guidi, M., Capitani, G., Mantecca, P., and Zanchetta, G. (2015). Ash leachates from some recent eruptions of Mount Etna (Italy) and Popocatépetl (Mexico) volcanoes and their impact on amphibian. *Biogeosciences*, *12*, 7087–7106. https://doi.org/10.5194/bg-12-7087-2015
2. Agudelo-Londoño, P. A., Rivera-Caycedo, J. E., Bernal-Vera, M. E., and Castaño-Ramírez, E. (2012). Caracterización del riesgo de contaminación por actividades pecuarias en el río Molinos , Villamaría (Caldas,Colombia). *Veterinaria y Zootecnía*, *6*(2), 56–82.
3. Arango, E. E., Buitrago, A. J., Cataldi, R., Ferrara, G. C., Panichi, C., and Villegas, V. J. (1970). Preliminary study on the Ruiz geothermal project (Colombia). *Geothermics*, *2*(PART 1), 43–56. https://doi.org/10.1016/0375-6505(70)90005-2
4. Bendix, J., Homeier, J., Cueva Ortiz, E., Emck, P., Breckle, S.-W., Richter, M., and Beck, E. (2008). Seasonality of weather and tree phe- nology in a tropical evergreen mountain rain forest. *Int. J. Biome-Teorol.*, (50), 370–384. https://doi.org/10.1007/s00484-006-0029-8, 2006.
5. Bernal, R., Gradstein, R., and Celis, M. (2016). *Catálogo de plantas y líquenes de Colombia. Vol 1 y 2*. Universidad Nacional de Colombia.
6. Bershaw, J., Saylor, J., Garzione, C., Leier, A., and Sundell, K. (2016). Stable isotope variations (Delta 18O and delta - D) in modern waters across the Andean Plateau. *Geochimica et Comochimica Acta*, *194*, 310–324.
7. Betancur, T., and Palacio, P. (2007). Identificación de fuente y zonas de recarga a un sistema acuifero apartir de isótopos estables del agua. *Investigacion*, *10*, 167–182.
8. Burbano, M., and Figueroa, A. (2015). Variabilidad espacio-temporal de aniones (SO4 -2 y Cl-) en el agua lluvia de Popayán, Colombia. *Revista Ingenierías Universidad de Medellín*, *14*(26), 13–28. https://doi.org/10.22395/rium.v14n26a1
9. Buytaert, W., Célleri, R., De Bièvre, B., Cisneros, F., Wyseure, G., Deckers, J., and Hofstede, R. (2006). Human impact on the hydrology of the Andean páramos. *Earth-Science Reviews*, *79*, 53–72. https://doi.org/10.1016/j.earscirev.2006.06.002
10. CARDER. (2007). *Plan de Manejo Integrado de Aguas Subterráneas en Pereira y Dosquebradas. Pereira, Colombia.*
11. CARDER, and IAvH. (2014). *Estudios técnicos, económicos, sociales y ambientales Complejo de páramos los Nevados*. Bogotá D.C.
12. Castrillon, F., Quiroz, O., Bermoudes, O., and Aravena, R. (2003). Evaluation of the origin and residence time of the groundwater in a regional aquifer system, rio de Bogotá basin, Colombia. *International Symposium on Isotope Hydrology and Integrated Water Resources Management*, 229–230.
13. Ceballos, J. L., Euscátegui, C., Ramírez, J., Cañon, M., Huggel, C., Haeberli, W., and Machguth, H. (2006). Fast shrinkage of tropical glaciers in Colombia. *Annals of Glaciology*, *43*, 194–201. https://doi.org/10.3189/172756406781812429
14. Clark, I., and Fritz, P. (1997). *Environmental isotopes in Hydrogeology*. New York: Lewis Publisher.
15. Clayton, R. N., and Steyner, A. (1975). Isotopes in hydrothermal systems 1975.pdf. *Geochimica et Comochimica Acta*, *39*, 1179–1186.
16. Corpocaldas, and Conservacion Internacional. (2007). *Plan de Manejo de los Páramos del Departamento de Caldas*. Manizales.
17. Cortes, A., Durazo, J., and Farvolden, R. (1997). Studies of isotopic hydrology of the basin of Mexico and vicinity: annotated bibliography and interpretation. *Journal of Hydrology*, *198*, 346–376.
18. Craig, H. (1961). Isotopic variations in meteoric waters. *Science*, *133*, 1702–1708.
19. Crawford, J., Hughes, C., and Lykoudis, S. (2014, October 30). *Freeware to calculate a local meteoric water line for your data using a variety of precipitation weighted and non-weighted regressions*.
20. Cuesta-Mosquera, A. P., González-Duque, C. M., Velasco-García, M., and Aristizábal, B. H. (2018). Distribución Espacial De Concentraciones De SO2 , NOx O3 En el Aire Ambiente de Manizales. *Revista Internacional de Contaminacion Ambiental*, *34*(3), 489–504. https://doi.org/10.20937/RICA.2018.34.03.11
21. Dansgaard. (1954). Oxygen-18 Abundance in Fresh Water. *Geochimica et Comochimica Acta*, *6*, 241–260.
22. Dansgaard, W. (1964). Stable isotopes in precipitation. *Tellus XVI*, *4*.
23. Diaz-Granados, A. (1988). *Resumen del Estudio Hidrogeológico del Flanco nororiental de la Serrania de San Jacinto y de la Zona litoral del Golfo de Morrosquillo*.
24. Doria, C., and Castillo, J. F. (2016). Chemical characterization of particulated atmospheric matter PM10 in Guajira, Colombia. *Revista Colombiana de Quimica*, *45*(2), 19–29. https://doi.org/10.15446/rev.colomb.quim.v45n2.56991

25. Doria, Carlos. (2017). Metales pesados (Cd , Cu , V , Pb) en agua lluvia de la zona de mayor influencia de la mina de carbón en La Guajira , Colombia. *Revista Colombiana de Química*, *46*(2), 37–44. https://doi.org/2357-3791.
26. Erazo, D., Londoño, A., and Aristizábal, B. (2015). Estudio del impacto de los fluidos volcánicos en el recurso hídrico de la cuenca del río Chinchiná. *Gestion y Ambiente*, *18*(2), 81–93.
27. Eslava, J. (1985). Consideraciones sobre los aspectos meteorologicos y efectos relacionados con la dispersión de fragmentos y gases emitidos por el volcán Arenas del Nevado del Ruiz el 13 de Noviembre de 1985. *Geologia Colombiana*, *14*, 165–173.
28. Esquivel-Hernández, G., Mosquera, G. M., Sánchez-Murillo, R., Quesada-Román, A., Birkel, C., Crespo, P., … Boll, J. (2019). Moisture transport and seasonal variations in the stable isotopic composition of rainfall in Central American and Andean Páramo during El Niño conditions (2015–2016). *Hydrological Processes*, 1–41. https://doi.org/10.1002/hyp.13438
29. Federico, C., Inguaggiato, S., Chacón, Z., Londoño, J. M., Gil, E., and Alzate, D. (2017). Vapour discharges on Nevado del Ruiz during the recent activity: Clues on the composition of the deep hydrothermal system and its effects on thermal springs. *Journal of Volcanology and Geothermal Research*, *346*, 40–53. https://doi.org/10.1016/j.jvolgeores.2017.04.007
30. Fernández-Turiel, J. L., Saavedra-Alonso, J., Ruggieri, F., Gimeno-Torrente, D., Perez-Torrado, F. J., Rodriguez-Gonzalez, A., … Galindo, G. (2012). Geoquímica de cenizas volcánicas a lo largo de dos transectas en Sudamérica: implicaciones ambientales. *Geo-Temas*, *13*, 2–5.
31. Fiorella, R. P. (2016). *Understanding Hydrological Cycling at High Elevations and in Forest Canopies using Stable Water Isotopes*. University of Michigan.
32. Fischer, T. P., Sturchio, N. C., Stix, J., Arehart, G. B., Counce, D., and Williams, S. N. (1997). The chemical and isotopic composition of fumarolic gases and spring discharges from Galeras Volcano, Colombia. *Journal of Volcanology and Geothermal Research*, *77*, 229–253. https://doi.org/10.1016/S0377-0273(96)00096-0
33. Flórez, A. (1992). *Los nevados de Colombia, glaciares y glaciaciones.* Santa fe de Bogotá, D.C: Instituto Geográfico Agustín Codazzi.
34. Froehlich, K., Gibson, J. J., and Aggarwal, P. (2002). Deuterium Excess In Precipitation And Its Climatological Significance. *Journal of Geophysical Research-Atmospheres*, (July), 2.
35. García, M., Villalba, F., Araguás - Araguás, L., and Rozanski, K. (1997). The role of atmospheric circulation patterns in controlling the regional distribution of stable isotope contents in precipitation: Preliminary results from two transects in the Ecuadorian Andes. *Isotope Techniques in The Study of Environmental Change - Proceedings of a Symposium, Vienna*, 127–141.
36. Gat, J. R. (1996). Oxygen and Hydrogen Isotopes in the Hydrologic Cycle. *Annual Review of Earth and Planetary Sciences*, *24*(1), 225–262. https://doi.org/10.1146/annurev.earth.24.1.225
37. Gomez, S., Taupin, J. D., and Rueda, A. (2015). Estudio hidrodinámico, geoquímico e isotópico de las formaciones acuíferas de la región de Bucaramanga (Colombia) Hydrodynamic, geochemical and isotopic study of formations aquifers in the region of Bucaramanga (Colombia). *Revista Peruana Geo-Atmosferica RPGA*, (4), 44–61.
38. Gonfiantini. (1998). *On the isotopic composition of precipitation*.
39. Gonfiantini, R., and Panichi, C. (1978). Environmental isotopes in geothermal environments.pdf. *Geothermics*, *6*, 143–161.
40. Gonfiantini, R., Roche, M., Olivry, J., Fontes, J., and Zuppi, G. (2001). The altitude effect on the isotopic composition of tropical rains. *Chemical Geology*, *181*, 147–167. https://doi.org/10.3402/tellusa.v20i4.10040
41. González-Duque, C. M., Cortés-Araujo, J., and Aristizábal-Zuluaga, B. H. (2015). Influence of meteorology and source variation on airborne Pm10 levels in a high relief tropical Andean city. *Revista Facultad de Ingenieria*, *1*(74), 200–212.
42. González, C. M., and Aristizábal, B. H. (2012). Acid rain and particulate matter dynamics in a mid-sized Andean city: The effect of rain intensity on ion scavenging. *Atmospheric Environment*, *60*, 164–171. https://doi.org/10.1016/j.atmosenv.2012.05.054
43. Henderson-Sellers, A., and McGuffie, K. (2006). Shift in stable water isotopes in precipitation in the Andean Amazon: Implications of deforestation or greenhouse impacts? In *Radioactivity in the Environment* (Vol. 8). https://doi.org/10.1016/S1569-4860(05)08003-4
44. Herrera, H., Vargas, M., and Taupin, J. (2009). Estudio Hidrogeológico con Enfasis en Hidrogeoquímica del Acuífero Morroa (Colombia). *Estudios de Hidrología Isotópica En América Latina 2006*, 29–46.
45. Hoefs, J. (2009), Stable Isotopes geochemistry, University of Göttingen, 6th edition, Springer.
46. Honório, B. A. D., Horbe, A. M. C., and Seyler, P. (2010). Chemical composition of rainwater in western Amazonia — Brazil. *Atmospheric Research*. https://doi.org/10.1016/j.atmosres.2010.08.001
47. Hughes, C. E., and Crawford, J. (2012). A new precipitation weighted method for determining the meteoric

water line for hydrological applications demonstrated using Australian and global GNIP data. *Journal of Hydrology*, *464–465*, 344–351. https://doi.org/10.1016/j.jhydrol.2012.07.029
48. IAEA. (1992). *Statistical treatment of data on environmental isotopes in precipitation* (Technical).
49. IAEA. (1997). *Isotope techniques in the study of environmental change*. Vienna.
50. IAEA. (2000). Environmental isotopes in the hydrological cycle. In UNESCO – IAEA (Ed.), *Technical documents in hydrology* (Vol. 1). Retrieved from http://www.hydrology.nl/images/docs/ihp/Mook_VI.pdf
51. IAEA. (2003). *International Symposium on Isotope Hydrology and Integrated Water Resources Management*. Vienna.
52. IAEA. (2019). GNIP/Colombia (IDEAM and IAEA). Retrieved June 15, 2019, from https://nucleus.iaea.org/Pages/GNIPR.aspx
53. IDEAM. (2010). *Informe de actividades glaciológicas 2010 - Volcán nevado Santa Isabel Y Sierra nevada de El Cocuy*. Bogotá, D.C.: Subdirección de Ecosistemas e Información Ambiental.
54. IDEAM. (2013). *Aguas Subterráneas en Colombia: una Visión General.* Retrieved from http://acuiferosuraba.net/wp-content/uploads/2016/08/Libro-Aguas-Subterráneas-en-Colombia-Una-Visión-General.pdf
55. IDEAM. (2019a). Volcán nevado del ruiz. Retrieved July 15, 2019, from http://www.ideam.gov.co/web/ecosistemas/volcan-nevado-ruiz
56. IDEAM. (2019b). Volcán Nevado Santa Isabel. Retrieved February 2, 2019, from http://www.ideam.gov.co/web/ecosistemas/volcan-nevado-santa-isabel
57. IDEAM, and UPME. (2017). *Atlas de viento de Colombia* (IDEAM and UPME, Eds.). Bogotá.
58. Ingeominas. (1998). *Geologia de la Plancha 225 Nevado del Ruiz* (p. Escala 1:100000). p. Escala 1:100000. Bogotá D.C.
59. Jaramillo, A. (2005). Clima andino y café en Colombia. In *CENICAFE*.
60. Jouzel, J., Delaygue, G., Landais, A., Masson-Delmotte, V., Risi, C., and Vimeux, F. (2013). Water isotopes as tools to document oceanic sources of precipitation. *Water Resources Research*, *49*(11), 7469–7486. https://doi.org/10.1002/2013WR013508
61. Kendall, C., and Coplen, T. B. (2001). Distribution of oxygen-18 and deuteriun in river waters across the United States. *Hydrological Processes*, *15*(7), 1363–1393. https://doi.org/10.1002/hyp.217
62. Koeniger, P., Margane, A., Abi-Rizk, J., and Himmelsbach, T. (2017). Stable isotope-based mean catchment altitudes of springs in the Lebanon Mountains. *Hydrological Processes*, *31*(21), 3708–3718. https://doi.org/10.1002/hyp.11291
63. Lachniet, M. S., and Patterson, W. P. (2009). Oxygen isotope values of precipitation and surface waters in northern Central America (Belize and Guatemala) are dominated by temperature and amount effects. *Earth and Planetary Science Letters*, *284*(3–4), 435–446. https://doi.org/10.1016/j.epsl.2009.05.010
64. Lavado, R. S. (1983). Evaluación de la relación entre la coposición química del agua de lluvia y el grado de salinidad y sodicidad de distintos suelos. *Rev. Facultad de Agronomía*, *4*(2), 135–139.
65. Leibundgut, C., Maloszewski, P., and Külls, C. (2009). *Tracers in Hydrology*. Retrieved from http://www.ghbook.ir/index.php?name=فرهنگ و رسانه های نوینandoption=com_dbookandtask=readonlineandbook_id=13650andpage=73andchkhashk=ED9C9491B4andItemid=218andlang=faandtmpl=component
66. Lizcano, A., Herrera, M. C., and Santamarina, J. C. (2006). Suelos derivados de cenizas volcánicas en colombia. *Revista Internacional de Desastres Naturales*, *6*(2), 167–198.
67. Mariño-Martinez, J., Veloza-Franco, J., and Martínez-Sánchez, A. (2018). Analysis of precipitation and recharge of aquifers in Tota and Ibagué (Colombia) from stable isotopes (18O and 2H). *Revista Facultad de Ingeniería*, *27*(47).
68. Martinelli, L. A., Victoria, R. L., Sternberg, L. S. L., Ribeiro, A., and Moreira, M. Z. (1996). Using stable isotopes to determine sources of evaporated water to the atmosphere in the Amazon basin. *Journal of Hydrology*, *183*(3–4), 191–204. https://doi.org/10.1016/0022-1694(95)02974-5
69. Medina, G., Paez, G., Vargas, M., and Taupin, G. (2009). Estudio Hidrogeológico con Enfasis en Hidrogeoquímica de los Acuíferos en la Zona Sur del Departamento del Valle del Cauca (Colombia). *Estudios de Hidrología Isotópica En América Latina 2006*, 47–65.
70. Mello, W Z De. (2001). Precipitation chemistry in the coast of the Metropolitan Region of Rio de Janeiro , Brazil. *Environmental Pollution*, *114*, 235–242.
71. Mello, William Z De, and Almeida, M. D. De. (2004). Rainwater chemistry at the summit and southern flank of the Itatiaia massif , Southeastern Brazil. *Environmental Pollution*, *129*, 63–68. https://doi.org/10.1016/j.envpol.2003.09.026
72. Michelsen, N., Reshid, M., Siebert, C., Schulz, S., Knöller, K., Weise, S. M., … Schüth, C. (2015). Isotopic and chemical composition of precipitation in Riyadh , Saudi Arabia. *Chemical Geology*, *413*, 51–62. https://doi.org/10.1016/j.chemgeo.2015.08.001
73. Michelsen, N., Reshid, M., Siebert, C., Schulz, S., Rausch, R., Knöller, K., … Schüth, C. (2015). Isotopic

composition of Riyadh rainfall, Saudi Arabia. *Chemical Geology*, *413*, 51–62. https://doi.org/10.1016/j.chemgeo.2015.08.001
74. Mimura, A. M. S., Almeida, J. M., Vaz, F. A. S., Oliveira, M. A. L. De, Ferreira, C. C. M., and Silva, J. C. J. (2016). Chemical composition monitoring of tropical rainwater during an atypical dry year. *Atmospheric Research*, *169*, 391–399. https://doi.org/10.1016/j.atmosres.2015.11.001
75. MMADT-MPS. (2007). *Resolucion 2115 - Por medio de la cual se señalan características, instrumentos básicos y frecuencias del sistema de control y vigilancia para la calidad del agua para consumo humano*. Retrieved from https://www.google.com.co/webhp?sourceid=chrome-instantandion=1andespv=2andie=UTF-8#
76. Mölg, N., Ceballos, J. L., Huggel, C., Micheletti, N., Rabatel, A., and Zemp, M. (2017). Ten years of monthly mass balance of conejeras glacier, Colombia, and their evaluation using different interpolation methods. *Geografiska Annaler, Series A: Physical Geography*, *99*(2), 155–176. https://doi.org/10.1080/04353676.2017.1297678
77. Morán-Tejeda, E., Ceballos, J., Peña, K., Lorenzo-Lacruz, J., and López-Moreno, J. (2018). Recent evolution and associated hydrological dynamics of a vanishing tropical Andean glacier : Glaciar de Conejeras , Colombia. *Hydrology and Earth Sciences Systems*, *22*, 5445–5461.
78. Mosquera, G., Lazo, P., Cárdenas, I., and Crespo, P. (2013). Identificación de las principales fuentes de agua que aportan a la generación de escorrentía en zonas Andinas de páramo húmedo: mediante el uso de isótopos estables deuterio (^{2}H) y oxígeno (18O. *Revista Semestral de DIUC*, *3*(2), 87–105.
79. Mosquera, Giovanny, Crespo, P., Célleri, R., Lazo, P., Vaché, K. B., and Steven S., P. (2016). Combined use of isotopic and hydrometric data to conceptualize ecohydrological processes in a high-elevation tropical ecosystem. *Hydrological Processes*, *30*(17), 2930–2947.
80. Ocampo-López, O. (2012). *Análisis de Vulnerabilidad de la cuenca del río Chinchiná para condiciones estacionarias y de cambio climático*. Universidad Nacional de Colombia.
81. Ortiz, L., and Reyes, M. (2009). Los páramos en Colombia: un ecosistema vulnerable. In *Escuela de Econonomía*. Retrieved from http://www.unilibrebaq.edu.co/ojsinvestigacion/index.php/ingeniare/article/view/704
82. Osorio, J. ., López, J., and Hermelin, M. (2003). Balance geoquímico para la cuenca alta del río Medellín, Cordillera Central (Antioquia, Colombia). *Rev. Acad. Colomb. Cienc.*, *27*(102), 71–84.
83. Otálvaro, D., Arias, G., and Vélez, E. (2008). Uso de métodos geofísicos e isotópicos en la construcción de un modelo hidrogeológico conceptual para los acuíferos de Pereira y Dosquebradas, Colombia. *Recursos Naturales y Ambiente*, (58), 89–96. Retrieved from http://repositorio.bibliotecaorton.catie.ac.cr/bitstream/handle/11554/6887/Uso_de_metodos_geofisicos_pdf.pdf?sequence=1andisAllowed=y
84. Otálvaro, D., Arias, G., Vélez, M., García, J., De la Rosa, P., Taupin, J., and Vargas, M. (2009). Plan de Manejo Integral del Agua Subterránea Modelo Hidrogeológico Conceptual Preliminar del Acuífero de Pereira, Colombia. *Estudios de Hidrología Isotópica En América Latina 2006*, 11–27.
85. Panarello, H., and Albero, M. (1981). Tritium, oxygen-18 and deuterium contents of Buenos Aires rainwater. In *Interamerican symposium on isotope hydrology* (pp. 91–109). Bogotá D.C.
86. Peña, K. (2016). *Análisis de la variabilidad hidroclimática y dinámica glaciar en la cuenca alta de Río Claro (Villamaría Caldas, Colombia), Estudio científico como base para la adaptación y mitigación al cambio climático en la alta montaña colombiana*. Pontificia Universidad Javeriana.
87. Pfahl, S., and Sodemann, H. (2014). What controls deuterium excess in global precipitation? *Climate of the Past*, *10*(2), 771–781. https://doi.org/10.5194/cp-10-771-2014
88. Poveda, G., Waylen, R., and Pulwarty, W. (2006). Annual and inter-annual variability of the present climate in northern South America and South Mesoamerica. *Paleogeography, Palaeoclimatol¬ogy, Palaeoecology*, *234*, 3–27.
89. Poveda, G., Waylen, P. R., and Pulwarty, R. S. (2006). Annual and inter-annual variability of the present climate in northern South America and southern Mesoamerica. *Palaeogeography, Palaeoclimatology, Palaeoecology*, *234*, 3–27. https://doi.org/10.1016/j.palaeo.2005.10.031
90. Prieto, A. (2008). *Cuantificación de la población ubicada en la cuenca alta del Río Claro (Volcán Nevado Santa Isabel), identificación de uso del suelo, análisis del recurso hídrico en términos de uso, abastecimiento, calidad y disponibilidad, y análisis de la vulnerabilida*. Bogotá, D.C.
91. Rabatel, A., Ceballos, J. L., Micheletti, N., Jordan, E., Braitmeier, M., González, J., … Zemp, M. (2018). Toward an imminent extinction of Colombian glaciers? *Geografiska Annaler, Series A: Physical Geography*, *100*(1), 75–95. https://doi.org/10.1080/04353676.2017.1383015
92. Ramírez Arcila, H., and Ospina Zúñiga, O. (2014). Evaluación de la calidad del agua de lluvia para su aprovechamiento y uso doméstico en la ciudad de Ibagué, Tolima, Colombia. *Ingeniería Solidaria*, *10*(17), 125–138. https://doi.org/10.16925/in.v9i17.812
93. Rodríguez, C. (2004). Isotopic Meteoric Line for Colombia. *Meteorología Colombiana*, (8), 43–51.

94. Rohrmann, A., Strecker, M. R., Bookhagen, B., Mulch, A., Sachse, D., Pingel, H., … Montero, C. (2014). Can stable isotopes ride out the storms ? The role of convection for water isotopes in models , records , and paleoaltimetry studies in the central Andes. *Earth and Planetary Science Letters*, *407*, 187–195. https://doi.org/10.1016/j.epsl.2014.09.021
95. Rozanski, K., and Araguas, L. A. (1995). Spatial and temporal variability of stable isotope composition of precipitation over the South American continent. *Bulletin de l'Institut Francais d'etudes Andines*, *24*(3), 379–390. Retrieved from papers3://publication/uuid/0DBCD095-3531-4286-B818-8CA24DA75DB6
96. Ruiz Carrascal, D., Moreno, H., Gutierrez-Lagoueyte, M., and Zapata, P. (2008). Changing Climate and Endangered High Mountain Ecosystems in Colombia. *The Science of the Total Environment*, *398*, 122–132. https://doi.org/10.1016/j.scitotenv.2008.02.038
97. Ruiz, D. (2009). Signals of climate variability/change in surface water supply of high-mountain watersheds-case study: Claro River high mountain basin, Los Nevados Natural Park, Andean Central Mountain Range, Colombia. In *World Bank Group*. Envigado, Antioquia.
98. Ruiz, D., Arroyave, M., Gutierrez, M., and Zapata, P. (2011). Increased Climatic Stress on High-Andean Ecosystems in the Cordillera Central of Colombia. *Research Gate*, 182–191. https://doi.org/10.13140/2.1.3718.4969
99. Ruiz, D., Arroyave, M., Molina, A., Barros, J., Gutiérrez, M., and Zapata, P. (2009). Estudio del recurso hídrico en la alta montaña frente a condiciones climáticas cambiantes . Estudio de caso : cuenca alta río Claro , Parque Nacional Natural Los Nevados. *Segundo Congreso Mundial de Paramos*, 10. Grupo de Investigación Gestión del Ambiente para el Bienestar Social – GABiS.
100. Salati, E., Dall'Olio, A., Matsui, E., and Gat, J. R. (1979). Recycling of water in the Amazon Basin: An isotopic study. *Water Resources Research*, *15*(5), 1250–1258. https://doi.org/10.1029/WR015i005p01250
101. Samuels-Crow, K. E., Galewsky, J., Hardy, D. R., Sharp, Z. D., Worden, J., and Braun, C. (2014). Upwind convective influences on the isotopic composition of atmospheric water vapor over the tropical Andes. *Journal of Geophysical Research*, *119*(12), 7051–7063. https://doi.org/10.1002/2014JD021487
102. Sánchez-Murillo, R., Durán-Quesada, A. M., Birkel, C., Esquivel-Hernández, G., and Boll, J. (2017). Tropical precipitation anomalies and d-excess evolution during El Niño 2014-16. *Hydrological Processes*, *31*(4), 956–967. https://doi.org/10.1002/hyp.11088
103. Sánchez-Murillo, R., Esquivel-Hernández, G., Welsh, K., Brooks, E. S., Boll, J., Alfaro-Solís, R., and Valdés-González, J. (2013). Spatial and Temporal Variation of Stable Isotopes in Precipitation across Costa Rica: An Analysis of Historic GNIP Records. *Open Journal of Modern Hydrology*, *03*(04), 226–240. https://doi.org/10.4236/ojmh.2013.34027
104. Santa, D., Martínez, D., and Betancur, T. (2008). Uso de la hidroquimica e isótopos ambientales para la evaluación de la conexión hidrológica entre el agua subterránea y el humedal ciénaga Colombia. *Gestion y Ambiente*, *11*, 21–38.
105. Saylor, J. E., Mora, A., Horton, B. K., and Nie, J. (2009). Controls on the isotopic composition of surface water and precipitation in the Northern Andes, Colombian Eastern Cordillera. *Geochimica et Cosmochimica Acta*, *73*(23), 6999–7018. https://doi.org/10.1016/j.gca.2009.08.030
106. Seinfeld, J., and Pandis, S. (2006). *Atmospheric Chemistry and Physics: From Air Pollution to Climate Change*. https://doi.org/10.5194/acp-5-139-2005
107. Servicio Geológico Colombiano. (2015). *Mapa de Amenaza Volcánica del Volcán Nevado del Ruiz*.
108. Servicio Geológico Colombiano. (2016). *Informe técnico anual de la actividad volcánica del segmento volcánico norte de Colombia*. Manizales.
109. Servicio Geológico Colombiano. (2017). *Informe técnico anual de la actividad volcanica del segmento norte de colombia*. Manizales.
110. Servicio Geológico Colombiano. (2018a). *Informe emisiones de cenizas del volcán nevado del ruiz, 4 y 5 de septiembre del 2018*. Manizales.
111. Servicio Geológico Colombiano. (2018b). *Informe técnico – Operativo de la actividad volcánica segmento volcánico norte de Colombia - Septiembre de 2018*. Manizales.
112. Servicio Geológico Colombiano. (2019). Generalidades Volcán Nevado del Ruíz. Retrieved July 15, 2019, from https://www2.sgc.gov.co/sgc/volcanes/VolcanNevadoRuiz/Paginas/generalidades-volcan-nevado-ruiz.aspx
113. Siegenthaler, U., and Oeschger, H. (1980a). Correlation of 18O in precipitation with temperature and altitude. *Nature*, *285*(5763), 314–317. https://doi.org/10.1038/285314a0
114. Siegenthaler, U., and Oeschger, H. (1980b). Correlation of 18O in precipitation with temperature and altitude. *Nature*, *285*(5763), 314–317. https://doi.org/10.1038/285314a0
115. Sklenáj, P., Luteyn, J., Ullua, C., Jorgensen, P., and Dillon, M. (2005). Flora Genérica des los Páramos: guía ilustrada de las plantas vasculares (Memoirs of the New York Botanical Garden 92). In

Hardback (Ed.), *Memoirs of the New York Botanical Garden*. https://doi.org/10.1179/eck.16.1.289166007176p043

116. Stewart, C., Johnston, D. M., Leonard, G. S., Horwell, C. J., Thordarson, T., and Cronin, S. J. (2006). Contamination of water supplies by volcanic ashfall : A literature review and simple impact modelling. *Journal of Volcanology an Geothermal Research*, *158*, 296–306. https://doi.org/10.1016/j.jvolgeores.2006.07.002
117. Sturm, C., Hoffmann, G., and Langmann, B. (2007). Simulation of the stable water isotopes in precipitation over South America: Comparing regional to global circulation models. *Journal of Climate*, *20*(15), 3730–3750. https://doi.org/10.1175/JCLI4194.1
118. Toro, L., Calderón, J., Taupin, J., and Vargas, M. (2009). Exploración de Aguas Subterráneas en Maicao (Colombia) Mediante Técnicas Hidroquímicas e Isotópicas. *Estudios de Hidrología Isotópica En América Latina 2006*, 67–82.
119. Universidad Nacional de Colombia. (2014a). Plan de ordenación y manejo ambiental de la cuenca hidrográfica del río Chinchiná en el departamento de Caldas - Colombia. POMCA 2014. In *Plan de ordenación y manejo ambiental de la cuenca hidrográfica del río Chinchiná en el departamento de Caldas - Colombia. POMCA 2014* (Corpocalda). Manizales: Corpocaldas.
120. Universidad Nacional de Colombia. (2014b). *Plan de Ordenamiento de la Subcuenca del Rio Guacaica*. Manizales: Corpocaldas.
121. UPME and Universidad Nacional de Colombia. (2000). *Atlas hidrológico de Colombia*. Medellin: Facultad de Minas - Posgrado en Aprovechamiento de Recursos Hidraúlicos.
122. USGS. (2015). Volcanic Ash Impacts and Mitigation. https://doi.org/10.1016/B978-0-7506-6843-9.X0001-7
123. Vallet-Coulomb, C., Gasse, F., and Sonzogni, C. (2008). Seasonal evolution of the isotopic composition of atmospheric water vapour above a tropical lake: Deuterium excess and implication for water recycling. *Geochimica et Cosmochimica Acta*, *72*, 4661–4674. https://doi.org/10.1016/j.gca.2008.06.025
124. Vélez, Duque, N., Orozco, M., and Aristizábal, B. (2015). *Entendimiento de fenómenos ambientales mediante el análisis de datos* (Gerard Oli). Manizales: Universidad Nacional de Colombia.
125. Vélez, M., and Rhenals, R. (2008). Determinación de la recarga con con isótopos ambientales en los acuíferos de Santa fe de Antioquia. *Revista Boletin Ciencias de La Tierra*, *24*, 37–54.
126. Vet, R., Artz, R. S., Carou, S., Shaw, M., Ro, C. U., Aas, W., … Reid, N. W. (2014). A global assessment of precipitation chemistry and deposition of sulfur, nitrogen, sea salt, base cations, organic acids, acidity and pH, and phosphorus. *Atmospheric Environment*, *93*, 3–100. https://doi.org/10.1016/j.atmosenv.2013.10.060
127. Villacis, M., Vimeux, F., and Taupin, jean denis. (2008). Analysis of the climate controls on the isotopic composition of precipitation (δ18O) at Nuevo Rocafuerte, 74.5°W, 0.9°S, 250 m, Ecuador. In *Comptes Rendus Geoscience* (Vol. 340). https://doi.org/10.1016/j.crte.2007.11.003
128. Vimeux, F., Gallaire, R., Bony, S., Hoffmann, G., and Chiang, J. (2005). What are the climate controls on dD in precipitation in the Zongo Valley (Bolivia)? Implications for the Illimani ice core interpretation. *Earth and Planetary Science Letters*, *240*, 205–220. https://doi.org/10.1016/j.epsl.2005.09.031
129. Vimeux, F., Tremoy, G., Risi, C., and Gallaire, R. (2011). A strong control of the South American SeeSaw on the intra-seasonal variability of the isotopic composition of precipitation in the Bolivian Andes. *Earth and Planetary Science Letters*, *307*(1–2), 47–58. https://doi.org/10.1016/j.epsl.2011.04.031
130. Vuille, M., Bradley, R., Werner, M., Healy, R., and Keimig, F. (2003). Modeling δ 18 O in precipitation over the tropical Americas: 1. Interannual variability and climatic controls. *Journal of Geophysical Research*, *108*(D6). https://doi.org/10.1029/2001JD002038
131. Vuille, M., and Werner, M. (2005). Stable isotopes in precipitation recording South American summer monsoon and ENSO variability: Observations and model results. *Climate Dynamics*, *25*(4), 401–413. https://doi.org/10.1007/s00382-005-0049-9
132. Wetang, G. N., and Wamalwa, H. M. (2015). Trace Elements in Rainfall Collected around Menengai Area Kenya. *World Geothermal Congress 2015*, (April), 19–25.
133. WGMS. (2017). *Global Glacier Change Bulletin No. 2 (2014–2015)* (Vol. 2; M. Zemp, S. U. Nussbaumer, I. Gärtner-Roer, J. Huber, H. Machguth, F. Paul, and M. Hoelzle, Eds.). Zurich, Switzerland: ICSU(WDS)/IUGG(IACS)/UNEP/ UNESCO/WMO,.
134. Windhorst, D., Waltz, T., Timbe, E., Frede, H. G., and Breuer, L. (2013). Impact of elevation and weather patterns on the isotopic composition of precipitation in a tropical montane rainforest. *Hydrology and Earth System Sciences*, *17*(1), 409–419. https://doi.org/10.5194/hess-17-409-2013
135. World Health Organization. (2018). *A global overview of national regulations and standards for drinking-water quality*. Retrieved from

http://apps.who.int/iris/bitstream/handle/10665/272345/9789241513760-eng.pdf?sequence=1andisAllowed=y

136. Wu, Y., Xu, Z., Liu, W., Zhao, T., Zhang, X., Jiang, H., … Zhou, X. (2016). Chemical compositions of precipitation at three non-urban sites of Hebei Province , North China : Influence of terrestrial sources on ionic composition. *Atmospheric Research*, *181*, 115–123. https://doi.org/10.1016/j.atmosres.2016.06.009